3-24-2020 12:00 PM

Multimodality imaging to quantify the pulmonary vascular tree in COPD

Andrea L. Barker Odhiambo
The University of Western Ontario

Supervisor
Parraga, Grace
The University of Western Ontario

Graduate Program in Medical Biophysics
A thesis submitted in partial fulfillment of the requirements for the degree in Master of Science

Abstract

Chronic obstructive pulmonary disease (COPD) is a progressive and debilitating disease resulting in chronic cough, shortness of breath, activity limitation and decreased pulmonary function. Developments in imaging technology have provided sensitive and reliable modalities for evaluating regional lung function and disease progression, and there is a growing interest in the role of imaging the vasculature in COPD. The ability to predict whether a patient is at risk of accelerated decline is important to disease management strategies. We hypothesize that CT blood vessel volume measurements are significantly different in ex-smokers without COPD than in those with this disease and will be related to disease severity. 90 participants completed both baseline and follow-up visits: 41 ex-smokers without COPD (71±10yrs) and 49 participants with COPD (71±8yrs). From baseline to follow-up, RA_{950} increased significantly for ex-smokers and GOLD II participants, while PV_1 decreased significantly for GOLD I. There were no differences in VDP when grouped according to ΔFEV_1. Participants whose FEV_1 increased by more than 20mL/year experienced a significantly smaller change in RA_{950} compared to those whose FEV_1 decreased by more than 40mL. Independent samples t-tests indicate a significant difference in the rate of PV_1 progression between COPD groups with and without emphysema, but not VDP or RA_{950}. Emphysema, or COPD phenotype, is related to vascular structure within the lung and the progression of vascular remodelling. Future work should include investigations of sex-differences in airways disease, and the use of machine learning to predict disease progression with optimized CT imaging parameters. (247/250)

Keywords

Obstructive lung disease, chronic obstructive pulmonary disease, hyperpolarized gas lung imaging, ^{3}He MRI, pulmonary vascular structure, remodeling, disease progression, computed tomography

Summary for Lay Audience

Chronic obstructive pulmonary disease (COPD) is a progressive and debilitating disease resulting in chronic cough, breathlessness, activity limitation and reduced lung function. Developments in imaging technology have permitted the evaluation and visualization of the complex effects of COPD within the lung. The ability to predict how a patient's disease will progress is important to managing it. Further, we do not fully understand how the disease develops, progresses, and how to predict who will get worse quickly. We can use MRI ventilation to image the lungs and see where air can or cannot go, which has allowed us to better understand their function. Similarly, measurements of small vessels that may be associated with inflammation, destruction, and disappear with damage, may help us better understand the disease process. We hypothesize that measurements of small blood vessel volume are significantly different in participants without COPD than in those with this disease and related to disease severity. We evaluated 90 participants: 41 ex-smokers without COPD and 49 participants with COPD at baseline and 2.5 years later. Ex-smokers and moderate COPD participants had more emphysema at follow-up, while participants with mild COPD had decreased small vessel volume and no change in emphysema. Both ex-smokers and participants with COPD had less ventilated lung at follow-up. Participants whose clinical measurements of lung function increased from baseline to follow-up experienced an increase in emphysema but significantly less change in small blood vessel volume compared to those whose lung function decreased the most in our sample. Participants with COPD who did not have emphysema experienced a decrease in small vessel volume. Vascular structure within the lung and how it changes with disease appears to be related to emphysema and disease severity. Measuring small vessel volume was more sensitive to changes in clinical lung function than lung ventilation. This research demonstrates that using multiple modalities to evaluate lung disease over time can help researchers and clinicians to better predict a patient's outcome and provide more specific and timely treatment.

(329/350)

Co-Authorship Statement

The following thesis contains one manuscript that has been submitted for publication. As the first author of this work, I was a significant contributor to all aspects of the study as well as manuscript preparation and submission. I was responsible for conception of the study, experimental design, image processing, statistical analyses and interpretation, as well as manuscript preparation and submission. Grace Parraga, as the Principal Investigator and thesis Supervisor, provided continued guidance and was responsible for the conception of the study, experimental design, data interpretation and drafting and approval of manuscripts. She was also the guarantor of the data integrity and responsible for Good Clinical Practice. Patient study visits and acquisition of pulmonary function data were performed under the supervision of Lyndsey Reid-Jones, Rachel Eddy and Danielle Knipping. Polarization of hyperpolarized gas was performed by Andrew Wheatley, Dante PI Capaldi, Heather Young, and Andrew Westcott. MRI acquisition was performed by Trevor Szekeres and David Reese. Below the specific contributions for all co-authors for Chapter 2 are outlined.

Chapter 2 is an original research article entitled "CT pulmonary vessels and MRI ventilation in Chronic Obstructive Pulmonary Disease: Relationship with worsening FEV_1 in the TINCan cohort study" and it was accepted to the journal *Academic Radiology* on March 5th, 2020. The manuscript was coauthored by Rachel Eddy, Jonathan MacNeil, Miranda Kirby, David McCormack, and Grace Parraga. I was responsible for conceptual development, experimental design, image processing, statistical analyses and interpretation, as well as manuscript preparation and submission. Rachel Eddy was responsible for data collection, conceptual development and manuscript revisions, Jonathan MacNeil assisted in data interpretation and manuscript revisions, Miranda Kirby assisted in data interpretation and manuscript revisions, and David McCormack assisted in data interpretation and manuscript revisions.

Acknowledgments

I would first like to thank my supervisor, Grace Parraga. The opportunities you have provided me are incredibly unique; from working on publications, book chapters, presentations and abstracts, to the opportunity to collaborate with colleagues and interact with patients on a daily basis. You have pushed me to grow personally and professionally even more than I could have anticipated through this experience.

I would also like to thank the members of my advisory committee: Jefferson Frisbee, Daniel Goldman and Cory Yamashita, for your support and guidance. The committee meetings were thought provoking and immensely helpful, and I left with many great ideas and the understanding that I had a great deal of support from experts as I completed this project. Further thanks goes to the amazing support of the Medical Biophysics department, including: Kathleen Petts, Wendy Hough, Jefferson Frisbee, Aaron Ward and Jennifer Devlin. The opportunities provided and excellent communication make me confident I was lucky enough to be a part of one of the best departments there is.

A special thank you goes to everyone within the Parraga lab – each and every one of you have made Robarts and our lab an incredibly special place to work. To Lyndsey Reid-Jones, thank you for always keeping it real; I am grateful that I met you here. To Danielle Knipping, thank you for your endless guidance, patience, and for always encouraging me to do all of the things that at one point I did not feel I could. I have learned to approach problems with a lot more confidence and curiosity thanks to you. To Tamas Lindenmaier, thank you for being a friendly and kind support in this lab. Whether it was collecting patient data, fixing my computer, or even just discussing course material, you always found a way to either help me or support me and I very much appreciate that.

To Rachel Eddy, thank you for being my mentor, go-to person, desk buddy, and friend. I respect and admire your kindness, resilience and tenacity when approaching challenges. Whether it was remembering something that I had forgotten, teaching me how to collect patient data, or discussing future plans, you selflessly shared valuable insight and unique ideas. To Jonathan MacNeil, thank you for your willingness to collaborate on projects. Your skills and insight were invaluable to me in getting this project done. Thank you for all of the laughs and puns. To Cathy Ong Ly, thank you for being my first friend here at Western, the best Starbucks buddy, for showing me how to get to class without going outside, and for all of the laughs. I you are the hardest worker that I know. To Andrew Westcott, thank you for being a positive

and caring lab mate and friend. I truly enjoyed all of our conversations about life and science. Thank you for constantly helping me to fix my code after I tried to fix it and made it worse. To Cathy Ong-Ly, thank you for being my first friend here and go-to coffee buddy! I truly enjoyed our time together, and you have shown me how to really think outside the box. To Fabio Salerno, thank you for providing endless insight into the clinical questions and applications of my work; you always left me feeling curious and inspired to learn more. To Maksym Sharma, I always enjoyed a discussion with you about family, school or life. To Alexander Matheson, thank you for teaching me so much about machine learning and physics. I will never look at fun facts the same way after having met you. To Marrissa McIntosh, thank you for your friendship and support. Your maturity and attitude set an example for everyone around you.

To the students of Robarts and Western, thank you for all of the friendships and fun. I am grateful to have met all of you through this experience, and you have all made my time at Western enjoyable and memorable, as well as setting the bar high for everything we do here.

To Kevin Shoemaker, Kim Hellemans, Baraa Al-Khazraji and Matt Holahan, thank you for providing me with such positive academic opportunities and training during my undergraduate years which inspired me to follow in your footsteps.

And finally, thank you to my friends and family outside of Western for checking in on me and supporting me. I feel so lucky to know how many people are on my team. To Natalie and Brendan, thank you for your constant patience, confidence and support. To Joan and Ross, all I can say is that I simply could not have done this without you. Thank you for everything you do to support me.

Table of Contents

List of Tables

List of Figures

List of Appendices

List of Abbreviations

AATD	Alpha-1 Antitrypsin Deficiency
ADC	Apparent Diffusion Coefficient
BL	Baseline
COPD	Chronic Obstructive Pulmonary Disease
CT	Computed Tomography
CSA	Cross-sectional Area
DL_{CO}	Diffusing Capacity for Carbon Monoxide
ES	Ex-smoker
^{19}F	Fluorine-19
FD	Fourier Decomposition
FEV_1	Forced Expiratory Volume in 1 Second
FRC	Functional Residual Capacity
FU	Follow-up
Hb	Hemoglobin
HbO_2	Oxyhemoglobin
$HbCO_2$	Carbaminohemoglobin
^{3}He	Helium-3
HU	Hounsfield Unit
LA	Lumen Area
MRI	Magnetic Resonance Imaging
6MWT	Six Minute Walk Test
PAH	Pulmonary Arterial Hypertension
PFT	Pulmonary Function Test
RA_{950}	Relative Area Under -950 HU
RF	Radiofrequency
RPE	Rating of Perceived Exertion
RV	Residual Volume
SaO_2	Blood Oxygen Saturation
SGRQ	St. George's Respiratory Questionnaire
TCV	Thoracic Cavity Volume
TLC	Total Lung Capacity
TV	Tidal Volume
UTE	Ultra-short Echo Time
VDP	Ventilation Defect Percent
WA	Wall Area
WT	Wall Thickness
^{129}Xe	Xenon-129

CHAPTER 1

1 INTRODUCTION

The lung is a complex organ that allows for the distribution and exchange of gases in and out of the bloodstream for all tissues in the body. In this chapter we will establish the basis for COPD research (1.1), discuss the basic structures within the lung and their function (1.2) followed by an investigation of the consequences of COPD on these structures and overall lung function in section 1.3. Section 1.4 will briefly discuss the significance of disease progression in COPD. In section 1.5, clinical measurements of lung function are discussed, followed by imaging technologies and their applications in the study of COPD (1.6). This chapter serves to establish the background and basis for the following chapters. Finally, the hypothesis and objectives of this thesis are described in section 1.7.

1.1 Motivation and Rationale

Prevalence and Burden

Chronic obstructive pulmonary disease (COPD) is a progressive and debilitating disease resulting in chronic cough, shortness of breath, activity limitation and decreased pulmonary function for those affected. Approximately 2 million Canadians over the age of 35 are currently diagnosed with COPD,[1] and will be a continued burden on the healthcare system[2] due to an aging population with a smoking history and environmental pollution.[1] The major risk factor for developing COPD is tobacco smoke, as approximately 25% of smokers will develop COPD in their lifetime,[3] with a lifetime risk of diagnosis of approximately the same by the age of 80.[4] This lung disease is predominantly considered to be smoking-related, and often affects people who are current or ex-smokers. However, it is possible to also develop COPD based on a genetic mutation[5] or after exposure to environmental or occupational hazards where inhaled particulates can cause lung damage.[6] Women and men are affected in relatively equal proportions.[1]

Patients experience frequent exacerbation leading to hospitalization with COPD being the leading cause of hospitalization in Canada,[7] as is illustrated in **Figure 1.1**. Further, comorbidities such as bronchiectasis increase the morbidity and mortality of COPD.[8] It is challenging to predict which patients will be at risk of disease exacerbation, which can contribute to extended hospital stays, increased morbidity, and increased risk of further exacerbation or death. Disease exacerbation is the most costly to the healthcare system at $10,000 per patient per hospital stay, adding up to an annual cost of over $600 million in Canada.[9] Current diagnostic techniques probe the whole lung and large airways, yet they are insensitive to the regional heterogeneity of disease presentation and progression observed within and between patients;[10] developments to imaging technology have provided sensitive and reliable modalities for evaluating regional lung function, as well as evaluating disease progression.[11]

COPD has historically been considered to have two distinct phenotypes.[12] As our understanding of this disease has developed, we now know that there are multiple disease phenotypes based on the cause of the disease.[1,13,14] Despite this evidence, treatment in the clinical setting is largely focused on symptom management as opposed to disease modifying therapies with a targeted and patient specific approach to the prevention of exacerbation.[6] Accordingly further study of the etiology, progression, and treatment of this disease is crucial in providing targeted, patient centred and specifically effective treatment.

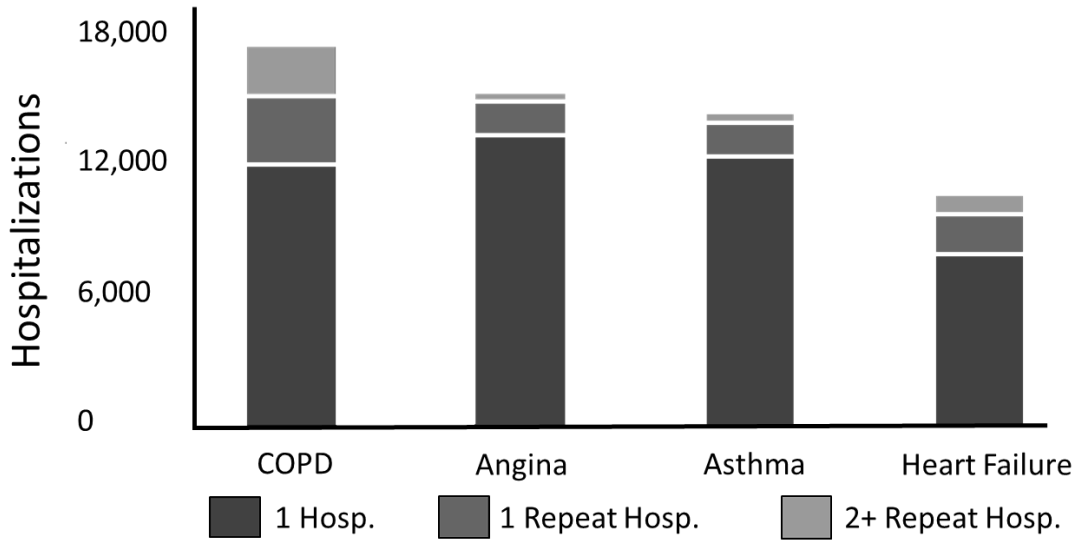

Figure 1.1: Canadian hospitalizations due to COPD.
This figure demonstrates that cases of COPD represent the greatest number of hospitalizations in Canada, more than angina, asthma and heart failure. COPD patients also have more repeated hospitalizations than in other causes. Figure Adapted from Canadian Institute for Health Information, Health Indicators Report 2008.[2]

Gaps in Clinical Measurements

Given the alarming and progressive disease morbidity and burden, there is a specific need to better identify patients at risk of disease development or progression. One way to inform this gap in our understanding of COPD progression is to investigate the role of vascular changes relative to clinical measurements. We understand that COPD is a heterogeneous disease and current clinical diagnostic measurements do not always reflect this variability in symptoms and disease presentation or progression. There is an urgent need to further our understanding of this disease in order to characterize disease phenotypes and ultimately improve treatment and management strategies.

1.2 Structure and Function of the Lung

The purpose of the respiratory system is to facilitate gas exchange by providing oxygen for the blood to circulate to tissues within the body and the removal of gaseous waste products, such as carbon monoxide (CO_2), ultimately maintaining the body's tightly regulated homeostasis. The structure of the lung consists of the airways, parenchyma and vasculature. An organized network of these structures is optimized to allow for efficient and effective

function. In a healthy lung, this process is highly optimized and during daily activities or resting, humans do not use this organ to its fullest capacity.[15] This however, this changes drastically in the context of diseases such as COPD, wherein damage to the parenchyma and airways can result in remodeling and inflammation of these structures with catastrophic and permanent effects on the lung's ability to properly serve its function. In this section, we will discuss the basic structures of the lung and a discussion of how these structures are affected in the context of disease will follow in the next (**1.3**).

1.2.1 Airways

The adult human lung comprises an extensive and highly organized network of airways. The large airways consisting of generations 0 (trachea) to 7. More proximal airways are encompassed by cartilaginous rings which allow them to stay open during the process of ventilation. The airway walls are comprised of a smooth muscle layer, allowing them to dilate or constrict, and which may become inflamed in COPD, restricting airflow.[16] The innermost layer is the airway epithelium which contains cilia that move mucous and dirt out of the airways.[15] The clearance of mucous is an important process in the prevention and removal of airway obstructions which would prevent downstream ventilation and regional loss of function. The main airway bifurcates to each lung, and then each lobe, and finally to each segment. Each segmental bronchus then bifurcates to form sub-segmental bronchi, sub-sub-segmental bronchi, and so on to ventilate 19 distinct bronchopulmonary segments.[15] As is outlined in **Figure 1.2**, the first 16 generations are conducting airways and no gas exchange occurs in this region; conversely, the last 7 are considered to be the respiratory zone of the lung, where gas exchange occurs.[15] The smallest airways, terminal airways, end in alveoli, the site of gas exchange in the lung.

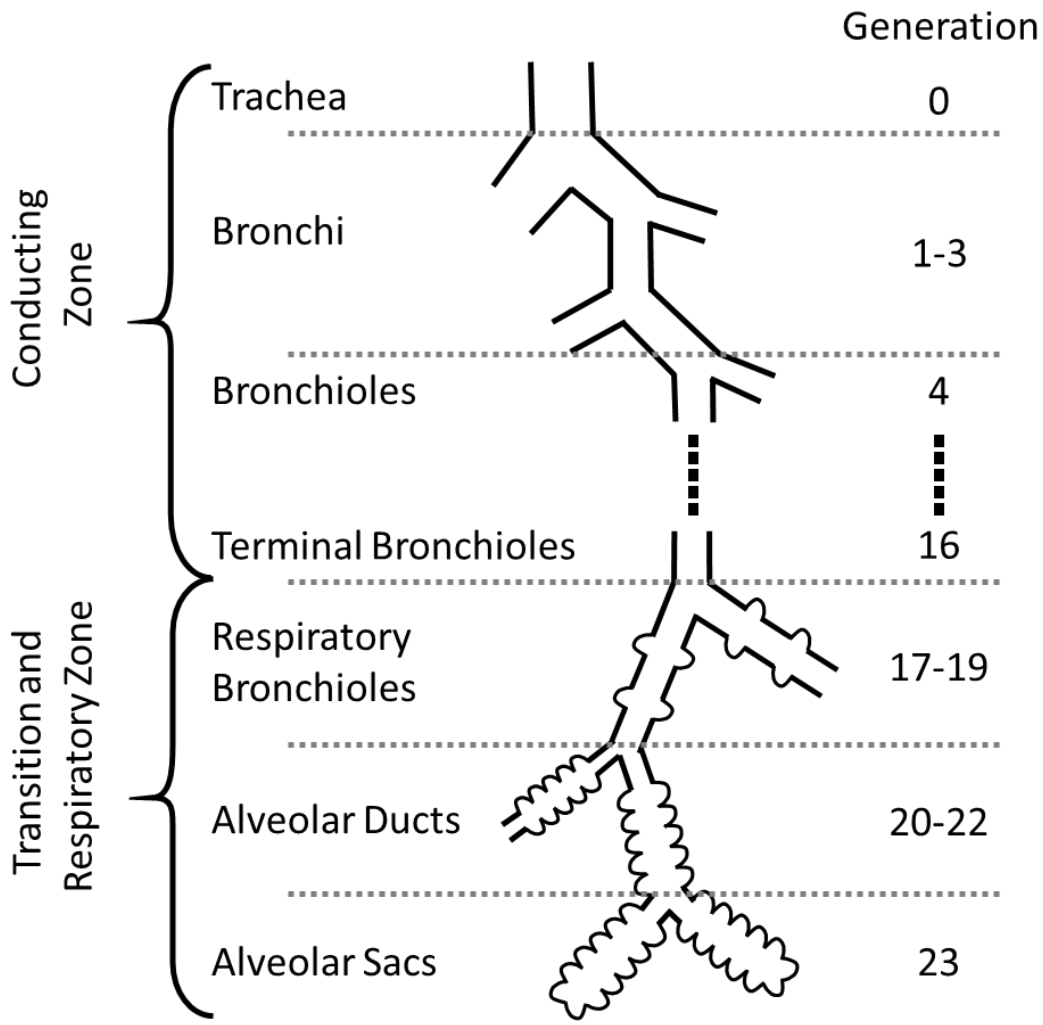

Figure 1.2: Idealized human airway generation diagram.
Adapted from Respiratory Physiology: The Essentials 10th edition.[15]

1.2.2 Parenchyma

In the healthy lung, the parenchyma is made up of approximately 500 million alveoli,[15] which fill with air upon inspiration. At the individual level, each alveolus is a small sac with a wall thickness of one cell, surrounded by a network of capillaries. When filled with air, the laws of partial pressures govern the exchange of gasses across this thin membrane; both oxygen (O_2) and carbon dioxide (CO_2) diffuse down their concentration gradients into and out of the bloodstream, respectively.[15]

1.2.3 Vessels

The pulmonary circulation is comprised of two distinct circuits: bronchial and pulmonary. The bronchial circulation makes up a relatively small volume of the total pulmonary vasculature, approximately 1%,[17] and is responsible for supplying oxygen to the bronchial tree and removing waste products as part of the systemic circulation. This circuit stems from the descending aorta, following the posterior aspect of the bronchial tree. The arteries form a plexus within the muscular layer of the bronchial wall and extending down to the terminal bronchioles. The bronchial venules drain to veins, as illustrated in **Figure 1.5**, which then either flow into the pulmonary circulation via anastomoses.[17]

The pulmonary circulation is that with which we are the most familiar and is fundamentally important as it permits gas exchanged at the alveolus to enter the bloodstream and travel to all tissues in the body. The pulmonary circulation leaves the right ventricle through the pulmonary artery, carrying deoxygenated blood to the lungs for gas exchange to occur. A network of capillaries surrounds each individual alveolus, and following gas exchange, oxygenated blood returns to the left atrium via the pulmonary veins, and leaves the left ventricle via the aorta to circulate through the rest of the systemic circulation.[15]

Within each capillary are a stream of red blood cells containing the protein hemoglobin (Hb) or carbaminohemoglobin ($HbCO_2$). Carbon dioxide is passively unloaded at the capillaries following its concentration gradient and diffusing into the alveolus to be exhaled. Similarly, oxygen diffuses down its concentration gradient into the bloodstream and binds to Hb forming oxyhemoglobin (HbO_2).[15] This process is illustrated in **Figure 1.3**.

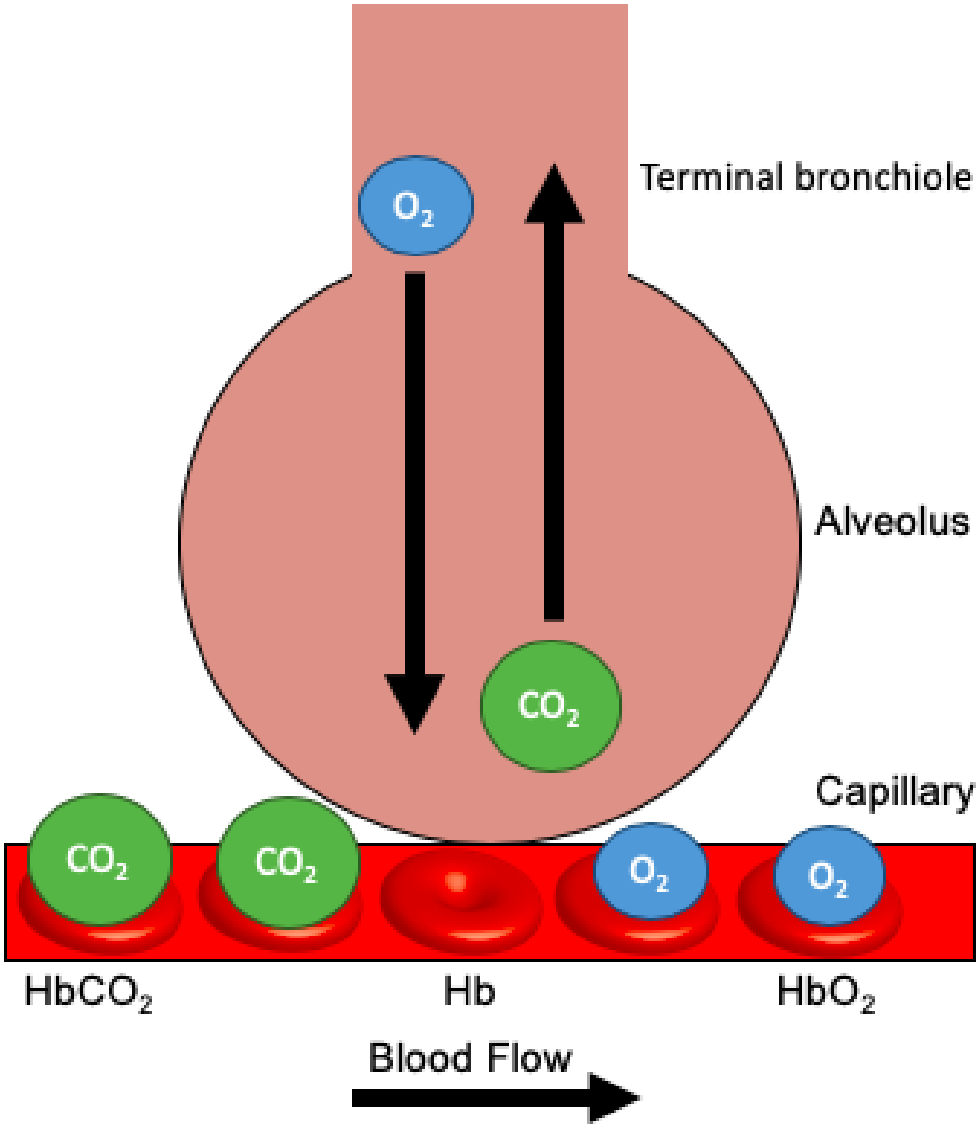

Figure 1.3: Diagram of gas exchange from the alveolus into the pulmonary capillary. This figure illustrates oxygen (blue) entering the alveolus, diffusing across the alveolar capillary membrane into the bloodstream to bind with hemoglobin on red blood cells. Carbon dioxide (green) diffuses from the bloodstream to the alveolus and is removed upon exhalation. Based on Respiratory Physiology: The Essentials 10th edition.[15]
O_2=oxygen, CO_2=carbon dioxide, $HbCO_2$=carbaminohemoglobin, Hb=hemoglobin, HbO_2=oxyhemoglobin.

The pulmonary vessels are important in the context of disease. Muscular arteries consist of a smooth muscle layer which, similar to airways, is able to contract and relax in order to decrease or increase the vascular lumen area. This smooth muscle layer allows for the tightly controlled regulation of blood pressure within the pulmonary circuit. Further,

receptors embedded in the vascular endothelium are sensitive to changes in blood gas concentration and inflammatory signaling molecules from neighbouring or distant tissues. [18] The pulmonary vasculature is an extremely important component in support of proper lung function, and as will be discussed in subsequent sections, is susceptible to changes in the disease state.

1.3 Pathophysiology of Chronic Obstructive Pulmonary Disease

Despite the lungs being over-engineered to facilitate gas exchange, damage can occur to the tissues due to smoking or environmental exposures to toxins that reduce the lung's abilities to properly perform this task. In COPD, this exposure leads to airway remodeling and tissue destruction that increases as the disease progresses.

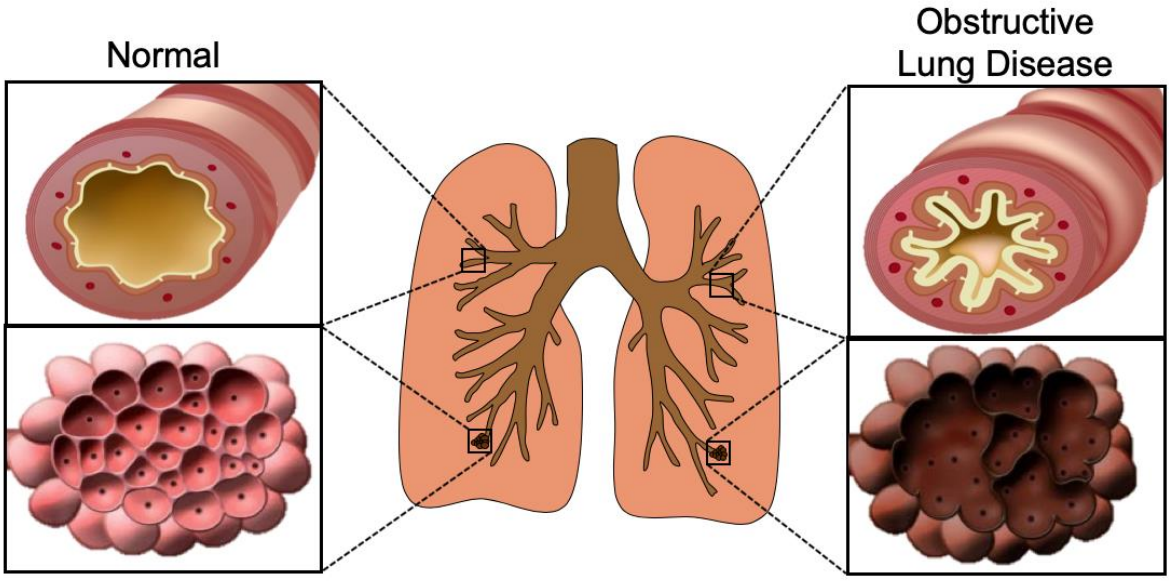

Figure 1.4: Lung parenchyma and airways in healthy lungs and in obstructive lung disease.
The top images in this figure illustrate the airway lumen and wall in a normal healthy lung, as compared to a lung with obstructive lung disease. The airway wall is inflamed, and the lumen is narrowed. The bottom row illustrates the lung parenchyma in healthy cases with many alveoli, as compared to emphysema, which occurs in obstructive lung disease where alveolar walls are destroyed.

1.3.1 Emphysema

In many cases, destruction of alveolar air sacs results in a loss of density within the lung parenchyma termed emphysema. As Illustrated in **Figure 1.4**, this loss of surface area within the lung results in enlarged airspaces, loss of terminal bronchioles, and ultimately a reduced capacity of the lung to exchange gases consistent with the extent of emphysematous lung volume.[12,19]

Three distinct types of emphysema exist, overlap of pathologies in clinical diagnoses with unique aetiologies. Centrilobular is associated with chronic cigarette smoking and is present in the central regions close to the bronchi with normal distal tissue. Panlobular emphysema is present in the lower portions of the lungs and distributed evenly from proximal to distal regions of the lungs; this type of emphysema is most common in alpha-1 antitrypsin deficiency, a genetic mutation that results in the development of emphysema in patients irrespective of smoking history. Finally, paraseptal emphysema is also related to smoking, but can be caused by fibrosis and lung infection as well, and presents as distal or peripheral tissue destruction.[5,20,21] Clinical cases often include multiple pathological presentations of emphysema.[20]

1.3.2 Chronic Bronchitis

Inflammation and obstruction within the airway results in an inflammatory response of the airway smooth muscle, as illustrated in **Figure 1.4**. Chronic bronchitis is the clinical term used to describe symptoms of excessive mucous production, generally as a result of chronic inflammation. Excess mucous can cause airway obstruction and a cough, as well as an inability to ventilate regions of the lung, causing reduced function.[12]

1.3.3 Pulmonary Vascular Remodeling

Late stage COPD can in some cases impair cardiovascular function.[22] Patients with COPD experience a drop in blood oxygen saturation (SaO_2) as their disease progresses and their lungs lose the ability to exchange gases efficiently.[12] In response to low levels of blood oxygen (hypoxia), the pulmonary vasculature constricts in order to optimize

ventilation/perfusion efficiency. In cases of chronic hypoxic vasoconstriction, a subsequent increase in pulmonary arterial pressure becomes pathological. In pulmonary arterial hypertension (PAH), wherein pathological changes within the lung place additional stress on the cardiovascular system, the right ventricular wall is thickened and cardiac function impaired.[23,24] Oxygen therapy is ultimately used in COPD in order to overcome the chronic hypoxemia experienced by patients and to decrease pulmonary arterial pressure.[24,25]

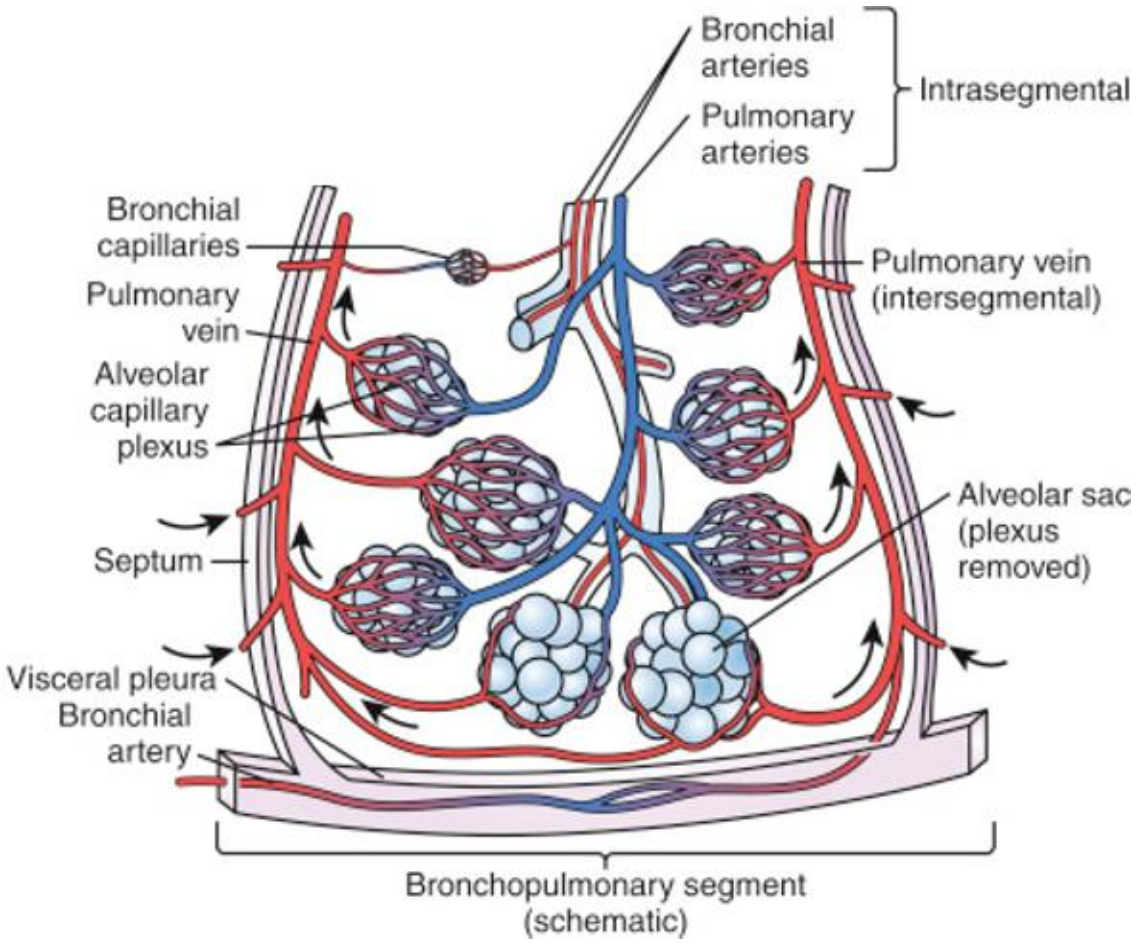

Figure 1.5: **Pulmonary and bronchial vascular structure within the lung.**

This figure illustrates the anatomy of vascular and pulmonary veins and arteries within a single bronchopulmonary segment. Adapted from "Structure and Function of the Respiratory System," Pediatric Critical Care 4th edition. Elsevier 2011.[26] Permission to reproduce is included in **Appendix B.**

The end stage of PAH is termed *cor pulmonale,* and is the result of chronic pulmonary arterial hypertension caused by chronic lung disease.[24] This occurs in approximately 50% of patients; however, the prevalence is challenging to accurately determine.[25] The

consideration of this condition is therefore important to our understanding of the complex interplay between the pulmonary and cardiovascular systems.

While the relationship between vascular remodeling and COPD has been long established,[27-29] there has been a growing interest in the role of imaging the vasculature in COPD,[30,31] and the literature contains a number of more recent studies evaluating small vessel volume in various populations.[32-35] Recent studies have demonstrated that vascular pruning occurs in COPD resulting in a loss of small vessels and decreased vessel density, which has been validated using histology.[36] Cigarette smoke has been identified as a mediator of these changes, and can directly result in vascular remodeling,[33,35] which is consistent with previous work related to the effects of smoking.[29] It has also been hypothesized that airway damage observed in bronchiectasis is driven by remodeling of the pulmonary vasculature.[37] A recent study reported that remodeling of the pulmonary vasculature does progress in direct correlation with emphysema over a two-year follow-up period.[38] Other groups have utilized similar methodology in order to investigate vascular remodeling in lung disease.[39-41]

Histological studies have also been conducted, and have reported bronchial arterial wall hypertrophy;[30] remodeling of the pulmonary vasculature such as wall thickening, lumen narrowing and pruning in COPD have all been published.[22,30] These changes are believed to be attributed to increased inflammatory cytokine signaling within the lung as well as a paradoxically upregulated growth factor signaling.[42]

The detrimental effects of smoking on the lung vasculature have been well characterized. Tobacco smoke can directly affect the vasculature by promoting vascular remodeling.[31] Further, as the alveolar walls are destroyed as in the case of emphysema, destruction of capillary and small arterioles within these tissues are removed as well.[35,36]

Within the clinical setting, cardiovascular comorbidities represent a large proportion of hospitalizations in patients with COPD and contribute to increased morbidity and mortality.[1,22] While this direct relationship is not the focus of this work, it is an important example of the complex relationships between the vascular and pulmonary systems in the disease state. Developing a better understanding of the complex relationships between the

cardiovascular and respiratory systems in the context of COPD serves an unmet clinical need and provides an opportunity for the application of imaging technologies to determine intermediate disease endpoints.

1.4 Disease Progression

Disease progression in COPD can be affected by a number of factors. Firstly, age-related decline in lung function is a normal physiological process, wherein peak lung function is achieved around the age of 25, and declines steadily with age.[43,44] **Figure 1.6** illustrates the effect that tobacco smoking has on this decline, although not all smokers experience the same negative effects, as some are more susceptible to cigarette smoke than others. Disease exacerbation is another factor that can affect the rate of lung function decline, as well as patient quality of life in COPD.[9,11,38,45] The ability to predict whether a patient is at risk of exacerbation or accelerated decline is important to treatment and management strategies. While difficult to predict, this is currently measured using pulmonary function testing and self-assessments of symptoms and quality of life, as discussed in section 1.5.

1.5 Clinical Measures of Global Lung Function

1.5.1 Pulmonary Function Testing

Spirometry

The diagnosis of COPD is based predominantly on pulmonary function testing results. Airflow obstruction can be measured using spirometry. A handheld spirometer is illustrated in **figure 1.7**. Pulmonary function testing results can be reported as absolute values in units of volume, or as a percent predicted (%pred). These predicted values are based on a population mean according to the patients' race, sex, age and height.[46] In considering the forced expiratory volume in one second (FEV_1), this describes the percentage of total lung volume that a person can blow out in the first second of expiration. When divided by the forced vital capacity (FVC), the total amount of air that a person can forcibly expire, the FEV_1/FVC ratio provides a measure of airflow obstruction.[15]

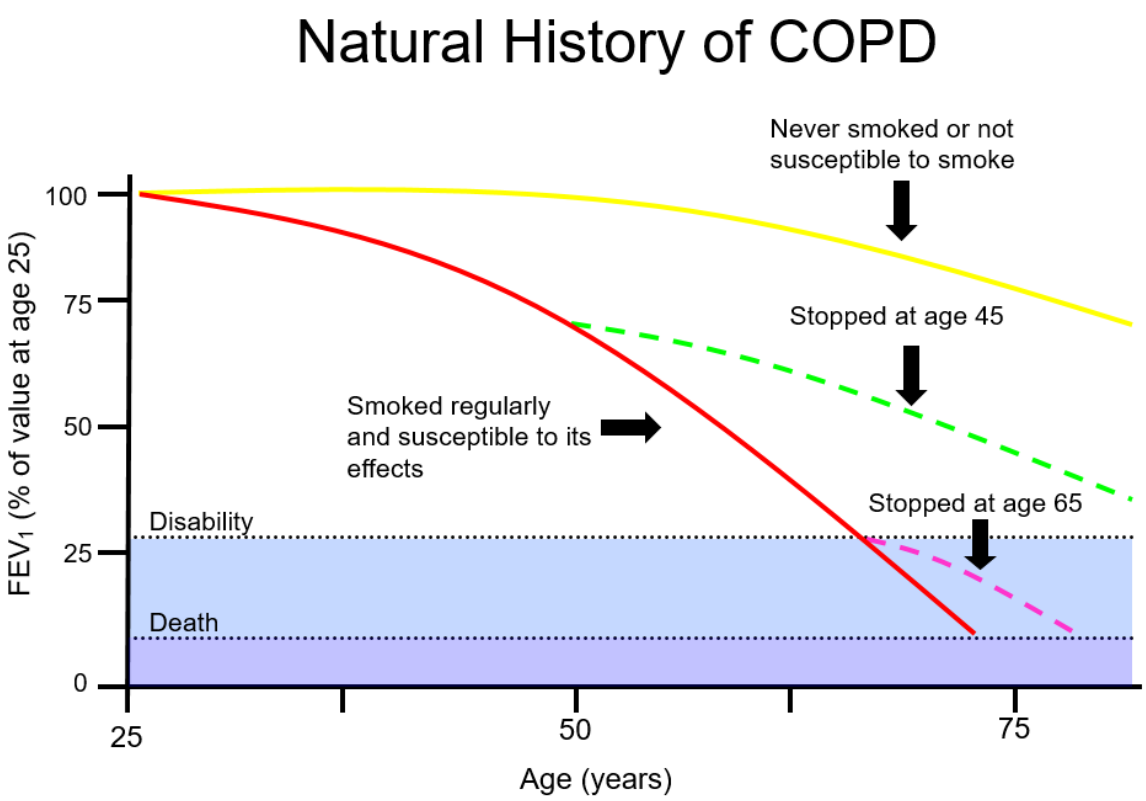

Figure 1.6: Natural history of COPD through the lifespan.

This diagram demonstrates the trajectory of normal age-related decline of lung function in never-smokers (yellow) from its peak at age 25. By contrast, in regular current smokers susceptible to the detrimental effects of tobacco smoke, this decline is accelerated (red) towards disability and death. In ever smokers who quit, this decline can be slowed towards the trajectory of normal decline (green and purple), illustrating the lung's ability to partially recover. Adapted from Fletcher & Peto 1977.[43]

Lung function peaks around the age of 25, and normal lung function decline occurs with age. As is illustrated in **Figure 1.6**, smoking can increase age-related lung function decline. An abnormal ratio of FEV_1/FVC less than 0.70 is indicative of airflow limitation characteristic of COPD.[6] Table 1-1 outlines the pulmonary function testing criteria for the diagnosis and grading of COPD as per the GOLD criteria.[6] Another important component of diagnosing COPD is the investigation of parenchymal tissue integrity, or the presence of emphysema. This can be done by measuring the diffusing capacity of the lung to carbon monoxide (DL_{CO}),[15] the current gold-standard for the assessment of emphysema; this can also be accomplished by imaging the lung using computed tomography[6] as discussed below, and these measurements have been shown to have good agreement.[47]

Figure 1.7: Clinical plethysmography box and handheld spirometer.
Plethysmography box for measuring lung volumes (left) and handheld spirometer.

Diffusing capacity is evaluated using a mixture of gases of a known concentration. This typically consists of a small amount of carbon monoxide (CO) (1-2%), an inert tracer gas such as neon (Ne), and balanced with nitrogen (N_2) and oxygen (O_2).[6,48] The patient inhales the gas mixture, holds their breath for a short amount of time, compared to the amount inhaled, compared to a predicted value and reported as a percentage of that (%pred). A high diffusing capacity is expected in a healthy person, whereas reduced DL_{CO} in COPD indicative of the presence of emphysema.

Pulmonary function testing is also used to classify the severity of a patient's disease according to the Global Initiative for Chronic Lung Disease guidelines, on a scale of 1-4[6], as outlined in **Table 1.1**.

Table 1.1: Pulmonary function testing diagnostic cut-offs from the Global Initiative for Chronic Lung Disease (GOLD).

	FEV_1/FVC	FEV_1
GOLD Grade I	<0.70	>80%
GOLD Grade II	<0.70	$>50\%_{pred}$, $<80\%_{pred}$
GOLD Grade III	<.070	$>30\%_{pred}$, $<50\%_{pred}$
GOLD Grade IV	<0.70	$<30\%_{pred}$

These criteria do not differentiate the relative causes of obstruction, airway inflammation or emphysema, and do not provide information regarding the heterogeneity of the disease throughout the lungs. Additionally, while this process is standardized for reproducible results,[49] assuring good results in children or patients with difficulty following instructions or performing testing to completion may have inaccurate results. In the next section, we will discuss imaging technologies used in order to overcome these limitations.

Plethysmography

Whole body plethysmography may be used to measure lung volumes by applying Boyle's law, which describes the relationships between pressure and volume in a closed system at a constant temperature.[50] In a box of known volume, as illustrated in **Figure 1.7**. when a participant applies pressure by inhaling or exhaling the volume change can be measured and reported.[50] **Figure 1.8** illustrates commonly reported lung volumes.

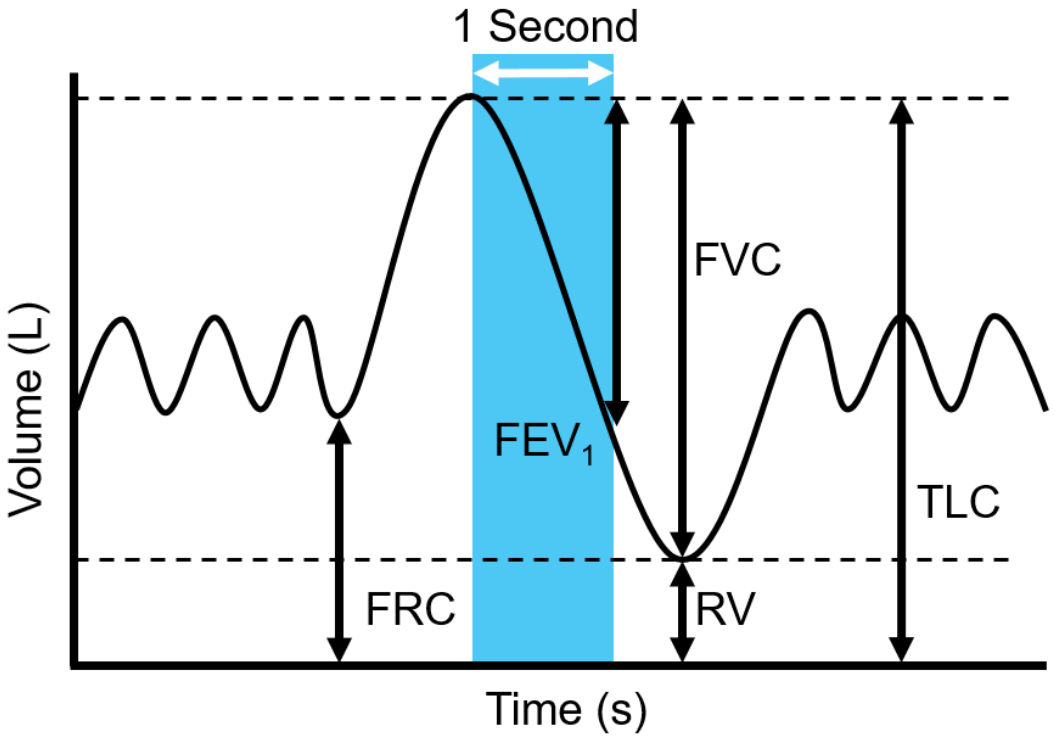

Figure 1.8: Representative schematic of lung volumes during tidal breathing and forced expiration.
This figure illustrates a time-volume graph during a patient's tidal breathing, followed by an inhalation, full expiration, and return to tidal breathing.
FRC=functional residual capacity, FEV_1=forced expiratory volume in 1 second, FVC=forced vital capacity, RV=residual volume, TLC=total lung capacity.

An increase in residual volume occurs in patients with COPD due to parenchymal tissue remodeling, which reduces the lung's elastic properties and make it challenging to expel gas upon exhalation. Further, airway inflammation and obstruction impair the movement of air in but also out of the lungs. Both of these cases result in gas trapping and might lead to characteristic hyperinflation of lung volumes in COPD. This can be observed by increases in both the patient's residual volume (RV) and total lung capacity (TLC), and functional residual capacity (FRC). An increased FRC means that the patient's tidal breathing occurs at volumes closer to TLC than what is observed in a healthy person.

1.5.2 Symptom Reporting

The investigation of COPD impact on quality of life can also be achieved using questionnaires with the aim of establishing the disease burden on the patient. The St.

George's Respiratory Questionnaire is an established tool used in the evaluation of COPD.[51] Questions evaluate the effects of obstructive lung disease on the patients' daily activities including the symptoms that they experience day to day, exacerbations and control of symptoms, as well as activity limitations. The report provides a symptom score, activity score, impact score and total score. A low score is indicative of low burden. A change of 4 points for the total score is the minimum clinically significant indication of a change in symptoms.[52] A limitation of using self-report measures to evaluate chronic disease is the bias introduced by variables that may affect symptom reporting such as the patients' sex.[53] Further, patients with chronic disease may have unconsciously modified their activities in order to manage their disease over time, and may not identify specifically that, for example, they do not take the stairs due to exercise limitations related to their COPD.

It is possible to evaluate a patient's activity limitation by evaluating a patients' rating of perceived exertion (RPE) and dyspnea using the Borg Scale.[54] The RPE scale ranges from 6-20 and uses brief descriptions of each level from 6 "no effort" to 20 "maximum effort". The Borg dyspnea scale is similar, ranging from 0 to 10.[55] This scale is commonly used to evaluate exertion during exercise testing, which is discussed in the following section.

1.5.3 Exercise Testing & Activity Limitation

A more objective method of investigating activity limitation in COPD is the use of exercise testing. The six-minute walk test (6MWT) is a simple measure of sub-maximal exercise capacity. The outcome measure is the distance walked by a patient over 6 minutes, doing laps of a 100 foot (30 meters) straight hallway at their own pace. A clinically important change in this measurement is 70 m in COPD.[56] Sub-maximal exercise testing is well tolerated in in this group, and while other methods of testing exist, the 6MWT was among the most strongly correlated to FEV_1.[57] A limitation of exercise testing to evaluate disease burden is that some patients have physical limitations unrelated to their COPD, for example, a knee or hip replacement, which may reduce their ability to perform the test regardless of disease severity.

Lifestyle changes are recommended as part of managing COPD in the clinical setting, primarily quitting smoking. As is illustrated in **Figure 1.6**, research has demonstrated that some of the damage incurred from chronic tobacco smoking can be reversed and quitting can alter the course of lung decline in smokers.[43] Further, cardio-pulmonary rehabilitation has been shown to improve symptoms in COPD, as well as overall patient quality of life. Maintaining or improving a patient's exercise capacity is an important factor for overall health, as inactivity puts the patient at risk for a number of comorbidities.[1]

1.5.4 Limitations of pulmonary function testing and the role of imaging

While the assessments of lung function, symptom reporting, and exercise capacity discussed above are well understood within the clinical setting, they are limited by the fact that they provide general information only. By contrast, imaging measurements provide regional information about the lung's structure and function, which can be assessed both qualitatively and quantitatively. In section **1.6**, we will explore various imaging technologies applied in lung imaging, including structural methods (1.6.1) such as x-ray, computed tomography, and proton magnetic resonance imaging (MRI). Additionally, we will explore quantitative analysis techniques (1.6.2) applied in COPD, including hyperpolarized gas MRI, ultra-short echo time and Fourier decomposition MRI. Imaging technologies better characterize the heterogeneity of disease presentation within a single patient and have been established as sensitive and reliable measurement tools which correlate with global assessments. These technologies have benefits and downsides and will be discussed in detail below. The application of imaging technologies in the study of COPD is imperative to the overarching goal of this thesis.

1.6 Imaging Pulmonary Structure and Function

1.6.1 Structural and Anatomical Imaging

Planar X-ray

The most commonly available imaging modality for chest imaging is planar x-ray, or projectional radiography. This imaging techniques functions by sending x-rays from a

source, through the sample and the x-ray attenuation is measured by a detector. The resulting imaging is a two-dimensional reconstruction of the sample, as demonstrated in **Figure 1.9**. Benefits of this technique is that it provides a good image resolution, and is abundantly available in the clinical setting.[58]

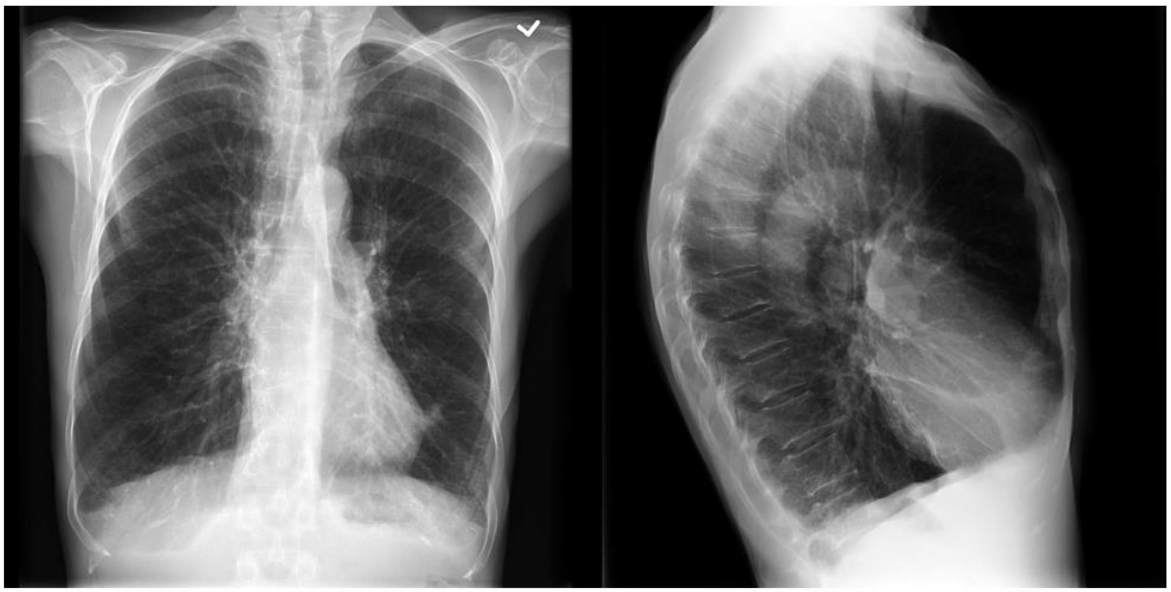

Figure 1.9: Chest x-ray in a patient with COPD showing lung hyperinflation as a result of emphysema.
A flattened diaphragm is a common sign of lung hyperinflation in COPD. Case courtesy of A. Prof Frank Gaillard, Radiopaedia.org, rID: 8512. CC BY-NC-SA 3.0 License (Creative Commons) information is included in **Appendix B**

Computed Tomography

Computed tomography (CT) has been used to image the chest and lungs since the late 1970's.[59,60] Based on known linear attenuation coefficients, researchers soon determined that emphysematous regions of the lung could be easily visualized using chest CT,[61] and that the presence of emphysema correlated with pulmonary function measurements.[19,61]

High resolution CT (HRCT) is the current gold-standard of lung imaging for the clinical setting. It provides high resolution structural information, giving precise and detailed insight into structures such as the airways, vessels, and parenchymal tissue integrity. Attenuation coefficients are measured based on density, wherein -1000 Hounsfield units (HU) indicates the presence of air and 0 HU establishes the presence of water. The attenuation of emphysematous or low density lung tissue is therefore close to that of air,

and the most commonly reported threshold is -950 HU,[62] although -910 is sometimes used.[63] A chest CT in an ex-smoker, as well as participants with COPD are shown in **Figure 1.10**. A major benefit to using CT imaging is that the spatial resolution is exceptionally high compared to other imaging modalities. A limitation of using CT is of course the radiation dose associated with imaging. The low-dose, high resolution CT protocol used in our lab gives a dose of 1.8 mSv to the patient. Micro-CT images have been acquired in order to measure the airways and vasculature; however, this method is only indicated in ex-vivo or animal studies.

The ability to quantify and measure structures and volumes of the lungs has become an important tool for the diagnosis and monitoring of lung disease. Quantitative CT analysis has been used to investigate changes in parenchyma, airway and vessels count, number and density in COPD[33,37,64] leading to increased application of this method in the clinical setting.[65] Analysis of airways count and measurements,[64] low attenuating area, low attenuating clusters,[38] blood vessel density and volume,[34,36] peripheral vessel volume and cross-sectional area[33,35] have all been reported in COPD from clinical CT, and are illustrated in **Figure 1.10**. Measurements such as airway wall thickness (WT, mm) and lumen area (LA, mm^2) can be measured from the cross-section of an airway in a CT image. Normal lung tissue has an attenuation threshold of approximately -700 HU. Emphysematous lung volume is calculated by dividing the volume of lung attenuating below -950 HU by the total lung volume (RA_{-950}). Gas trapping may also be measured using CT, as trapped tissue is less dense, but is denser than emphysematous lung regions. The most broadly accepted threshold is of -856 HU.[66]

Blood vessel volume can be calculated using a combination of density threshold method followed by a circularity filter and line-tracing algorithm to assure continuity.[67] More recent methods have taken advantage of machine learning methods.[39,68,69] Studies have reported increased volumes of emphysematous tissues within the lungs of patients with COPD, and these levels correlate with the severity of the patient's disease.[20] Studies investigating changes in the airways of patients with COPD have identified that the airway walls of COPD patients are thicker than those of healthy controls,[70] and when counted, have reduced numbers in relation to the patient's disease severity.[64] Analysis techniques

for vascular structure have been used to evaluate the relationship between CT emphysema, pulmonary arterial pressure,[31] and small vessel cross-sectional area ($CSA_{5\%}$).[38] The authors determined that vascular pruning, or a loss of small vessels within the lung, is related to the extent of emphysema within the lung and also related to increased pulmonary arterial pressure, indicative of vascular disease.[31]

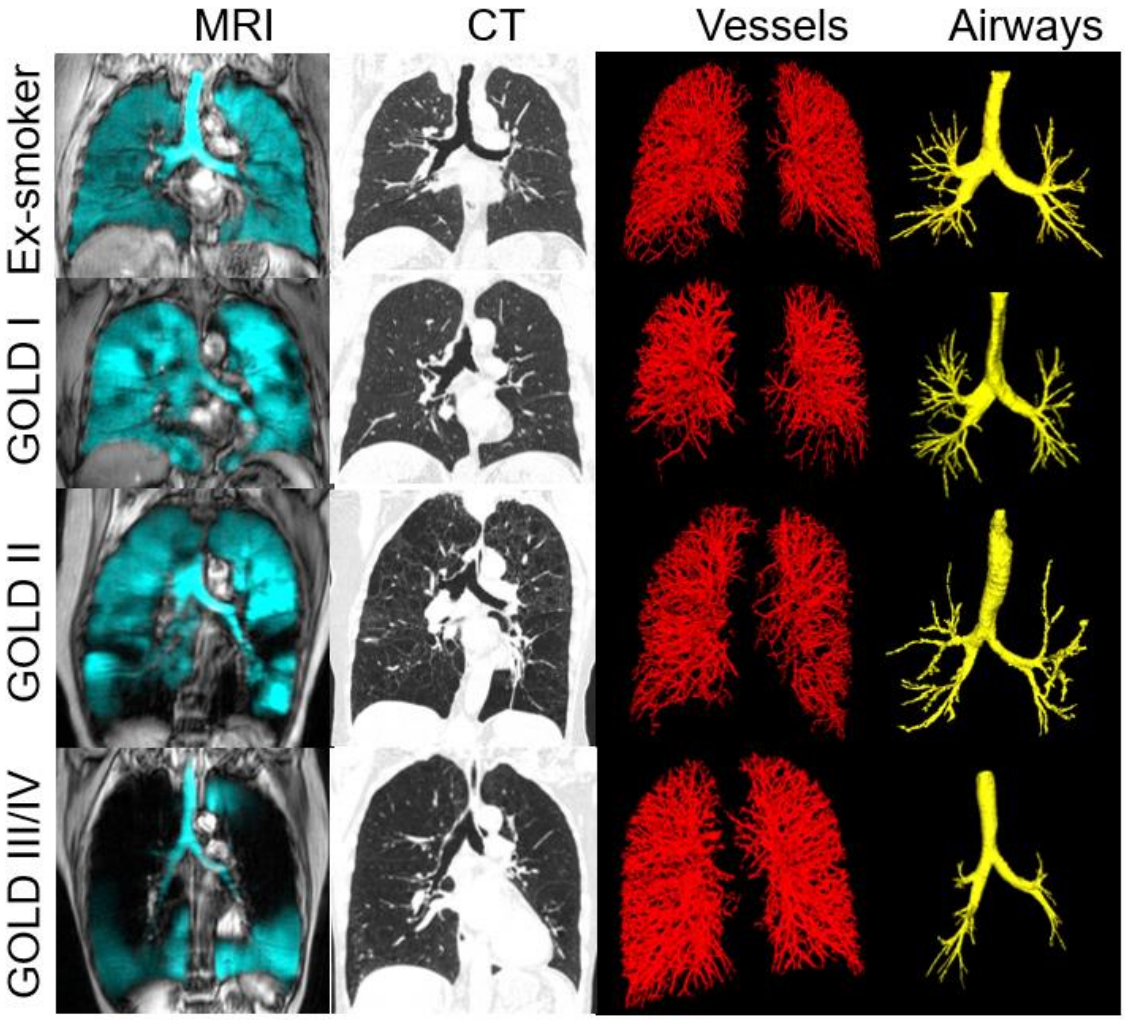

Figure 1.10: ^{3}He MRI and computed tomography images and 3D models of vascular structure and airways in an ex-smoker without COPD as well as participants COPD. Left panel: chest CT in an ex-smoker without COPD, as well as representative participants with GOLD I, II and III/IV COPD. Middle panel: 3D rendering of vascular trees. Right panel: 3D rendering of airway trees demonstrating a decrease in the number of airways with increasing disease severity.
Ex-smoker: 80-year-old male, VDP=4%, RA_{950}=1%, TBV=151mL; GOLD I: 67-year-old male, VDP=8% RA_{950}=2%, TBV=115mL; GOLD II: 60-year-old female, VDP=16% RA_{950}=27%, TBV=106mL; GOLD IV: 68-year-old female, VDP=34%, RA_{950}=33%, TBV=162mL.

GOLD=global initiative for obstructive lung disease, 3D=three dimensional, CT=computed tomography, VDP=ventilation defect percent, RA_{950}=relative area of the lung with attenuation below -950 HU, TBV=total blood volume.

While the consequences of disease on these organs are relatively well characterized, only recently have researchers begun to explore how imaging can be used to detect pulmonary vascular remodeling as a biomarker for disease stage or progression. Advances in both high resolution and functional image acquisition techniques as well as advanced image analysis methodologies have provided the opportunity to quantitatively evaluate vascular structures within the lungs, and how it relates to lung function, something that was previously next to impossible to accomplish.[71] These techniques will be discussed further in section 1.5.1.

Parametric response mapping has emerged as a technique that applies multiple methods of quantitative CT analysis in order to elucidate multiple COPD phenotypes. By acquiring inspiration-expiration CT scans and generating voxel-wise maps of emphysema, gas trapping, and functional small airways disease, researchers were able to identify relative volumes of each in participants with COPD.[72,73] Parametric response mapping has been utilized in order to elucidate multiple imaging phenotypes of COPD.

Proton Magnetic Resonance Imaging

It is possible to image the lungs using magnetic resonance imaging (MRI), however due to extensive air-tissue interfaces, it is challenging to acquire images with adequate signal, and tissue destruction due to disease leaves even less tissue to image. This is due to a rapid loss of signal following the radio frequency (RF) pulse. A benefit of using MRI is that this method does not deliver any radiation dose to the patient, and therefore is ideal for longitudinal studies. Beyond the technical limitations with this technique, access and cost are also barriers to its widespread application in the clinical setting.

Ultra-short Echo Time

Ultrashort echo time (UTE) MR imaging can be used to acquire very high-resolution images that provide better resolution than conventional proton MR techniques. This is accomplished by using a very small flip-angle and a short echo time (TE). A short TE means that there is very short relaxation time that overcomes the rapid signal decay due to

air-tissue interfaces within the lungs.[74] This method provides images with signal intensity values which are directly related to tissue density.[75]

1.6.2 Functional Imaging

Hyperpolarized Gas Magnetic Resonance Imaging

In order to overcome the limitations of proton MRI, hyperpolarized noble gas MR imaging may be used to measure ventilation within the lungs. Gasses, such as helium-3 (^{3}He) and xenon-129 (^{129}Xe) are stable isotopes that can be hyperpolarized in order to increase their MR signal.[74,76] Hyperpolarized gas images are acquired during a single breath-hold and are well tolerated by patients.[77-80] Gas images are superimposed onto proton images at the same lung volume for anatomical reference.[81] This was first accomplished in 1994 using ^{129}Xe, a safe general anesthetic, in the mouse lungs,[82] and shortly thereafter in humans;[83] however, the field quickly switched to ^{3}He imaging. While ^{3}He has a greater gyromagnetic ratio and provides greater signal in imaging, ^{129}Xe is less expensive and a far more abundant resource,[74] and therefore the field has transitioned back to ^{129}Xe imaging.[84]

Dynamic wash-in and wash-out methods have been used in both healthy and diseased lungs. The theory behind this technique is that regions that might appear as ventilation defects on a single breath-hold MR image are regions with slower time constants for filling than in a single breath-hold due to tissue properties or airflow obstructions,[85] and therefore the ventilation of partially obstructed regions may be investigated. This can be accomplished using hyperpolarized gas such as ^{3}He or ^{129}Xe, or fluorinated gas.[86,87] This technique is accomplished by administering a known amount of hyperpolarized gas over time using either the wash-in or wash-out methods, and reporting ventilation defect percent as well as wash-in/out time.[85,88] This method is less clinically applicable due to the extended imaging time and doses of gas required,[88] however, could provide valuable information regarding tissue properties and gas trapping.[89]

Single breath-hold MRI of the lung has been extensively used in the study of COPD.[90,91] There is strong agreement between CT measurements of emphysema, pulmonary function testing and MRI ventilation defect percent (VDP),[11,92] wherein participants with decreased

pulmonary function testing measured using spirometry have increased VDP.[11] MRI has been used by our group to evaluate disease progression in COPD, and these measurements are importantly related to, and sensitive to changes in, participants' self-reported quality of life.[11,92] Upon imaging, bright areas are regions that are filled with gas, whereas dark areas are termed ventilation defects as can be visualized in **Figure 1.10**. This can be expressed as a percent of the total lung area that is not ventilated, known as the VDP. The minimal clinically important difference in VDP using ^{3}He MRI is of 2% or 110mL.[93] This is important for evaluating a change in disease severity in patients in longitudinal studies or for evaluating a treatment response.

Despite the shortcomings of conventional proton MR imaging for generating tissue signal within the lung, hyperpolarized gas MRI can be used to assess tissue integrity using the apparent diffusion coefficient (ADC). Measured in units of cm^2/s, ADC provides a measure of the distance a gas particle travels within the lung in a certain period of time. In healthy lung tissues, alveoli and alveolar septa divide the parenchymal space into extremely small compartments that limit the movement of any individual gas particle. When alveolar walls and septa are destroyed, as is in the case of emphysema, the gas particles are free to travel further distances within the lung in a similar amount of time, producing a high ADC value.[78,94] This technique is exciting due its application as an indirect spatial measurement of emphysema within the lung without exposure to ionizing radiation.[95] A limitation of the ADC technique is that it is impossible to evaluate tissue integrity for regions of the lung that are not ventilated, as no gas is able to travel there and no coefficient can be generated.

Xenon Dissolved-phase MRI

Xenon gas, unlike helium and fluorine, is uniquely able to diffuse into the blood stream. Single breath-hold ^{129}Xe imaging therefore allows for measurements of both regional lung ventilation as well as gas exchange; when this gas diffuses into the bloodstream it is associated with a chemical shift that can be differentiated from the gas phase Xe within the lungs.[89] This method provides a measurement not only of how well the lungs are ventilated upon inhalation, but also of how well ventilated regions are able to exchange gases at the alveolar-capillary level.

Fourier Decomposition MRI

Fourier decomposition (FD) MRI is a technique that provides a voxel-wise map of ventilation and perfusion within the lung. A frequency signal for blood flow according to the cardiac rhythm, as well as for the respiratory rate is generated within in each voxel. In collecting a time series of images of the lungs, ventilation and perfusion maps can be generated based on mean signal intensity over a period of minutes.[96] This method has recently been compared to ^{19}F washout MRI in patients with COPD. The authors demonstrated that FD-MRI correlated strongly with pulmonary function testing measurements as well as washout results.[97] This method has also been compared to ^{3}He MR imaging with good agreement.[98]

Summary

Overall, imaging technologies provide important structural and functional information that allows a deeper understanding of the heterogeneity of lung disease within a single patient. Various structural and functional modalities exist, each with benefits and downsides. When combined with clinical measures of lung function, we can gain insight which is clinically understood and grounded in the clinical setting, while improving the information available to physicians and researchers, allowing the identification of novel endpoints and biomarkers in COPD.

1.7 Thesis Objectives and Hypotheses

COPD is a chronic, debilitating and irreversible disease, with a significant economic burden, and for which disease exacerbation is related to increased morbidity and mortality.[6] Although the role of vascular remodeling,[17,22-24,31] angiogenesis[18,30,42] and pruning in COPD[32,35,36] have been explored, recent work has demonstrated the potential for CT vascular structure as a biomarker of disease severity and progression.[38] The relationship of CT vascular measurements with and lung ventilation has, to our knowledge, yet to be elucidated.

The overarching objective of this thesis is to explore the role of vascular structure and how it relates to established measures of lung structure and function in a unique dataset. Specifically, we aim to:

1) To compare CT blood vessel volume measurements in ex-smokers without COPD and those with mild, moderate, and severe disease,

2) To evaluate relationships between imaging and clinical biomarkers of chronic obstructive pulmonary disease, and

3) To investigate disease progression in COPD using multimodality imaging.

We hypothesize that CT blood vessel volume measurements are significantly different in ex-smokers without COPD than in those with this disease, and that CT blood vessel measurements are strongly and significantly related to MRI ventilation in ex-smokers. This work will conclude with a discussion both the impact and limitations of this work and will explore potential future directions.

1.8 References

1 Bartholemew, S., Desjardins, S., Ellison, J., Evans, J., Gabora, N., Jun Gao, Y., Gilbert, C., et al. (ed Public Health Agency of Canada (PHAC)) (Government of Canada, Canada, 2018).

2 CIHI. (Canadian Institute of Health Indicators, Ottawa, 2008).

3 Lokke, A., Lange, P., Scharling, H., Fabricius, P. & Vestbo, J. Developing COPD: a 25 year follow up study of the general population. *Thorax* **61**, 935-939, doi:10.1136/thx.2006.062802 (2006).

4 Gershon, A. S., Warner, L., Cascagnette, P., Victor, J. C. & To, T. Lifetime risk of developing chronic obstructive pulmonary disease: a longitudinal population study. *Lancet* **378**, 991-996, doi:10.1016/s0140-6736(11)60990-2 (2011).

5 Thurlbeck, W. M. & Muller, N. L. Emphysema: definition, imaging, and quantification. *AJR Am J Roentgenol* **163**, 1017-1025, doi:10.2214/ajr.163.5.7976869 (1994).

6 GOLD. Global Strategy for the Diagnosis, Management and Prevention of Chronic Obstructive Pulmonary Disease. (2017).

7 Evans, J., Chen, Y., Camp, P. G., Bowie, D. M. & McRae, L. Estimating the prevalence of COPD in Canada: Reported diagnosis versus measured airflow obstruction. *Health Rep* **25**, 3-11 (2014).

8 Patel, I. S. *et al.* Bronchiectasis, exacerbation indices, and inflammation in chronic obstructive pulmonary disease. *Am J Respir Crit Care Med* **170**, 400-407, doi:10.1164/rccm.200305-648OC (2004).

9 Mittmann, N. *et al.* The cost of moderate and severe COPD exacerbations to the Canadian healthcare system. *Respir Med* **102**, 413-421, doi:10.1016/j.rmed.2007.10.010 (2008).

10 Kirby, M. *et al.* COPD: Do Imaging Measurements of Emphysema and Airway Disease Explain Symptoms and Exercise Capacity? *Radiology* **277**, 872-880, doi:10.1148/radiol.2015150037 (2015).

11 Kirby, M. *et al.* MRI ventilation abnormalities predict quality-of-life and lung function changes in mild-to-moderate COPD: longitudinal TINCan study. *Thorax* **72**, 475-477, doi:10.1136/thoraxjnl-2016-209770 (2017).

12 West, J. B. *Respiratory Pathophysiology: The Essentials*. 3rd edn, (Williams & Wilkins, 1987).

13 Galban, C. J. *et al.* Computed tomography-based biomarker provides unique signature for diagnosis of COPD phenotypes and disease progression. *Nat Med* **18**, 1711-1715, doi:10.1038/nm.2971 (2012).

14 Han, M. K. *et al.* Chronic obstructive pulmonary disease phenotypes: the future of COPD. *Am J Respir Crit Care Med* **182**, 598-604 (2010).

15 West, J. B., Luks, A.M. *Respiratory Physiology: The Essentials*. 10th edn, 238 (Wolters Kluwer, 2016).

16 Jeffery, P. K. Remodeling in asthma and chronic obstructive lung disease. *Am J Respir Crit Care Med* **164**, S28-38, doi:10.1164/ajrccm.164.supplement_2.2106061 (2001).

17 Kumar, A., Raju, S., Das, A. & Mehta, A. C. Vessels of the Central Airways: A Bronchoscopic Perspective. *Chest* **149**, 869-881, doi:10.1016/j.chest.2015.12.003 (2016).

18 Zanini, A., Chetta, A. & Olivieri, D. Therapeutic perspectives in bronchial vascular remodeling in COPD. *Ther Adv Respir Dis* **2**, 179-187, doi:10.1177/1753465808092339 (2008).

19 Bergin, C. *et al.* The diagnosis of emphysema. A computed tomographic-pathologic correlation. *Am Rev Respir Dis* **133**, 541-546, doi:10.1164/arrd.1986.133.4.541 (1986).

20 Smith, B. M. *et al.* Pulmonary emphysema subtypes on computed tomography: the MESA COPD study. *Am J Med* **127**, 94 e97-23, doi:10.1016/j.amjmed.2013.09.020 (2014).

21 Takahashi, M. *et al.* Imaging of pulmonary emphysema: a pictorial review. *Int J Chron Obstruct Pulmon Dis* **3**, 193-204, doi:10.2147/copd.s2639 (2008).

22 Barbera, J. A. Mechanisms of development of chronic obstructive pulmonary disease-associated pulmonary hypertension. *Pulm Circ* **3**, 160-164, doi:10.4103/2045-8932.109949 (2013).

23 Dunham-Snary, K. J. *et al.* Hypoxic Pulmonary Vasoconstriction: From Molecular Mechanisms to Medicine. *Chest* **151**, 181-192, doi:https://doi.org/10.1016/j.chest.2016.09.001 (2017).

24 Lai, Y. C., Potoka, K. C., Champion, H. C., Mora, A. L. & Gladwin, M. T. Pulmonary arterial hypertension: the clinical syndrome. *Circ Res* **115**, 115-130, doi:10.1161/circresaha.115.301146 (2014).

25 Shujaat, A., Minkin, R. & Eden, E. Pulmonary hypertension and chronic cor pulmonale in COPD. *Int J Chron Obstruct Pulmon Dis* **2**, 273-282 (2007).

26 Fuhrman, B. P. & Zimmerman, J. J. *Pediatric Critical Care E-Book*. (Elsevier Health Sciences, 2011).

27 Wright, J. L. *et al.* The structure and function of the pulmonary vasculature in mild chronic obstructive pulmonary disease. The effect of oxygen and exercise. *Am Rev Respir Dis* **128**, 702-707, doi:10.1164/arrd.1983.128.4.702 (1983).

28 Weitzenblum, E., Schrijen, F., Mohan-Kumar, T., Colas des Francs, V. & Lockhart, A. Variability of the pulmonary vascular response to acute hypoxia in chronic bronchitis. *Chest* **94**, 772-778, doi:10.1378/chest.94.4.772 (1988).

29 Santos, S. *et al.* Characterization of pulmonary vascular remodelling in smokers and patients with mild COPD. *Eur Respir J* **19**, 632-638, doi:10.1183/09031936.02.00245902 (2002).

30 Zanini, A., Chetta, A., Imperatori, A. S., Spanevello, A. & Olivieri, D. The role of the bronchial microvasculature in the airway remodelling in asthma and COPD. *Respir Res* **11**, 132, doi:10.1186/1465-9921-11-132 (2010).

31 Matsuoka, S. *et al.* Quantitative CT measurement of cross-sectional area of small pulmonary vessel in COPD: correlations with emphysema and airflow limitation. *Acad Radiol* **17**, 93-99, doi:10.1016/j.acra.2009.07.022 (2010).

32 Diaz, A. A. *et al.* Pulmonary vascular pruning in smokers with bronchiectasis. *ERJ Open Res* **4**, doi:10.1183/23120541.00044-2018 (2018).

33 Diaz, A. A. *et al.* Quantitative CT Measures of Bronchiectasis in Smokers. *Chest* **151**, 1255-1262, doi:10.1016/j.chest.2016.11.024 (2017).

34 Synn, A. J. *et al.* Radiographic pulmonary vessel volume, lung function and airways disease in the Framingham Heart Study. *Eur Respir J* **54**, doi:10.1183/13993003.00408-2019 (2019).

35 Estepar, R. S. *et al.* Computed tomographic measures of pulmonary vascular morphology in smokers and their clinical implications. *Am J Respir Crit Care Med* **188**, 231-239, doi:10.1164/rccm.201301-0162OC (2013).

36 Rahaghi, F. N. *et al.* Pulmonary vascular density: comparison of findings on computed tomography imaging with histology. *Eur Respir J* **54**, doi:10.1183/13993003.00370-2019 (2019).

37 Diaz, A. A. *et al.* Bronchoarterial ratio in never-smokers adults: Implications for bronchial dilation definition. *Respirology* **22**, 108-113, doi:10.1111/resp.12875 (2017).

38 Takayanagi, S. *et al.* Longitudinal changes in structural abnormalities using MDCT in COPD: do the CT measurements of airway wall thickness and small pulmonary

vessels change in parallel with emphysematous progression? *Int J Chron Obstruct Pulmon Dis* **12**, 551-560, doi:10.2147/copd.s121405 (2017).

39 Jin, D. *et al.* A semi-automatic framework of measuring pulmonary arterial metrics at anatomic airway locations using CT imaging. *Proc SPIE Int Soc Opt Eng* **9788**, doi:10.1117/12.2216558 (2016).

40 Rahaghi, F. N. *et al.* Quantification of the Pulmonary Vascular Response to Inhaled Nitric Oxide Using Noncontrast Computed Tomography Imaging. *Circ Cardiovasc Imaging* **12**, e008338, doi:10.1161/circimaging.118.008338 (2019).

41 Iyer, K. S. *et al.* Quantitative Dual-Energy Computed Tomography Supports a Vascular Etiology of Smoking-induced Inflammatory Lung Disease. *Am J Respir Crit Care Med* **193**, 652-661, doi:10.1164/rccm.201506-1196OC (2016).

42 Voelkel, N. F., Gomez-Arroyo, J. & Mizuno, S. COPD/emphysema: The vascular story. *Pulm Circ* **1**, 320-326, doi:10.4103/2045-8932.87295 (2011).

43 Fletcher, C. & Peto, R. The natural history of chronic airflow obstruction. *Br Med J* **1**, 1645-1648, doi:10.1136/bmj.1.6077.1645 (1977).

44 Jones, P. W. Health status and the spiral of decline. *COPD* **6**, 59-63, doi:10.1080/15412550802587943 (2009).

45 Vestbo, J. *et al.* Evaluation of COPD Longitudinally to Identify Predictive Surrogate Endpoints (ECLIPSE). *Eur Respir J*, doi:10.1183/09031936.00111707 (2008).

46 Quanjer, P. H. *et al.* (Eur Respiratory Soc, 2012).

47 Grydeland, T. B. *et al.* Quantitative CT measures of emphysema and airway wall thickness are related to D(L)CO. *Respir Med* **105**, 343-351, doi:10.1016/j.rmed.2010.10.018 (2011).

48 Brusasco, V., Crapo, R. & Viegi, G. Coming together: the ATS/ERS consensus on clinical pulmonary function testing. *Eur Respir J* **26**, 1-2, doi:10.1183/09031936.05.00034205 (2005).

49 Miller, M. R. *et al.* Standardisation of spirometry. *Eur Respir J* **26**, 319-338, doi:10.1183/09031936.05.00034805 (2005).

50 Quanjer, P. H. *et al.* (Eur Respiratory Soc, 1993).

51 Jones, P. W., Quirk, F. H., Baveystock, C. M. & Littlejohns, P. A self-complete measure of health status for chronic airflow limitation. The St. George's Respiratory Questionnaire. *Am Rev Respir Dis* **145**, 1321-1327, doi:10.1164/ajrccm/145.6.1321 (1992).

52 Jones, P. W. St. George's Respiratory Questionnaire: MCID. *COPD* **2**, 75-79, doi:10.1081/copd-200050513 (2005).

53 Raghavan, D. & Jain, R. Increasing awareness of sex differences in airway diseases. *Respirology* **21**, 449-459, doi:10.1111/resp.12702 (2016).

54 Borg, G. *Borg's perceived exertion and pain scales*. (Human kinetics, 1998).

55 Kendrick, K. R., Baxi, S. C. & Smith, R. M. Usefulness of the modified 0-10 Borg scale in assessing the degree of dyspnea in patients with COPD and asthma. *J Emerg Nurs* **26**, 216-222, doi:10.1016/s0099-1767(00)90093-x (2000).

56 ATS statement: guidelines for the six-minute walk test. *Am J Respir Crit Care Med* **166**, 111-117, doi:10.1164/ajrccm.166.1.at1102 (2002).

57 Bell, M. *et al.* Systematic Review of the Association Between Laboratory- and Field-Based Exercise Tests and Lung Function in Patients with Chronic Obstructive Pulmonary Disease. *Chronic Obstr Pulm Dis* **2**, 321-342, doi:10.15326/jcopdf.2.4.2014.0157 (2015).

58 Busch, H. Digital radiography for clinical applications. *European radiology* **7**, S66-S72 (1997).

59 Jost, R. G., Sagel, S. S., Stanley, R. J. & Levitt, R. G. Computed tomography of the thorax. *Radiology* **126**, 125-136, doi:10.1148/126.1.125 (1978).

60 Rosenblum, L. J. *et al.* Computed tomography of the lung. *Radiology* **129**, 521-524, doi:10.1148/129.2.521 (1978).

61 Goddard, P. R., Nicholson, E. M., Laszlo, G. & Watt, I. Computed tomography in pulmonary emphysema. *Clin Radiol* **33**, 379-387 (1982).

62 Gevenois, P. A. *et al.* Comparison of computed density and microscopic morphometry in pulmonary emphysema. *Am J Respir Crit Care Med* **154**, 187-192, doi:10.1164/ajrccm.154.1.8680679 (1996).

63 Muller, N. L., Staples, C. A., Miller, R. R. & Abboud, R. T. "Density mask". An objective method to quantitate emphysema using computed tomography. *Chest* **94**, 782-787, doi:10.1378/chest.94.4.782 (1988).

64 Kirby, M. *et al.* Total Airway Count on Computed Tomography and the Risk of Chronic Obstructive Pulmonary Disease Progression. Findings from a Population-based Study. *Am J Respir Crit Care Med* **197**, 56-65, doi:10.1164/rccm.201704-0692OC (2018).

65 Herth, F. J. F. *et al.* The Modern Art of Reading Computed Tomography Images of the Lungs: Quantitative CT. *Respiration* **95**, 8-17, doi:10.1159/000480435 (2018).

66 Lynch, D. A. & Al-Qaisi, M. L. Quantitative ct in copd. *Journal of thoracic imaging* **28**, 284 (2013).

67 Shikata, H., Hoffman, E. A. & Sonka, M. in *Medical Imaging 2004: Physiology, Function, and Structure from Medical Images.* 107-116 (International Society for Optics and Photonics).

68 Nardelli, P., Ross, J. C. & Estépar, R. S. J. in *International Conference on Medical Image Computing and Computer-Assisted Intervention.* 224-232 (Springer).

69 Nardelli, P. *et al.* Pulmonary Artery-Vein Classification in CT Images Using Deep Learning. *IEEE Trans Med Imaging* **37**, 2428-2440, doi:10.1109/tmi.2018.2833385 (2018).

70 Lee, Y. K., Oh, Y. M. & Lee, J. H. Quantitative assessment of emphysema, air trapping, and airway thickening on computed tomography. *Lung* **186**, 157 (2008).

71 Oswald-Mammosser, M. *et al.* Non-invasive diagnosis of pulmonary hypertension in chronic obstructive pulmonary disease. Comparison of ECG, radiological measurements, echocardiography and myocardial scintigraphy. *Eur J Respir Dis* **71**, 419-429 (1987).

72 Boes, J. L. *et al.* Parametric response mapping monitors temporal changes on lung CT scans in the subpopulations and intermediate outcome measures in COPD Study (SPIROMICS). *Acad Radiol* **22**, 186-194, doi:10.1016/j.acra.2014.08.015 (2015).

73 Capaldi, D. P. *et al.* Pulmonary Imaging Biomarkers of Gas Trapping and Emphysema in COPD: (3)He MR Imaging and CT Parametric Response Maps. *Radiology* **279**, 597-608, doi:10.1148/radiol.2015151484 (2016).

74 Fain, S., Schiebler, M. L., McCormack, D. G. & Parraga, G. Imaging of lung function using hyperpolarized helium-3 magnetic resonance imaging: Review of current and emerging translational methods and applications. *J Magn Reson Imaging* **32**, 1398-1408, doi:10.1002/jmri.22375 (2010).

75 Ma, W. *et al.* Ultra-short echo-time pulmonary MRI: evaluation and reproducibility in COPD subjects with and without bronchiectasis. *J Magn Reson Imaging* **41**, 1465-1474, doi:10.1002/jmri.24680 (2015).

76 Leawoods, J. C., Yablonskiy, D. A., Saam, B., Gierada, D. S. & Conradi, M. S. Hyperpolarized 3He gas production and MR imaging of the lung. *Concepts in Magnetic Resonance: An Educational Journal* **13**, 277-293 (2001).

77 Driehuys, B. *et al.* Chronic obstructive pulmonary disease: safety and tolerability of hyperpolarized 129Xe MR imaging in healthy volunteers and patients. *Radiology* **262**, 279-289, doi:10.1148/radiol.11102172 (2012).

78 Parraga, G. *et al.* Hyperpolarized 3He ventilation defects and apparent diffusion coefficients in chronic obstructive pulmonary disease: preliminary results at 3.0 Tesla. *Invest Radiol* **42**, 384-391, doi:10.1097/01.rli.0000262571.81771.66 (2007).

79 Shukla, Y. *et al.* Hyperpolarized 129Xe magnetic resonance imaging: tolerability in healthy volunteers and subjects with pulmonary disease. *Acad Radiol* **19**, 941-951, doi:10.1016/j.acra.2012.03.018 (2012).

80 Lutey, B. A. *et al.* Hyperpolarized 3He MR imaging: physiologic monitoring observations and safety considerations in 100 consecutive subjects. *Radiology* **248**, 655-661, doi:10.1148/radiol.2482071838 (2008).

81 Kirby, M. *et al.* Hyperpolarized ^{3}He magnetic resonance functional imaging semiautomated segmentation. *Acad Radiol* **19**, 141-152, doi:10.1016/j.acra.2011.10.007 (2012).

82 Albert, M. S. *et al.* Biological magnetic resonance imaging using laser-polarized 129Xe. *Nature* **370**, 199-201, doi:10.1038/370199a0 (1994).

83 Mugler, J. P., 3rd *et al.* MR imaging and spectroscopy using hyperpolarized 129Xe gas: preliminary human results. *Magn Reson Med* **37**, 809-815 (1997).

84 Woods, J. C. & Conradi, M. S. (3)He diffusion MRI in human lungs. *J Magn Reson* **292**, 90-98, doi:10.1016/j.jmr.2018.04.007 (2018).

85 Marshall, H. *et al.* Direct visualisation of collateral ventilation in COPD with hyperpolarised gas MRI. *Thorax* **67**, 613-617 (2012).

86 Ouriadov, A. V. *et al.* In vivo regional ventilation mapping using fluorinated gas MRI with an x-centric FGRE method. *Magnetic resonance in medicine* **74**, 550-557 (2015).

87 Couch, M. J. *et al.* Inert fluorinated gas MRI: a new pulmonary imaging modality. *NMR Biomed* **27**, 1525-1534, doi:10.1002/nbm.3165 (2014).

88 Gutberlet, M. *et al.* Free-breathing Dynamic (19)F Gas MR Imaging for Mapping of Regional Lung Ventilation in Patients with COPD. *Radiology* **286**, 1040-1051, doi:10.1148/radiol.2017170591 (2018).

89 Kruger, S. J. *et al.* Functional imaging of the lungs with gas agents. *Journal of Magnetic Resonance Imaging* **43**, 295-315 (2016).

90 Kirby, M., Pike, D., Coxson, H. O., McCormack, D. G. & Parraga, G. Hyperpolarized (3)He ventilation defects used to predict pulmonary exacerbations in mild to moderate chronic obstructive pulmonary disease. *Radiology* **273**, 887-896, doi:10.1148/radiol.14140161 (2014).

91 Lessard, E. *et al.* Pulmonary (3)He Magnetic Resonance Imaging Biomarkers of Regional Airspace Enlargement in Alpha-1 Antitrypsin Deficiency. *Acad Radiol* **24**, 1402-1411, doi:10.1016/j.acra.2017.05.008 (2017).

92 Salerno, M. *et al.* Emphysema: hyperpolarized helium 3 diffusion MR imaging of the lungs compared with spirometric indexes--initial experience. *Radiology* **222**, 252-260, doi:10.1148/radiol.2221001834 (2002).

93 Eddy, R. L., Svenningsen, S., McCormack, D. G. & Parraga, G. What is the Minimal Clinically Important Difference for (3)He MRI Ventilation Defects? *Eur Respir J*, doi:10.1183/13993003.00324-2018 (2018).

94 Saam, B. T. *et al.* MR imaging of diffusion of (3)He gas in healthy and diseased lungs. *Magn Reson Med* **44**, 174-179, doi:10.1002/1522-2594(200008)44:2<174::aid-mrm2>3.0.co;2-4 (2000).

95 Diaz, S. *et al.* Hyperpolarized 3He apparent diffusion coefficient MRI of the lung: reproducibility and volume dependency in healthy volunteers and patients with emphysema. *J Magn Reson Imaging* **27**, 763-770, doi:10.1002/jmri.21212 (2008).

96 Bauman, G. *et al.* Non-contrast-enhanced perfusion and ventilation assessment of the human lung by means of fourier decomposition in proton MRI. *Magn Reson Med* **62**, 656-664, doi:10.1002/mrm.22031 (2009).

97 Kaireit, T. F. *et al.* Comparison of quantitative regional ventilation-weighted fourier decomposition MRI with dynamic fluorinated gas washout MRI and lung function testing in COPD patients. *J Magn Reson Imaging* **47**, 1534-1541, doi:10.1002/jmri.25902 (2018).

98 Guo, F., Capaldi, D. P. I., McCormack, D. G., Fenster, A. & Parraga, G. A framework for Fourier-decomposition free-breathing pulmonary (1) H MRI ventilation measurements. *Magn Reson Med* **81**, 2135-2146, doi:10.1002/mrm.27527 (2019).

CHAPTER 2

2 CT PULMONARY VESSELS AND MRI VENTILATION IN CHRONIC OBSTRUCTIVE PULMONARY DISEASE: RELATIONSHIP WITH WORSENING FEV_1 IN THE TINCan COHORT STUDY

In the previous chapter we explored the structural and functional consequences of COPD, as well as various methods of measurement. The state of the literature was established, and this provided a basis for the application of multimodality imaging to elucidate the role of imaging the pulmonary vasculature in obstructive lung disease. In this chapter, the main thesis objectives and hypotheses are addressed. The purpose of this study is to evaluate the relationship between CT pulmonary vasculature with MRI lung ventilation, and to investigate how these relationships change over time.

This work was accepted to for publication Academic Radiology on March 5th, 2020.

2.1 Introduction

The 2020 statement of the Global Initiative for Chronic Lung Disease (GOLD)[1] reported that in 2010, the number of cases of Chronic Obstructive Pulmonary Disease (COPD) in persons aged 40 and over was at least 385 million and the global prevalence of COPD was 12%, both of which are predicted to increase in the next two decades. Global estimates of three million deaths/year are predicted to dramatically increase in the next 20 years because tobacco cigarette smoking rates are rising in the developing world and demographic aging is also climbing in the developed world.[2] The measurement of COPD airway, parenchyma and vascular phenotypes in patients to optimize care remains challenging[3,4] and because of this, GOLD staging criteria and the confirmatory diagnosis of COPD still rely on pulmonary function tests[1] based on expiratory flow measurements made at the mouth. Unfortunately, the onset of, and progression of COPD are believed to initiate in the terminal airways,[5,6] which are impossible to measure using pulmonary function tests. Moreover, cardiovascular comorbidities that cannot be measured or estimated using

pulmonary function tests are responsible for a large share of COPD hospitalizations and for increased COPD morbidity and mortality.[7,8]

Pulmonary imaging measurements of COPD promise improved disease phenotyping and better risk predictions for COPD exacerbations and accelerated disease progression. In this regard, thoracic x-ray computed tomography (CT) serves as the gold-standard COPD imaging approach and has been extensively used in COPD cohort studies including Genetic epidemiology of COPD Study (COPDGene),[9] Subpopulations and Intermediate Markers in COPD Study (SPIROMICS),[10] Multi-Ethics Study of Atherosclerosis (MESA),[11] Canadian Cohort of Obstructive Lung Disease Study (CanCOLD)[12] and Evaluation of COPD to Longitudinally Identify Predictive Surrogate Endpoints (ECLIPSE).[13] Hyperpolarized noble gas MRI has also been developed to sensitively measure ventilation heterogeneity[14] and airspace enlargement in COPD patients,[15] both of which are related to COPD severity,[16] exercise limitation[17] and symptoms.[18]

A recent longitudinal study of COPD demonstrated that the forced expiratory volume in one second (FEV_1) changed very little in patients in whom there was substantial vascular pruning and airway remodeling.[19] Pulmonary vessels with a cross-sectional diameter < 5mm were also shown to be related to emphysema and pulmonary hypertension[20] and other work demonstrated the relationship between cigarette smoking and small vessel volume,[21] as well as a relationship between pulmonary vascular tree pruning and COPD progression.[22,23] More recently, histological examinations confirmed pulmonary vascular trimming and airway wall remodeling in COPD patients.[24] Taken together, these findings support the notion that CT small vessel measurements may serve as an intermediate endpoint of COPD. To our knowledge, no study has investigated the relationships between CT pulmonary vasculature structure and MRI ventilation (airway function).

In the Thoracic Imaging Network of Canada (TINCan) study,[25] volume-matched CT and MRI was acquired in 176 ex-smokers; spatial correlations between MRI ventilation defects and conventional CT measurements of emphysema and airways disease were reported. This unique dataset provides an opportunity to investigate CT pulmonary vascular tree measurements and MRI ventilation over time in a relatively large group of ever-smokers.

We hypothesized that CT pulmonary vascular tree measurements would be significantly related to MRI ventilation and CT emphysema measurements in ex-smokers and that their change over time would be related to changes in emphysema. Hence, the objective of this study was to evaluate the relationship between CT pulmonary vasculature with MRI lung ventilation in ex-smokers and to investigate how these measurements change over a relatively short period of time.

Materials and Methods

2.1.1 Study Design and Participants

Participants provided written informed consent to an ethics-board approved (Institutional Ethics Board #00000984) and registered (NCT02279329 clinicaltrials.gov) protocol and underwent thoracic CT, MRI and pulmonary function tests as previously described.[25] Inclusion criteria included a history of cigarette smoking > 10 pack years, age between 50 and 85 years at baseline and exclusion criteria consisted of claustrophobia and any contraindications for MRI or CT. Ex-smokers had ceased smoking ≥1-year prior to the study visit but there was no maximum cut-off for when ex-smokers had ceased smoking. COPD was defined as post-bronchodilator forced expiratory volume in 1 second (FEV1)/forced vital capacity (FVC) ratio less than 0.70 according to the modified GOLD criteria.[1] This study was prospectively planned and performed from December 2010 to January 2019; participants underwent a single two-hour visit and performed spirometry, plethysmography, quality-of-life questionnaires, exercise capacity tests, MRI and CT as previously described.[25] Long-term follow-up was prospectively planned for 24 ±6 months and 120±12 months after the baseline visit.[25] All evaluations were performed 20 minutes after administering Novo-Salbutamol HFA using a metered-dose inhaler (four doses of 100 ug, Teva Novopharm Ltd., Toronto, ON, Canada) through a spacer (*AeroChamber Plus* spacer, Trudell Medical International, London, ON, Canada). All the data generated during the study are available from the corresponding author.

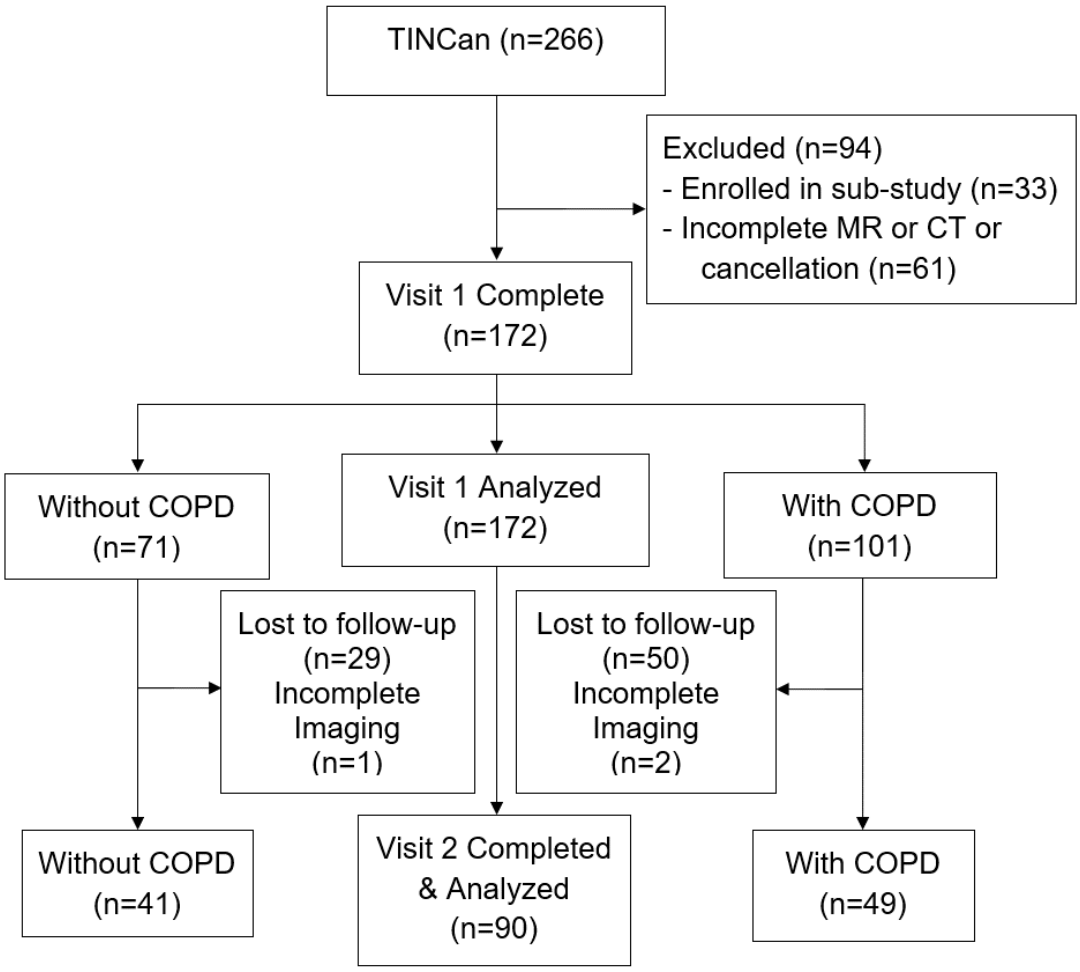

Figure 2.1: Consort diagram for TINCan Cohort Study and participants evaluated. hundred and sixty-six consented to participation and 172 participants completed the baseline visit (Visit 1) while 90 participants completed the follow-up visit (Visit 2) and were included in analysis.

2.1.2 Pulmonary Function and Quality of Life Tests

Spirometry, plethysmography, and measurement of the diffusing-capacity-of-the-lung for carbon-monoxide (DL_{CO}) were performed according to American Thoracic Society/European Respiratory Society guidelines[26-28] using a body plethysmograph (*MedGraphics Elite Series*, MGC Diagnostic Corporation, St. Paul, MN, USA) with an attached gas analyzer. The St. George's Respiratory Questionnaire was administered,[29] and a six-minute-walk-test to measure the six-minute walk-distance (6MWD) was also performed.[30]

2.1.3 MRI

Anatomical proton (^{1}H), hyperpolarized ^{3}He static ventilation, and diffusion weighted MRI were performed on a 3.0 T Discovery MR750 system (GE Healthcare, Milwaukee, WI, USA) with broadband imaging capabilities as previously described. ^{1}H MRI was acquired using a whole-body radio-frequency coil during a breath hold after inhalation of 1.0 L of N_2 as previously described.[25] ^{1}H and ^{3}He images were acquired using a fast gradient recalled echo pulse sequence with the following parameters respectively: (TR/TE/flip angle=4.7ms, 1.2ms, 30°) and (TR/TE/flip angle=4.3ms, 1.4ms 7°).[25,31] ^{3}He polarization was performed as previously described[25] and all ^{3}He MRI was performed using a single-channel rigid elliptical transmit-receive chest coil (RAPID Biomedical, Wuerzburg, Germany) as previously described.

2.1.4 CT

Within 30 minutes of the MRI, CT was acquired on a 64-slice Lightspeed VCT scanner (GE Healthcare, Milwaukee, WI, USA) under breath-hold after inhalation of 1.0 L N_2 from functional residual capacity.[25] CT images were acquired with the following parameters: beam collimation of 64 x 0.625mm, 120kVp, effective mAs of 100, 500ms tube rotation time, pitch of 1.25, and image reconstruction with a standard convolution kernel to 1.25mm.[25] Total effective dose was estimated as 1.8 mSv using the ImPACT CT patient dosimetry calculator (based on Health Protection Agency [UK] NRBP-SR250).

2.1.5 Image Analysis

^{3}He MRI ventilation defect percent (VDP) was semi-automatically segmented using in-house custom-built software using MATLAB (R2018a, Natick, MA, USA) as previously described.[31] Diffusion-weighted images were automatically processed to generate apparent diffusion coefficients (ADC).[17] CT image analysis was completed using VIDA Vision Software (VIDA Diagnostics Inc., Coralville, IA, USA) for measurements of the relative area of the lung with attenuation <-950 HU, and for pulmonary vascular measurements based on segmented vascular trees as previously described.[32] Briefly, for pulmonary vessel segmentation, the approach was based on tube enhancement using a cylindrical shape

model that employed an eigenvalue of the Hessian matrix which served as a filter to extract vessels. At junctions, vessel branch points were identified from noise by applying a thinning method which then allowed for the selection of objects with many branch points. Pulmonary vascular total blood volume (TBV) was calculated for the entire segmented vascular tree and a 1 voxel filter was used to generate and the percent of pulmonary vessels with a radius < one pixel (PV_1), similar to previously described results using VIDA Apollo software.[33]

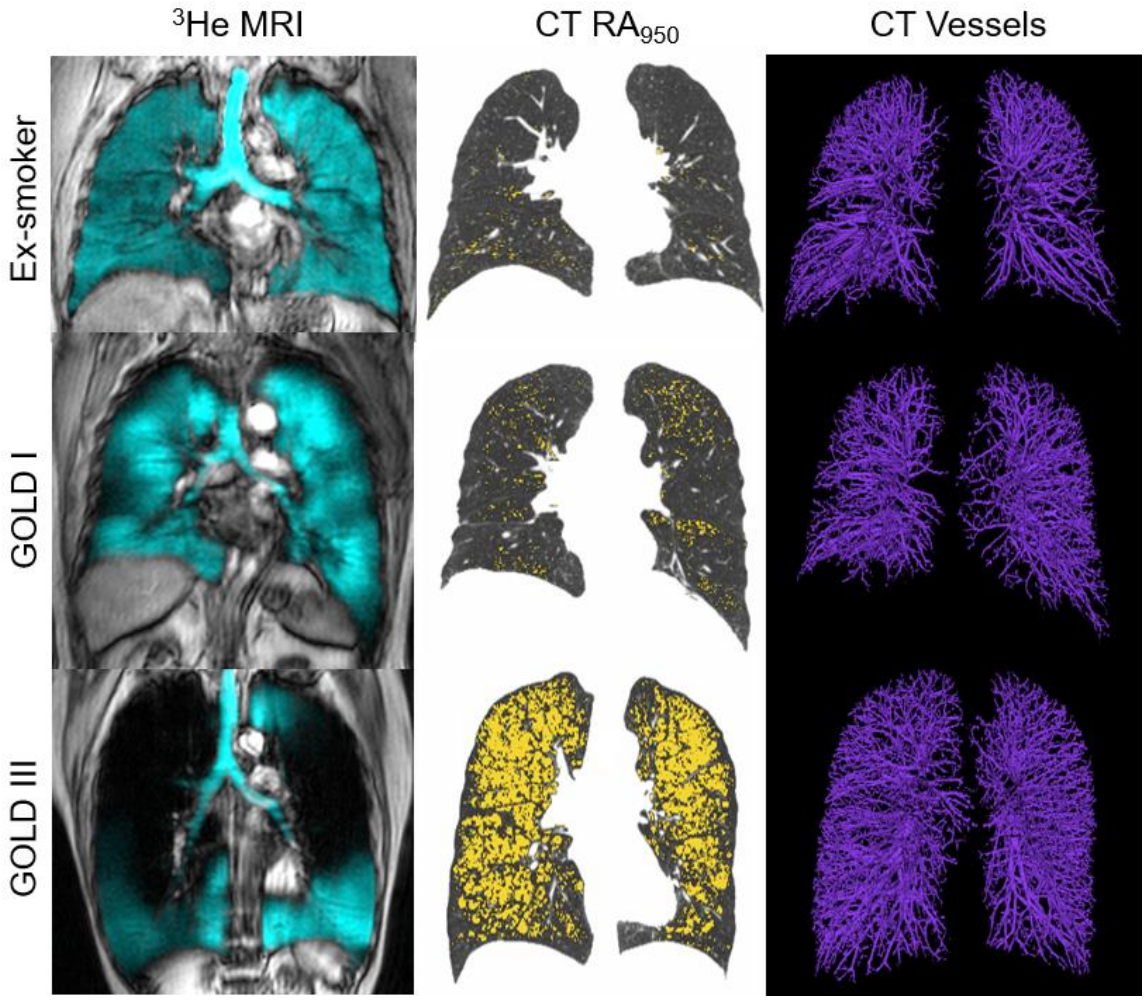

Figure 2.2: Baseline MR and CT images for representative ex-smoker without COPD and representative participant III COPD.
Left panel provides coronal centre-slice ^{3}He MRI ventilation in cyan co-registered with ^{1}H anatomical image; Middle panel provides coronal CT reconstruction of same slice with relative area of the lung with voxels < -950 Hounsfield units (RA_{950}) shown in yellow; Right panel provides 3D reconstruction of CT pulmonary vessels at baseline in purple.
Ex-smoker without COPD is an 83-year-old male, $FEV_{1\ \%pred}$=104%, VDP=4 =%, RA_{950}= 1%, TBV=150 mL, PV_1=45%

GOLD I COPD participant is an 88-year-old male, $FEV_{1\ \%pred}$=88%, VDP=10%, RA_{950}=4%, TBV=100 mL, PV_1=54%
GOLD III COPD participant is a 68-year-old female, $FEV_{1\ \%pred}$=37%, VDP=34%, RA_{950}= 33%, TBV=160 mL, PV_1=60%
MRI=magnetic resonance imaging; CT=computed tomography; GOLD=global initiative for chronic obstructive lung disease; FEV_1=forced expiratory volume in 1 second; VDP=ventilation defect percent; RA_{950}=relative area of the lung with CT attenuation < -950 HU.

2.1.6 Statistical Methods

Statistical analyses were completed using SPSS (ver. 25; IBM Statistics, Armonk, NY, USA). Longitudinal analyses were evaluated using repeated measures ANOVA as well as independent t-tests to determine relationships between baseline and follow-up measurements. Paired sample t-tests were used to determine subgroup (All participants, Ex-smokers, all COPD and GOLD I, II, III/IV) differences between time points for specific variables. The annual rate of change in FEV_1 was determined for all participants and they were stratified into three subgroups based on change in FEV_1/year as follows: 1) a decrease of greater than 40mL/year (n=40), 2) a change in FEV_1 between a 20mL/year increase and a 40mL/year decrease (n=25), and 3) an increase of greater than 20mL/year (n=25). Relationships were evaluated using linear regression in GraphPad Prism (Prism v8; La Jolla, CA, USA). All results were considered statistically significant when the probability of making a Type I error was less than 5%.

2.2 Results

As shown in the consort diagram provided in **Figure 2.1**, 266 participants enrolled in the study and 172 participants completed all imaging examinations at baseline. Of those participants who did not complete Visit 1, most simply did not attend after enrollment and consent (n=43) or did not complete MRI (because of coil fit, n=10 or claustrophobia, n=3) or CT (radiation dose concerns, n=5). After 31±7 months (range=8-50 months), 90 participants returned for a complete follow-up visit. There were 29 ex-smokers and 50 COPD participants lost to follow-up who could no longer be reached by telephone or email.

Table 2.1: Participant demographics at baseline for all ex-smokers with and without COPD and at baseline for those who returned for follow-up.

	All Participants			Participants with Follow-up			
Parameter (±SD)	All n=172	Without COPD n=71	With COPD n=101	All n=90	Without COPD n=41	With COPD n=49	*p*-value
Females n (%)	67 (39)	31 (44)	36 (36)	36 (42)	18 (44)	16 (33)	-
Age y	71 (10)	70 (10)	71 (10)	71 (9)	71 (10)	71 (8)	.642
BMI kg/m^2	27 (5)	29 (4)	26 (4)	28 (4)	30 (4)	26 (4)	.158
SaO_2 %	96 (3)	96 (4)	95 (3)	96 (3)	95 (5)	96 (2)	.808
6MWD m	386 (94)	403 (96)	373 (92)	404 (85)	398 (100)	408 (71)	.087
$FEV_{1\ \%pred}$	76 (29)	98 (19)	60 (24)	83 (27)	102 (18)	68 (23)	**.021**
$FVC_{\ \%pred}$	90 (18)	92 (17)	88 (20)	94 (17)	94 (17)	95 (18)	.054
FEV_1/FVC	62 (19)	81 (7)	49 (13)	65 (17)	81 (6)	52 (11)	.097
$RV_{\ \%pred}$	139 (49)	107 (22)	162 (50)	127 (41)	106 (20)	145 (45)	**.011**
$TLC_{\ \%pred}$	111 (18)	101 (13)	118 (18)	109 (15)	102 (12)	114 (16)	.164
$RV/TLC_{\ \%pred}$	123 (28)	106 (17)	135 (29)	115 (25)	103 (15)	125 (28)	**.004**
$DL_{CO\ \%pred}$	64 (23)	78 (21)	54 (20)	68 (21)	77 (17)	60 (20)	.129

BMI=body mass index, SaO_2=digital oxygen saturation, 6MWD=six minute walk distance, %pred=percent predicted, FEV_1=forced expiratory volume in 1 second, FVC=forced vital capacity, RV=residual volume, TLC=total lung capacity, DL_{CO}=diffusing capacity of the lung for carbon monoxide. A one-way ANOVA was used to test for differences between participants that attended both baseline and follow-up visits (n=90) and those that attended the baseline visit (n=172).

As shown in **Table 2.1**, of the 90 participants who completed both the baseline and follow-up visit, 41 were ex-smokers without spirometric evidence of COPD (71±10yrs) and 49 participants were ex-smokers with COPD (71±8yrs). **Table 2.1** also shows that the participants who completed both baseline and follow-up visits reported significantly greater (more normal) FEV_1, (p=0.02), RV (p=0.01) and RV/TLC (p=0.004) at baseline than all participants completing the baseline visit.

Figure 2.2 shows MRI and CT findings for representative participants at baseline including an ex-smoker without COPD and participants with GOLD grade I and grade III COPD. With increasing disease severity there were a qualitatively more and larger ventilation defects and a greater relative area of emphysema as shown in the yellow RA_{950} mask.

Figure 2.2 shows there were no visually obvious differences in CT total blood volume or PV_1 with increasing disease severity.

Table 2.2: Demographics for participants who attended both baseline and follow-up

	Ex-smoker			GOLD I			GOLD II			GOLD III/IV	
Parameter (±SD)	BL n=41	FU n=41	*p*-value	BL n=15	FU n=15	*p*-value	BL n=23	FU n=23	*p*-value	BL n=11	FU n=11
Female n (%)	18 (44)	18 (44)	-	1 (7)	1 (7)	-	11 (48)	11 (48)	-	4 (36)	4 (36)
Age y	71 (10)	73 (10)	**.0001**	75 (8)	78 (8)	**.0001**	68 (7)	72 (7)	**.0001**	70 (9)	72 (9)
BMI kg/m^2	30 (4)	30 (4)	.721	28 (4)	28 (4)	.766	26 (4)	25 (3)	.632	26 (6)	26 (5)
SaO_2 %	95 (5)	96 (2)	.791	96 (1)	95 (3)	.183	96 (2)	94 (3)	**.002**	95 (2)	94 (3)
6MWD m	417 (83)	404 (76)	.074	434 (39)	408 (59)	**.041**	423 (71)	407 (80)	.152	362 (84)	336 (97)
$FEV_{1\ \%pred}$	102 (18)	103 (21)	.465	97 (12)	99 (12)	.387	62 (8)	59 (14)	.164	40 (5)	39 (10)
$FVC_{\ \%pred}$	94 (17)	96 (19)	.112	111 (13)	110 (14)	.527	94 (13)	90 (12)	.099	75 (10)	67 (15)
FEV_1/FVC	81 (6)	79 (7)	**.027**	64 (4)	64 (5)	.942	50 (9)	50 (10)	.310	41 (7)	44 (10)
$RV_{\ \%pred}$	105 (20)	103 (20)	.336	116 (27)	119 (19)	.685	140 (25)	143 (32)	.505	202 (46)	193 (45)
$TLC_{\ \%pred}$	101 (11)	96 (12)	**.0001**	111 (11)	110 (10)	.744	113 (14)	111 (17)	.601	124 (22)	121 (17)
$RV/TLC_{\ \%pred}$	103 (15)	106 (16)	.338	104 (18)	107 (15)	.343	123 (17)	127 (16)	.388	160 (17)	157 (21)
$DL_{CO\ \%pred}$	79 (16)	86 (17)	**.0001**	76 (20)	78 (23)	.483	60 (16)	61 (20)	.463	45 (14)	45 (14)

BL=baseline, FU=Follow-up, BMI=body mass index, SaO_2=oxygen saturation, 6MWD=six minute walk distance, %pred=percent predicted, FEV_1=forced expiratory volume in 1 second, FVC=forced vital capacity, RV=residual volume, TLC=total lung capacity, DL_{CO}=diffusing capacity of the lung to carbon monoxide. Paired t-tests were used to test for within-group changes at follow-up.

As shown in **Table 2.3** (supplement), the ex-smoker subgroup reported significantly different RA_{950} (p<0.0001), VDP (p<0.0001), TBV (p<0.0001) and PV_1 (p=0.01) at baseline as compared to all COPD subgroups. There were significant differences between GOLD I and GOLD II subgroups for RA_{950}, VDP and PV_1, and between GOLD I and GOLD III/IV for all imaging measurements. VDP was also significantly different between GOLD III/IV and GOLD II subgroups at baseline. **Table 2.4** (supplement) also shows that at baseline, VDP was significantly different for the 23 participants with CT emphysema ($RA_{950} \geq 6.8\%$,[34]) as compared to the subgroup of COPD participants without emphysema (n=26). The subgroup of participants with CT emphysema also reported significantly different baseline VDP, TBV and PV_1 as compared to all ex-smokers.

Table 2.2 shows baseline and follow-up pulmonary function, lung volume, 6MWD and DL_{CO} measurements for all 90 participants who completed the follow-up visit including ex-smokers without COPD (n=41 at baseline and follow-up), GOLD I, (n=16 at baseline and n=15 at follow-up), GOLD II, (n=23 at baseline and n=21 at follow-up) and GOLD III+IV (n=11 at baseline and n=14 at follow-up) COPD. Paired t-tests revealed significant differences for each subgroup at follow-up; unpaired test results are shown in **Table 2.5 (**online supplement) because the subgroup sample sizes changed over time with some participants reported worsening pulmonary function at the follow-up visit. In the ex-smoker subgroup, there were significant but small changes in FEV_1/FVC, TLC and DL_{CO}, whilst in the GOLD I subgroup there was a significant decline in the 6MWD.

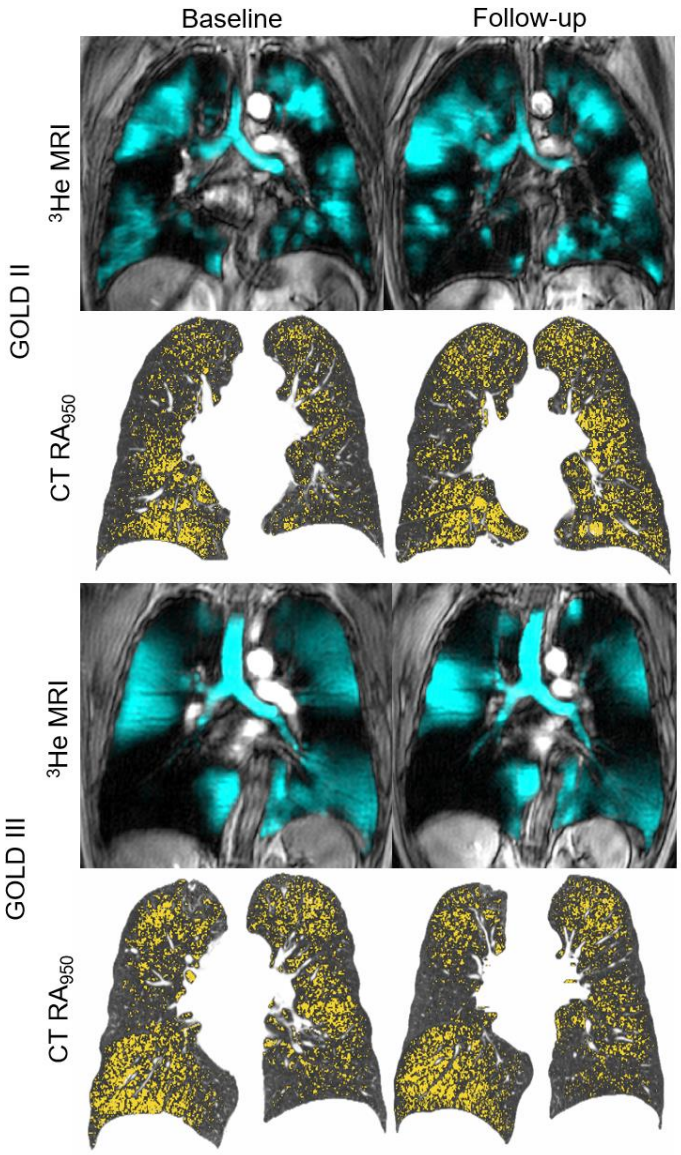

Figure 2.3: Baseline and follow-up CT and MR imaging for representative participants with COPD.
Top panels provide coronal centre-slice ^{3}He MRI ventilation in cyan co-registered with ^{1}H anatomical image; Bottom panels provide coronal CT reconstruction of same slice with relative area of the lung < -950 Hounsfield units (RA_{950}), shown in yellow.
GOLD II participant is a 76-year-old male, follow-up time=38 months, $FEV_{1\%pred}$=56% (BL) and 38% (FU); VDP=24% (BL) and 33% (FU); RA_{950}=11% (BL) and 19% (FU)
GOLD III participant is a 74-year-old male, follow-up time=28 months, $FEV_{1\%pred}$=34% (BL) and 30% (FU); VDP=34% (BL) and 45% (FU); RA_{950}=18% (BL) and 22% (FU).
MRI=magnetic resonance imaging; CT=computed tomography; GOLD=global initiative for chronic obstructive lung disease; FEV_1=forced expiratory volume in 1 second; %pred=percent predicted; VDP= ventilation defect percent; RA_{950}=relative area of the lung with CT attenuation < -950 HU.

Figure 2.3 shows MRI ventilation and CT RA_{950} masks and measurements for two representative COPD participants at baseline and follow-up. For both participants, there was qualitatively worse MRI ventilation (shown in cyan in top panel), and emphysema (shown using the RA_{950} mask in yellow in bottom panel) at the follow-up visit.

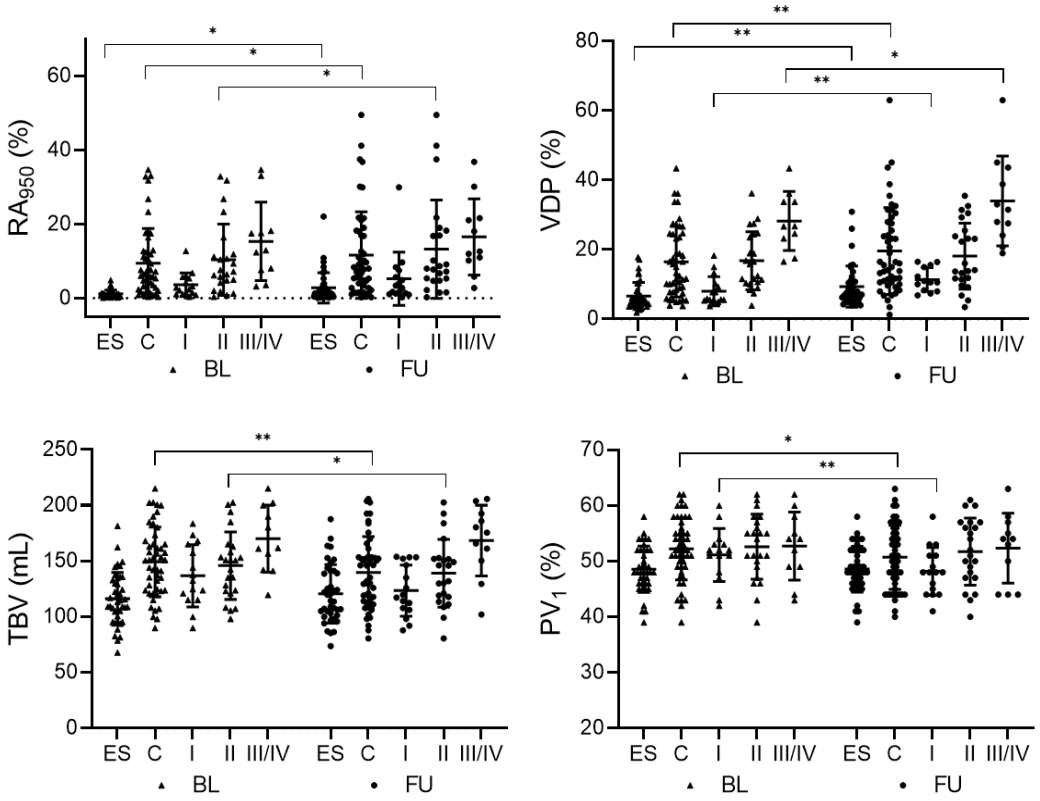

Figure 2.4: Imaging measurements at baseline and follow-up.
Paired t-tests were used to determine significance of within-group changes over time for: RA_{950}: ES=1±1% (BL) and 3±4% (FU), p<.02; C=9±9% (BL) and 11±12% (FU), p=.02; GOLD I=4±3% (BL) and 5±7% (FU) , p=.17; GOLD II=10±10% (BL) and 13±13% (FU) , p=.03; GOLD III/IV=15±11% (BL) and 17±10% (FU) , p=.70.

VDP: ES=7±4% (BL) and 9±6% (FU), p=.002; C=16±10% (BL) and 19±11% (FU), p=.005; GOLD I=8±4% (BL) and 11±3% (FU), p=.001; GOLD II=17±9% (BL) and 18±10% (FU), p=.42; GOLD III/IV=29±5% (BL) and 33±9% (FU), p=.04.

TBV: ES=114±24mL (BL) and 115±36mL (FU), p=.46; C=146±30mL (BL) and 142±35mL (FU), p=.005; GOLD I=134±29 (BL) and 142±29mL (FU), p=.06; GOLD II=145±27 (BL) and 132±34mL (FU), p=.03; GOLD III/IV=167±25 (BL) and 162±36mL (FU), p=.81.

PV_1: ES=49±4% (BL) and 49±5% (FU), p=.72; C=52±6% (BL) and 51±6% (FU), p=.02; GOLD I=51±5% (BL) and 48±4% (FU), p=.002; GOLD II=52±6% (BL) and 52±6% (FU), p=.40; GOLD III/IV=53±6% (BL) and 52±6% (FU), p=.69.

BL=baseline; FU=follow-up; RA_{950}=relative area of the lung with attenuation < -950 HU; VDP=ventilation defect percent; TBV=total blood vessel volume; PV_1=relative volume of pulmonary vessels with radius < 1 voxel; ES=ex-smokers without COPD; C=all participants with COPD; GOLD=global initiative for chronic obstructive lung disease; *p<.05, **p<.01

Quantitative results are shown in **Figure 2.4** for baseline and follow-up RA_{950}, VDP, CT pulmonary vascular total blood volume (TBV) and percent of pulmonary vessels with radius < one voxel (PV_1) measurements. For RA_{950} shown in the top left panel, there were significant changes at follow-up for ex-smokers (p=0.02), all COPD (p=0.002) and GOLD II COPD (p=0.03) subgroups. For VDP shown in the top right panel, there were significant changes at follow-up for ex-smokers (p=0.002), all COPD (p=0.005), GOLD I (p=.001) and GOLD III/IV (p=0.04) subgroups. For TBV shown in the bottom left panel, there were significant changes at follow-up for all COPD (p=0.005) and GOLD II subgroups (p=0.03) whereas there was a trend for a change at follow-up reported by GOLD I participants (p=0.06). Finally, there were significant changes at follow-up for PV_1 in the all COPD (p=0.02) and GOLD I COPD (p=0.002) subgroups.

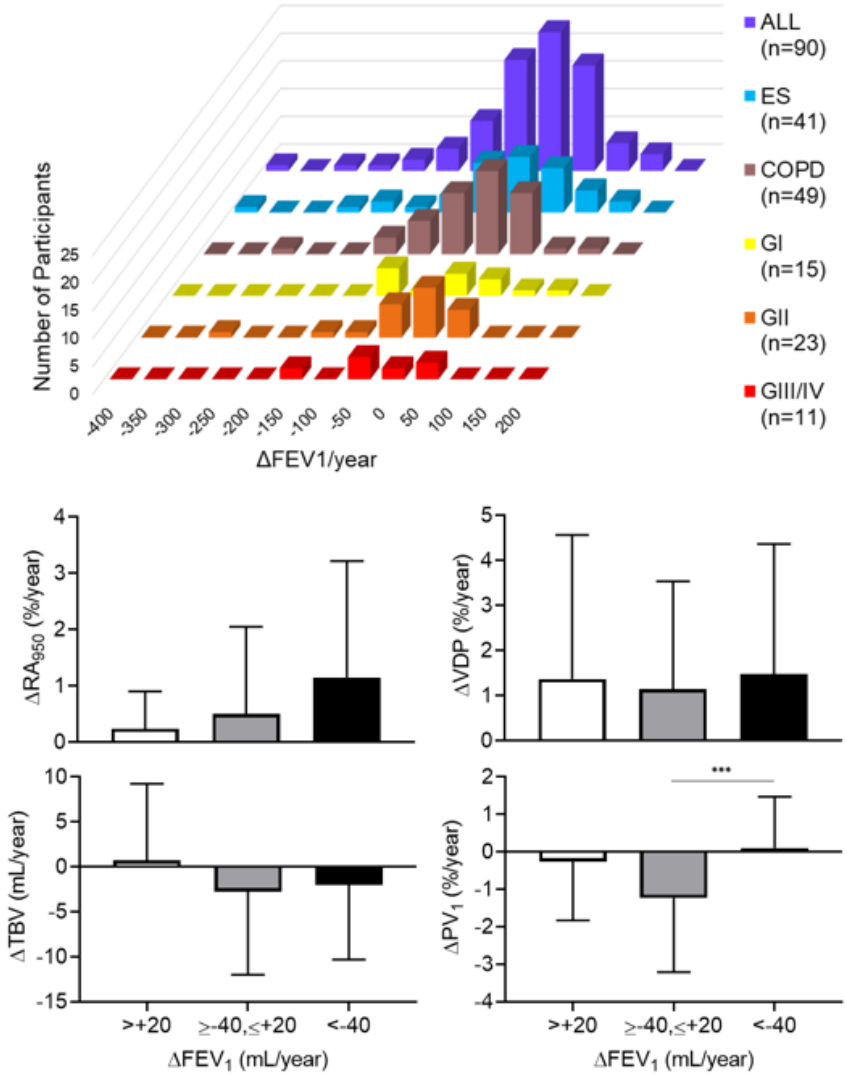

Figure 2.5: Change in imaging measurements at follow-up for participants stratified by mean annual change in FEV_1.

Top panel shows histograms for the FEV_1 rate of change for all participants (n=90, mean=-40±93mL/year), ES (n=41, mean=-42±107mL/year), C (n=49, mean=-39±80mL/year), GI (n=15, mean=22±93mL/year), GII (n=23, mean=-45±75mL/year) and GIII/IV (n=11, mean=-49±75mL/year). Participants who reported a decrease at follow-up in FEV_1 < -40mL/year (n=40), between -40 and +20mL/year (n=25) and >+20mL/year (n=25) are shown in white, grey and black ±SD, respectively for ΔRA_{950} ΔVDP ΔTBV and ΔPV_1. T-tests were used to evaluate subgroup differences as shown above.

ΔRA_{950} for ΔFEV_1>+20= -0.24±0.66 %/year, ≥-40, ≤+20= 0.50±1.6%/year, <-40= 1.2±2.1%/year,

Significant differences for >+20 and ≥-40mL to ≤+20, ***p*=.44**; ≥-40mL to ≤+20 and <-40, ***p*=.18**; >+20 and < -40, ***p*=.01.**

ΔVDP for ΔFEV_1>+20=1.4±3.2%/year, ≥-40, ≤+20= 1.1±2.4%/year, <-40=1.5±2.9%/year

Significant differences for subgroups: >+20 and ≥-40mL to ≤+20, ***p*=.77**; ≥-40mL to ≤+20 and <-40, ***p*=.63**; >+20 and < -40, ***p*=.89**.

ΔTBV for ΔFEV_1>+20=0.70±8.6mL/year, ≥-40, ≤+20= -2.7±9.2mL/year, <-40=-2.0±8.3mL/year

Significant differences for subgroups: >+20 and ≥-40mL to ≤+20, ***p*=.19**; ≥-40mL to ≤+20 and <-40, ***p*=.75**; >+20 and < -40, ***p*=.21.**
ΔPV_1 for ΔFEV_1: >+20= -.26±1.6%/year, ≥-40, ≤+20= -1.2±2.0%/year, <-40= .10±1.4%/year
Significant differences for subgroups >+20 and ≥-40mL to ≤+20, ***p*=.07;** ≥-40mL to ≤+20 and <-40, ***p*=.007**; >+20 and < -40, ***p*=.33**.
ALL=all participants; ES=ex-smokers; C=all participants with COPD; GOLD=global initiative for chronic obstructive lung disease; FEV_1=forced expiratory volume in 1 second; PV_1=relative volume of pulmonary vessels with radius <1 voxel; RA_{950}=relative area of the lung with CT attenuation <-950 HU; VDP=ventilation defect percent; TBV=total blood vessel volume. **p*<.05, ***p*<.01.

As shown in the frequency distributions provided in the top panel of **Figure 2.5**, the mean annual change in FEV_1 was -40±93mL/year for all participants, -42±107 mL/year for ES, -22±93mL/year for GOLD I, -45±75mL/year for GOLD II and -49±75mL/year for GOLD III/IV participants. A one-way ANOVA revealed no significant difference in the mean annual FEV_1 rate of change for the subgroups (*p*=0.87). We acknowledge that the mean annual change in FEV_1 measured here is greater than previous reports and with greater heterogeneity [9,35,36].

The bottom panels in **Figure 2.5** show the annual rate of change for RA_{950}, VDP, TBV and PV_1 for three subgroups stratified by the mean change in FEV_1/year (from right to left): a decrease of greater than 40mL/year (n=40), a change in FEV_1 between a 20mL/year increase and a 40mL/year decrease (n=25), and an increase of greater than 20mL/year (n=25) in white, grey and black bars respectively. The annual rate of RA_{950} change for participants with FEV_1 decrease of greater than 40mL/year was also significantly different compared to the subgroup with a 20mL/year FEV_1 increase (*p*=0.01). The annual rate of change for PV_1 for the subgroup with an FEV_1 decrease of greater than 40mL/year was also significantly different compared to the subgroup with a change in FEV_1 between a 20mL/year increase and a 40mL/year decrease (*p*=0.007). Finally, as shown in **Table 2.4,** the very small difference in mean annual change in PV_1 between ex-smokers without COPD and COPD participants with CT emphysema was significant (*p*=0.013), whilst no other imaging measurement annual changes were significantly between COPD subgroups with and without emphysema.

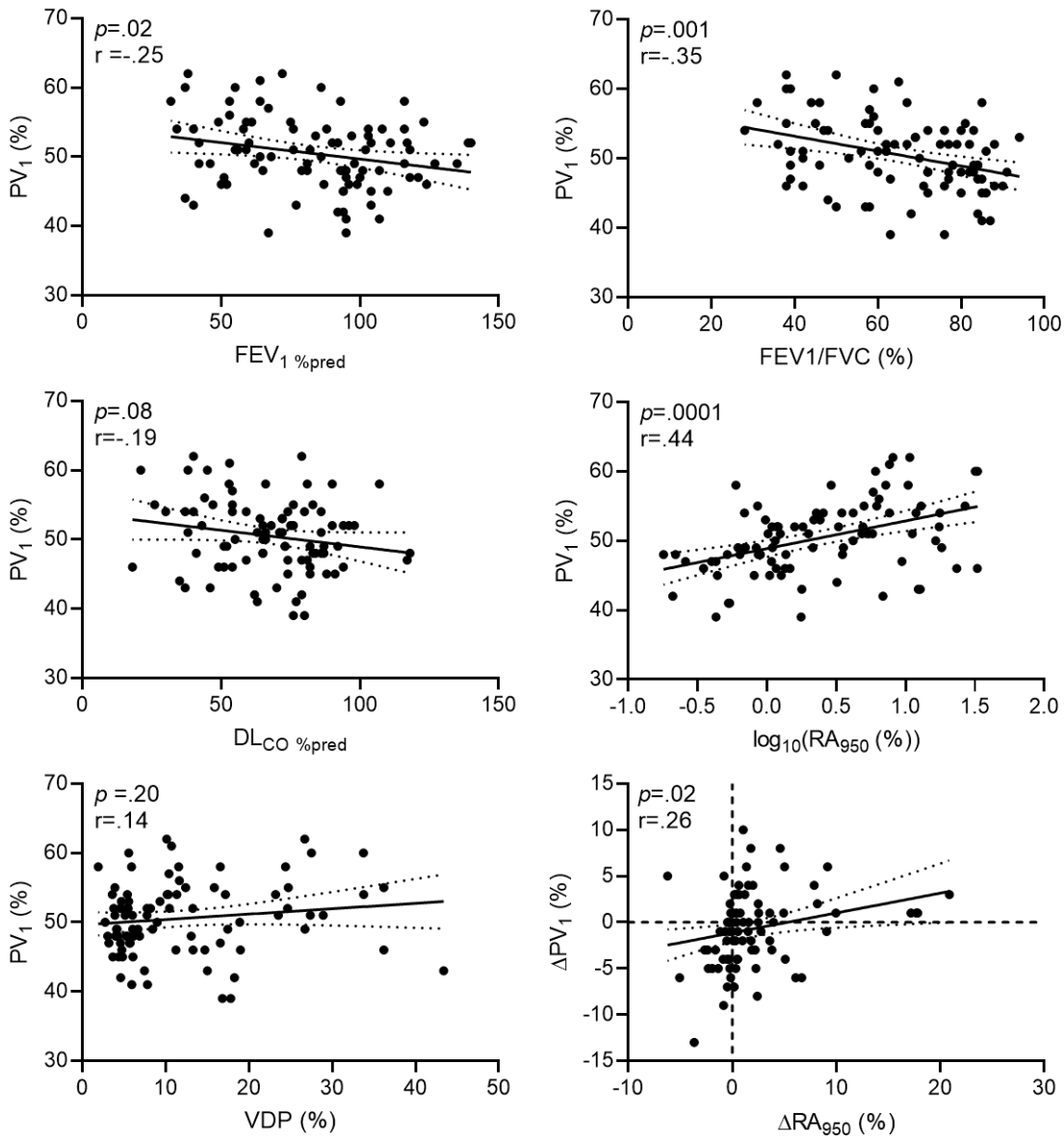

Figure 2.6: Relationships for PV_1 and pulmonary function test measurements.
PV_1 linear regression with FEV_1 y=-.047x+54.423, r=-.25, p=.02;
PV_1 linear regression with FEV_1/FVC: y =-.107x+57.483, r=.-35, p=.001;
PV_1 linear regression with $\log_{10}(RA_{950})$: y =4.000x+48.870, r=.44, p=.0001;
PV_1 linear regression with DL_{CO}: y=-.048x+53.743, r=-.19, p=.08;
PV_1 linear regression with VDP: y=.078x+49.632, r=.14, p=.20;
ΔPV_1 linear regression with ΔRA_{950}: y=.214x-1.126, r=.26, p=.02.

As shown in **Figure 2.6**, we also explored relationships for PV_1 with pulmonary function measurements. Baseline values of PV_1 weakly correlated with baseline values of $FEV_{1\ \%pred}$ (r=-.25; p=0.02), FEV_1/FVC (r=-.35; p=0.001) and log RA_{950} (r=.44; p=0.0001), but not DL_{CO} (r=-.19; p=0.08) or VDP (r=.14; p=0.20). **Figure 2.6** also shows that the mean change in PV_1 was also weakly but significantly related to the change in RA_{950} (r=.26; p=0.02) and the annual rates of change were also significantly but weakly related (r=.28, p=0.01) (data not shown).

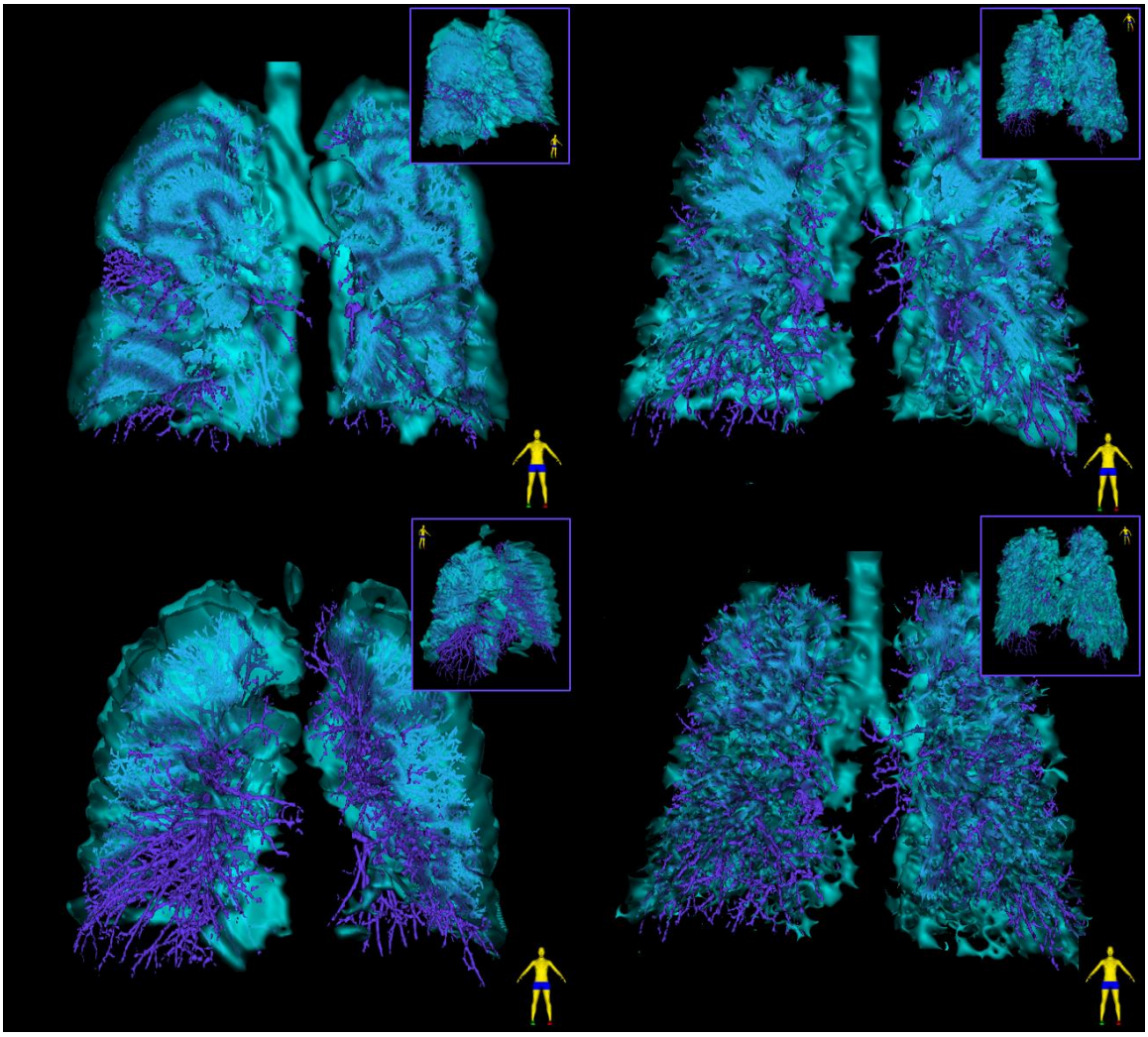

Figure 2.7: 3D model of ^{3}He MRI ventilation and CT vessels for four representative participants.
Ventilation (cyan) and vessels (purple) for representative participants who did and did not report the mean absolute change in FEV_1 at the follow-up visit:
Top panels show GOLD II COPD at follow-up with > mean absolute change in FEV_1:

67-year-old female, follow-up time=33 months, $FEV_{1\%pred}$=53% (BL) and 50% (FU); Absolute change in FEV_1= -110mL; VDP=12% (BL) and 10% (FU); TBV=110mL (BL) and 110mL (FU); PV_1=56% (BL) and 60% (FU); RA_{950}=6% (BL) and 8% (FU).
75-year-old male, follow-up time=33 months, $FEV_{1\%pred}$=108% (BL) and 79% (FU); Absolute change in FEV_1= -1170mL; VDP=17 (BL) and 26 (FU); TBV=182 (BL) and 153mL (FU); PV_1=54% (BL) and 52% (FU); RA_{950}=3% (BL) and 2% (FU).

Bottom panels show GOLD II COPD at follow-up with < mean absolute change in FEV_1:
71-year-old female, follow-up time=49 months, $FEV_{1\%pred}$=58% (BL) and 59% (FU); Absolute change in FEV_1= -60mL; VDP=11% (BL) and 12% (FU); TBV=120mL (BL) and 120mL (FU); PV_1=54% (BL) and 60% (FU); RA_{950}=12% (BL) and 17% (FU)
57-year-old male, follow-up time=34 months, $FEV_{1\%pred}$=62% (BL) and 62% (FU); Absolute change in FEV_1= 0mL; VDP=8 (BL) and 9% (FU); TBV=128 (BL) and 130mL (FU); PV_1=49% (BL) and 50% (FU); RA_{950}=1% (BL) and 2% (FU).

Figure 2.7 shows ^{3}He MRI ventilation co-registered with CT vessel trees at follow-up for four representative participants including two COPD participants at follow-up with a change in FEV_1 greater than the mean for all participants and two COPD at follow-up with FEV_1 change less than the mean for all participants. In the top two panels, regions of mismatched vascular structure and ventilation are shown in the top panels for two participants with follow-up time of` 33 months. For a 67-year-old female shown in the top left panel, the absolute change at follow-up in FEV_1 was -110mL, whilst the change for RA_{950} and VDP was 2% and PV_1 increased 4%. For a 75-year-old male, shown in the right panel, the absolute change in FEV_1 was a decrease of 1170mL, VDP worsened from 17% to 26%, TBV decreased from 182mL to 153mL, PV_1 increased from 52% to 54% and RA_{950} decreased 1% at follow-up.

In the bottom panels, regions of mismatched vessel tree and MRI ventilation are shown for two participants at follow-up with GOLD grade II COPD. For the 71-year-old female shown in the bottom left panel, the follow-up time was 49 months and there was an absolute change in FEV_1 of -60mL, whilst the change for RA_{950} and PV_1 were 5% and 6% respectively with negligible changes in VDP and TBV. For a 57-year-old male in the bottom right panel, there was no change in $FEV_{1\%pred}$ over 34 months and there were negligible changes in all other imaging measurements, although there appears to be substantial MRI ventilation-vessel tree mismatch in the anterior region of the lung.

2.3 Discussion

We measured pulmonary CT vessel measurements and MRI ventilation at baseline and 31±7 months later in 90 ex-smokers including 41 without COPD and 49 with COPD and observed: 1) participants who returned for follow-up reported significantly more normal FEV_1, RV and RV/TLC at baseline than all participants who completed the baseline visit, 2) significant differences in baseline RA_{950}, VDP, TBV and PV_1 between ex-smokers and COPD participants as well as VDP (but not TBV or PV_1) in COPD participants with and without emphysema, 3) while the annual rate of change in FEV_1 (-40±93mL/year) was not different among participant subgroups, the annual rate of change for RA_{950} and PV_1 was significantly different in participants with an accelerated annual rate of FEV_1 decline as compared to participants with a diminished annual rate of FEV_1 decline, and, 4) significant but weak relationships for PV_1 with FEV_1, FEV_1/FVC and RA_{950} and for the mean annual change in PV_1 with the mean annual change in RA_{950}.

First, we observed that participants who returned for follow-up had significantly more normal pulmonary function and lung volumes at baseline than all participants completing the baseline visit. This suggests that measurements reported here may provide conservative estimates of longitudinal change because they stem from participants who were in better health on their first visit so they were perhaps more likely to attend the follow-up visit. The follow-up period was also similar to ECLIPSE (3 years) [35] and CanCOLD (2.5 years)[36] but the TINCan cohort was a convenience and not a population sample.

Second, at baseline, and as expected, we observed significant differences in RA_{950}, VDP, TBV and PV_1 between ex-smokers and COPD participants. Differences between ex-smokers and participants with COPD for emphysema,[19,37] small vessel volume[20,38] and ventilation[17] have been previously observed. To our knowledge however this is the first report of ventilation and CT pulmonary vascularity at baseline and again 2.5 years later. In addition, we observed that VDP measurements were significantly different in COPD participants with and without emphysema whilst PV_1 measurements were significantly different between COPD participants with emphysema and ex-smokers, both findings in agreement with the concept that emphysema, ventilation and the pulmonary vasculature

are necessarily and mechanistically linked in COPD patients to avoid ventilation-perfusion mismatch.[24,38-41]

Third, we stratified participants based on the annual rate of change in FEV_1, similar to what was previously described in the ECLIPSE study.[13] While the annual rate of change in FEV_1 (-40 ±93mL/year) was not different among participant subgroups, the annual rate of change in RA_{950} and PV_1 was significantly different in participants with an accelerated annual rate of FEV_1 decline as compared to participants with a diminished annual rate of FEV_1 decline. Previous work also reported diminished small vessel volume in COPD patients over time[21,38,42,43] while others reported a significant increase in small vessel volume in ex-smokers over a similar follow-up time.[19] Possible ways to explain these divergent results include a role for angiogenesis in chronic inflammation and tissue repair and remodeling of both the pulmonary and bronchial vasculature,[44-47] previously validated in COPD patients.[24,47] Similar findings were not observed for the annual rate of change in VDP, indicative that changes in small airway function measured using VDP[17] poorly reflect changes in FEV_1, which is dominated by large airway function. In contrast, there was a significantly different rate of change in RA_{950} in participants in whom FEV_1 improved by more than 20mL/year as compared to the subgroup in whom FEV_1 decreased by more than 40mL. Moreover, the subgroup reporting the largest annual rate of FEV_1 decline was dominated by GOLD II participants (10/23 or 44%) which is important because the GOLD II subgroup was the only one to report significant worsening of emphysema.

Finally, we also observed that PV_1 weakly correlated with baseline $FEV_{1\ \%pred}$, FEV_1/FVC and RA_{950}, but not DL_{CO} or VDP. The mean PV_1 change was significantly related to the change in RA_{950} and the relationship for rate of change in both measurements was also significant. These findings are consistent with what has been previously reported, where pulmonary function and small vessel volume are related, but not consistently, in COPD patients.[48] Small vessel volume and emphysema were previously shown to be related in patients with COPD,[20] although worsening emphysema and pulmonary vessel volume were not related in a linear fashion over time.[19] Previous work investigating the relationship between ventilation and perfusion also reported their modest relationship which appeared to be independent of disease severity.[40] Given the potential relevance of these study

findings for the clinical management of COPD patients, we think it is time for the field to consider ways to implement ventilation MRI and especially CT in clinical workflows and this is especially the case for automated image analysis and data reporting, research that our group and others are currently undertaking.

We acknowledge a number of study limitations including the relatively small sample size compared to other cohort studies that included imaging measurements such as CanCOLD,[12] ECLIPSE,[9,13] and COPDGene,[9,13] although to our knowledge, no other COPD cohort study has evaluated lung volume matched MRI and CT datasets to probe ventilation and pulmonary vascular changes over time. In addition, as compared to other recent studies,[20,21,42] our CT measurement approach may underestimate the fraction of small pulmonary vessels in our results. It is important to note that the TINCan study was required to compromise between the acquisition of volume matched MRI and CT (at FRC+1L) versus full inspiration MRI and CT, mainly due to the costs of ^{3}He gas and because the standard in the field was to acquire MRI at FRC+1L. However, as compared to plethysmographic measurements of TLC, for the participants studied here, FRC+1L values were within 80% to 90% of plethysmographic TLC, which is similar to other CT studies for inhalation breath-holds in supine participants or patients. Moreover, Madani and colleagues[49] also previously reported that such differences related to lung volume are within a few percent for RA_{950} values and that these are unlikely to be clinically relevant.

2.4 Conclusions

We evaluated 90 ex-smokers with and without COPD over 2.5 years and observed that the annual RA_{950} and PV_1 rates of change were greater in participants with an accelerated FEV_1 decline. The annual changes in PV_1 were weakly related to the annual change in RA_{950} but not VDP. Taken together, these findings suggest that changes over time in the pulmonary vessels and ventilation may be asynchronous in ex-smokers and COPD patients.

2.5 Supplemental Data

Table 2.3: Imaging data at baseline by COPD subgroup

Parameter (±SD)	ES n=41	C n=49	GI n=15	GII n=23	GIII/IV n=11	*p*-value
RA_{950}	1 (1)	9 (9)*	4 (3)	10 (10)*#	15 (11)*#	**.0001**
VDP	7 (4)	17 (10)*	8 (4)	17 (9)*#	29 (5)*#!	**.0001**
TBV	116 (24)*	149 (31)*	134 (29)*	145 (27)*	167 (25)*#	**.0001**
PV_1	49 (4)	52 (6)*	51 (5)	52 (6)*#	53 (6)*#	**.01**

P-values reflect a one-way ANOVA testing for subgroup differences with Tukey's post-hoc correction for multiple comparisons. An independent t-test was used to determine differences between ES and C subgroups where * reflects significantly different than ES, # reflects significantly different than GI, and ‼ reflects significantly different than GII. ES=ex-smokers; C=all COPD; G=GOLD; I=mild; II=moderate; III/IV=severe; RA_{950}=relative area of lung with CT attenuation <-950 HU; VDP=ventilation defect percent; TBV=CT total blood volume; PV_1=relative volume of pulmonary vessels with radius <1 voxel.

Table 2.4: Baseline and rate of change imaging measurements in subgroups dichotomized by CT emphysema

Parameter (±SD)	All Ex-smokers n=41	COPD No CT emphysema n=26	COPD CT Emphysema n=23	*p*-value
RA_{950} %	1 (1)	3 (2)	17 (9)$^{*\#}$	**ND**
VDP %	7 (4)	11 (8)*	22 (9)$^{*\#}$	**.0001**
TBV mL	116 (24)	140 (31)*	159 (30)*	**.0001**
PV_1 %	49 (4)	51 (5)	53 (6)*	**.003**
ΔRA_{950} %/yr	1 (2)	0 (1)	0 (6)	.878
ΔVDP %/yr	1 (2)	1 (2)	2 (4)	.113
ΔTBV %/yr	1 (9)	-4 (10)	-3 (6)	.061
ΔPV_1 %/yr	0 (2)	-1 (2)*	0 (1)	**.013**

Participants with COPD were dichotomized based on the presence of CT emphysema using the validated CT RA_{950} threshold (≥ 6.8%). P-values reflect results of a one-way ANOVA for significant differences between subgroups with Tukey's post-hoc correction for multiple comparisons. An independent t-test was used to determine differences between subgroups whereby: * reflects significantly different than all ex-smokers, and $^{\#}$ reflects significantly different than COPD with no CT emphysema; ND=not done; TBV=CT total blood volume; VDP=ventilation defect percent; PV_1=relative volume of pulmonary vessels with radius <1 voxel; RA_{950}=relative area of lung CT attenuation <-950 HU.

Table 2.5: Demographics for participants who attended both baseline and follow-up: Unpaired analysis to account for changes in subgroup participants over time

	Ex-smoker			GOLD I			GOLD II			GOLD III/IV	
Parameter (±SD)	BL n=41	FU n=40	*p*-value	BL n=15	FU n=15	*p*-value	BL n=23	FU n=21	*p*-value	BL n=11	FU n=14
Female n (%)	18 (44)	17 (43)	-	1 (7)	1 (7)	-	11 (48)	11 (52)	-	4 (36)	2 (14)
Age y	71 (10)	73 (10)	.325	75 (8)	80 (8)	.243	68 (7)	72 (7)	.126	66 (16)	72 (11)
BMI kg/m^2	30 (4)	30 (4)	.813	28 (4)	27 (4)	.630	26 (4)	27 (4)	.411	26 (6)	25 (5)
SaO_2 %	95 (5)	96 (2)	.782	96 (1)	95 (3)	.088	96 (2)	95 (3)	.092	95 (2)	94 (3)
6MWD m	417 (83)	409 (74)	.593	434 (39)	397 (87)	.176	423 (71)	401 (57)	.463	358 (81)	363 (110)
$FEV_{1\ \%pred}$	102 (18)	103 (20)	.640	97 (12)	102 (13)	.556	62 (8)	63 (10)	.642	40 (5)	38 (7)
$FVC_{\ \%pred}$	94 (17)	96 (18)	.521	111 (13)	117 (12)	.235	94 (13)	88 (11)	.132	75 (10)	72 (17)
FEV_1/FVC	81 (6)	80 (6)	.414	64 (4)	62 (5)	.260	50 (9)	54 (9)	.219	41 (7)	40 (8)
$RV_{\ \%pred}$	105 (20)	101 (20)	.250	116 (27)	128 (32)	.141	140 (25)	136 (26)	.665	203 (44)	184 (46)
$TLC_{\ \%pred}$	101 (11)	96 (12)	**.028**	111 (11)	115 (18)	.252	113 (14)	108 (14)	.267	123 (21)	118 (17)
$RV/TLC_{\ \%pred}$	103 (15)	104 (16)	.800	104 (18)	110 (15)	.180	123 (17)	125 (14)	.701	162 (18)	152 (23)
$DL_{CO\ \%pred}$	79 (16)	85 (17)	**.037**	76 (20)	78 (21)	.654	60 (16)	62 (22)	.436	45 (13)	46 (13)

BL=baseline, FU=Follow-up, BMI=body mass index, SaO_2=oxygen saturation, 6MWD=six minute walk distance, %pred=percent predicted, FEV_1=forced expiratory volume in 1 second, FVC=forced vital capacity, RV=residual volume, TLC=total lung capacity, DL_{CO}=diffusing capacity of the lung to carbon monoxide. Unpaired Student's t-tests were used to test for group changes at follow-up.

2.6 References

1 *Global Strategy for the Diagnosis, Management and Prevention of Chronic Obstructive Pulmonary Disease 2020 Report*, <https://goldcopd.org/wp-content/uploads/2019/11/GOLD-2020-REPORT-ver1.0wms.pdf> (2020).

2 *Projections of Mortality and Causes of Death, 2016 and 2060.*, <http://www.who.int/healthinfo/global_burden_disease/projections/en/> (2019).

3 Galban, C. J. *et al.* Computed tomography-based biomarker provides unique signature for diagnosis of COPD phenotypes and disease progression. *Nat Med* **18**, 1711-1715, doi:10.1038/nm.2971 (2012).

4 Han, M. K. *et al.* Chronic obstructive pulmonary disease phenotypes: the future of COPD. *Am J Respir Crit Care Med* **182**, 598-604 (2010).

5 Hogg, J. C., Macklem, P. T. & Thurlbeck, W. M. Site and nature of airway obstruction in chronic obstructive lung disease. *N Engl J Med* **278**, 1355-1360 (1968).

6 McDonough, J. E. *et al.* Small-airway obstruction and emphysema in chronic obstructive pulmonary disease. *N Engl J Med* **365**, 1567-1575, doi:10.1056/NEJMoa1106955 (2011).

7 Mittmann, N. *et al.* The cost of moderate and severe COPD exacerbations to the Canadian healthcare system. *Respir Med* **102**, 413-421, doi:10.1016/j.rmed.2007.10.010 (2008).

8 Patel, I. S. *et al.* Bronchiectasis, exacerbation indices, and inflammation in chronic obstructive pulmonary disease. *Am J Respir Crit Care Med* **170**, 400-407, doi:10.1164/rccm.200305-648OC (2004).

9 Regan, E. A. *et al.* Genetic Epidemiology of COPD (COPDGene) Study Design. *COPD* **7**, 32-43, doi:10.3109/15412550903499522 (2011).

10 Couper, D. *et al.* Design of the Subpopulations and Intermediate Outcomes in COPD Study (SPIROMICS). *Thorax* **69**, 491-494, doi:10.1136/thoraxjnl-2013-203897 (2013).

11 Thomashow, M. A. *et al.* Endothelial microparticles in mild chronic obstructive pulmonary disease and emphysema. The Multi-Ethnic Study of Atherosclerosis Chronic Obstructive Pulmonary Disease study. *Am J Respir Crit Care Med* **188**, 60-68, doi:10.1164/rccm.201209-1697OC (2013).

12 Bourbeau, J. *et al.* Canadian Cohort Obstructive Lung Disease (CanCOLD): Fulfilling the Need for Longitudinal Observational Studies in COPD. *COPD* **11**, 125-132, doi:10.3109/15412555.2012.665520 (2014).

13 Vestbo, J. *et al.* Evaluation of COPD Longitudinally to Identify Predictive Surrogate Endpoints (ECLIPSE). *Eur Respir J* **34**, 869-873, doi:10.1183/09031936.00111707 (2008).

14 Virgincar, R. S. *et al.* Quantitative analysis of hyperpolarized ^{129}Xe ventilation imaging in healthy volunteers and subjects with chronic obstructive pulmonary disease. *NMR Biomed* **26**, 424-435, doi:10.1002/nbm.2880 (2013).

15 Swift, A. J. *et al.* Emphysematous changes and normal variation in smokers and COPD patients using diffusion ^{3}He MRI. *Eur J Radiol* **54**, 352-358, doi:10.1016/j.ejrad.2004.08.002 (2005).

16 Kirby, M. *et al.* Hyperpolarized ^{3}He and ^{129}Xe MR imaging in healthy volunteers and patients with chronic obstructive pulmonary disease. *Radiology* **265**, 600-610, doi:10.1148/radiol.12120485 (2012).

17 Kirby, M. *et al.* MRI ventilation abnormalities predict quality-of-life and lung function changes in mild-to-moderate COPD: longitudinal TINCan study. *Thorax* **72**, 475-477, doi:10.1136/thoraxjnl-2016-209770 (2017).

18 Kirby, M. *et al.* COPD: Do Imaging Measurements of Emphysema and Airway Disease Explain Symptoms and Exercise Capacity? *Radiology* **277**, 872-880, doi:10.1148/radiol.2015150037 (2015).

19 Takayanagi, S. *et al.* Longitudinal changes in structural abnormalities using MDCT in COPD: do the CT measurements of airway wall thickness and small pulmonary vessels change in parallel with emphysematous progression? *Int J Chron Obstruct Pulmon Dis* **12**, 551-560, doi:10.2147/copd.s121405 (2017).

20 Matsuoka, S. *et al.* Quantitative CT measurement of cross-sectional area of small pulmonary vessel in COPD: correlations with emphysema and airflow limitation. *Acad Radiol* **17**, 93-99, doi:10.1016/j.acra.2009.07.022 (2010).

21 Estepar, R. S. *et al.* Computed tomographic measures of pulmonary vascular morphology in smokers and their clinical implications. *Am J Respir Crit Care Med* **188**, 231-239, doi:10.1164/rccm.201301-0162OC (2013).

22 Diaz, A. A. *et al.* Bronchoarterial ratio in never-smokers adults: Implications for bronchial dilation definition. *Respirology* **22**, 108-113, doi:10.1111/resp.12875 (2017).

23 Barbera, J. A. Mechanisms of development of chronic obstructive pulmonary disease-associated pulmonary hypertension. *Pulm Circ* **3**, 160-164, doi:10.4103/2045-8932.109949 (2013).

24 Rahaghi, F. N. *et al.* Pulmonary vascular density: comparison of findings on computed tomography imaging with histology. *Eur Respir J* **54**, doi:10.1183/13993003.00370-2019 (2019).

25 Kirby, M. *et al.* Longitudinal Computed Tomography and Magnetic Resonance Imaging of COPD: Thoracic Imaging Network of Canada (TINCan) Study Objectives. *J COPD F* **1**, 200-211, doi:10.15326/jcopdf.1.2.2014.0136 (2014).

26 Miller, M. R. *et al.* Standardisation of spirometry. *Eur Respir J* **26**, 319-338, doi:10.1183/09031936.05.00034805 (2005).

27 Wanger, J. *et al.* Standardisation of the measurement of lung volumes. *Eur Respir J* **26**, 511-522, doi:10.1183/09031936.05.00035005 (2005).

28 Macintyre, N. *et al.* Standardisation of the single-breath determination of carbon monoxide uptake in the lung. *Eur Respir J* **26**, 720-735, doi:10.1183/09031936.05.00034905 (2005).

29 Jones, P. W., Quirk, F. H., Baveystock, C. M. & Littlejohns, P. A self-complete measure of health status for chronic airflow limitation. The St. George's Respiratory Questionnaire. *Am Rev Respir Dis* **145**, 1321-1327, doi:10.1164/ajrccm/145.6.1321 (1992).

30 Enright, P. L. The six-minute walk test. *Respir Care* **48**, 783-785 (2003).

31 Kirby, M. *et al.* Hyperpolarized ^{3}He magnetic resonance functional imaging semiautomated segmentation. *Acad Radiol* **19**, 141-152, doi:10.1016/j.acra.2011.10.007 (2012).

32 Shikata, H., McLennan, G., Hoffman, E. A. & Sonka, M. Segmentation of Pulmonary Vascular Trees from Thoracic 3D CT Images. *Int J Biomed Imaging* **2009**, 636240, doi:10.1155/2009/636240 (2009).

33 Schuhmann, M. *et al.* Computed tomography predictors of response to endobronchial valve lung reduction treatment. Comparison with Chartis. *Am J Respir Crit Care Med* **191**, 767-774, doi:10.1164/rccm.201407-1205OC (2015).

34 Gevenois, P. A. *et al.* Comparison of computed density and microscopic morphometry in pulmonary emphysema. *Am J Respir Crit Care Med* **154**, 187-192, doi:10.1164/ajrccm.154.1.8680679 (1996).

35 Vestbo, J. *et al.* Changes in forced expiratory volume in 1 second over time in COPD. *N Engl J Med* **365**, 1184-1192, doi:10.1056/NEJMoa1105482 (2011).

36 Kirby, M. *et al.* Total Airway Count on Computed Tomography and the Risk of Chronic Obstructive Pulmonary Disease Progression. Findings from a Population-based Study. *Am J Respir Crit Care Med* **197**, 56-65, doi:10.1164/rccm.201704-0692OC (2018).

37 Smith, B. M. *et al.* Pulmonary emphysema subtypes on computed tomography: the MESA COPD study. *Am J Med* **127**, 94 e97-23, doi:10.1016/j.amjmed.2013.09.020 (2014).

38 Synn, A. J. *et al.* Radiographic pulmonary vessel volume, lung function and airways disease in the Framingham Heart Study. *Eur Respir J* **54**, doi:10.1183/13993003.00408-2019 (2019).

39 Pompe, E. *et al.* Five-Year Progression of Emphysema and Air Trapping at CT in Smokers with and Those without Chronic Obstructive Pulmonary Disease: Results from the COPDGene Study. *Radiology*, ([Epub ahead of print] PMID: 32013794), doi:10.1148/radiol.2020191429 (2020).

40 Rodriguez-Roisin, R. *et al.* Ventilation-perfusion imbalance and chronic obstructive pulmonary disease staging severity. *J Appl Physiol* **106**, 1902-1908, doi:10.1152/japplphysiol.00085.2009 (2009).

41 Petersson, J. & Glenny, R. W. Gas exchange and ventilation-perfusion relationships in the lung. *Eur Respir J* **44**, 1023-1041, doi:10.1183/09031936.00037014 (2014).

42 Diaz, A. A. *et al.* Pulmonary vascular pruning in smokers with bronchiectasis. *ERJ Open Res* **4**, doi:10.1183/23120541.00044-2018 (2018).

43 Diaz, A. A. *et al.* Quantitative CT Measures of Bronchiectasis in Smokers. *Chest* **151**, 1255-1262, doi:10.1016/j.chest.2016.11.024 (2017).

44 Voelkel, N. F., Gomez-Arroyo, J. & Mizuno, S. COPD/emphysema: The vascular story. *Pulm Circ* **1**, 320-326, doi:10.4103/2045-8932.87295 (2011).

45 Zanini, A., Chetta, A., Imperatori, A. S., Spanevello, A. & Olivieri, D. The role of the bronchial microvasculature in the airway remodelling in asthma and COPD. *Respir Res* **11**, 132, doi:10.1186/1465-9921-11-132 (2010).

46 Jeffery, P. K. Remodeling in asthma and chronic obstructive lung disease. *Am J Respir Crit Care Med* **164**, S28-38, doi:10.1164/ajrccm.164.supplement_2.2106061 (2001).

47 Zanini, A., Chetta, A. & Olivieri, D. Therapeutic perspectives in bronchial vascular remodeling in COPD. *Ther Adv Respir Dis* **2**, 179-187, doi:10.1177/1753465808092339 (2008).

48 Mashimo, S. *et al.* Relationship between diminution of small pulmonary vessels and emphysema in chronic obstructive pulmonary disease. *Clin Imaging* **46**, 85-90, doi:10.1016/j.clinimag.2017.07.008 (2017).

49 Madani, A., Van Muylem, A. & Gevenois, P. A. Pulmonary emphysema: effect of lung volume on objective quantification at thin-section CT. *Radiology* **257**, 260-268, doi:10.1148/radiol.10091446 (2010).

CHAPTER 3

3 CONCLUSIONS AND FUTURE DIRECTIONS

In the previous chapter, main hypotheses and objectives of this thesis were addressed. In this section, the main findings of this work are summarized, and study limitations and future directions are explored. This section also contains a summary of the impact and significance of this work on the field and broader scientific community.

3.1 Overview and Research Questions

The purpose of this work is to explore the relationships between imaging and clinical biomarkers of chronic obstructive pulmonary disease, and specifically the role of CT measurements of vascular remodeling in informing disease stage and progression. The goal of this thesis was to address a gap in the literature by investigating the relationships between CT blood vessel volume measurements with hyperpolarized gas MR imaging in COPD. Additionally, we sought to determine whether small blood vessel volume measurements might serve as an informative structural biomarker that serves to indicate disease progression alongside established functional measurement methods.

3.2 Summary and Conclusions

In **Chapter 1**, we discussed the motivation and rationale for the study of COPD and the gaps in clinical knowledge that this work intends to inform. We also discussed the structure and function of the lungs, and the pathophysiological changes that occur respectively in the context of disease. We then reviewed clinical measures of lung function including pulmonary function testing, symptom reporting and exercise testing, as well as both structural and functional imaging methods. To conclude the chapter, we outlined the thesis hypotheses and objectives, which were:

1) To compare CT blood vessel volume measurements in ex-smokers without COPD and those with mild, moderate, and severe disease, and

2) To evaluate relationships between imaging and clinical biomarkers of chronic obstructive pulmonary disease, and
3) To investigate disease progression in COPD using multimodality imaging.

We hypothesized that CT blood vessel volume measurements were significantly different in ex-smokers without COPD than in those with this disease and will be related to disease severity. In **Chapter 2**, we addressed these aims:

1) In a cross-sectional sample of ex-smokers without COPD and participants with mild, moderate and severe disease, we confirmed our hypothesis and demonstrated that small blood vessel volume is significantly different in COPD than in ex-smokers without COPD and is related to disease severity. In this study we demonstrated that in 90 ex-smokers with and without COPD over a follow-up period of 2.5 years, there were significant differences between ex-smokers and mild, moderate and severe COPD for imaging measurements of CT RA_{950}, TBV, PV_1 and MRI VDP.

2) In this study, we also demonstrated that the rates of change in imaging measurements from baseline to follow-up were significantly different according to the rate of change in FEV_1; RA_{950} and PV_1 demonstrated changes between groups, whereas VDP was the same across each group, demonstrating that changes in small vessel volume and emphysema on CT are sensitive to changes in lung function that VDP is not.

3) Finally, changes in PV_1 according to the presence of emphysema in whereas other imaging measurements did not significantly differentiate groups according to phenotype. This indicates that disease progression occurs differently according to COPD phenotype.

We concluded that small blood vessel volume may be an important indicatory of disease progression, and that combining CT and MRI measurements of lung structure and function, respectively, can inform a deeper understanding of COPD progression.

3.3 Limitations

A limitation of this work is the consequence of non-isotropic CT voxel size on peripheral vascular structure measurements. Based on the algorithm that was used by VIDA Vision commercial software, peripheral vessels are defined as a vessel with a radius of less than one voxel. Because of the non-isotropic voxel size used in our acquisition protocol, it is unclear in which plane the radius is being measured, which would affect the threshold diameter of peripheral vessels. Despite this limitation, even if a radius of 1.25mm is used as a threshold, this would mean a cross sectional area of approximately 5mm^2, which is consistent with methods reported in other studies.[1-3] Other specific limitations were discussed in **Chapter 2**.

3.4 Future Directions

In the future, it would be interesting to spatially match hyperpolarized gas MRI and CT vascular structure in bronchiectasis, as a model of airway remodeling. In approximately 50% of COPD cases, patients experience an irreversible cycle of marked airway inflammation, infection, obstruction, and damage.[4] The current gold-standard for the diagnosis of bronchiectasis is CT, wherein the radiologist looks for the signet ring sign, a mismatched ratio between the cross-sectional diameter of the airway and its associated vessel. Another radiological marker of bronchiectasis is the traction sign, or airways that do not appear to taper as they travel distal from the main airways.[5] There is no way to reverse this disease. The consequences for the patient are symptoms such as chronic cough, repeated chest infection, shortness of breath and decreased pulmonary function. In patients with COPD, the presence of bronchiectasis results in decreased quality of life, increased rates of hospitalization and disease exacerbation, and increased morbidity and mortality.[4,6]

Further, the consideration of clinical COPD phenotypes in evaluating vascular changes within the lung should be considered. Studies in healthy never smokers and in ex-smokers without COPD have reported some emphysema on CT scans, however the upper limit of normal has been reported as 6.8%.[7] Differences in vascular measurements between the

chronic bronchitis predominant compared to emphysema predominant case may be reflective of different underlying physiological processes, as discussed in sections 1.3.1 to 1.3.3.

Another important future direction for this work is to investigate the of the role of sex differences in airways disease, as this factor is becoming an important consideration for COPD diagnosis and management.[8] Interestingly, bronchiectasis differentially affects men and women differently throughout their lifespan. In childhood, boys are more likely to be diagnosed with non-cystic fibrosis bronchiectasis. Later in adulthood, this trend is reversed, wherein women over the age of 60 are twice as likely to be diagnosed.[9] This likely represents a complex interplay between genetic, hormonal and environmental factors related to the disease.[8] Further, men and women experience chronic lung disease such as COPD differently; women are more likely to report greater symptom severity and to experience psychological effects of chronic disease than men.[8] An interesting future study would investigate sex differences in disease progression and vascular remodeling in consideration of disease severity and burden.

Finally, another potential future direction for this work given the results of this study would be the application of machine learning to predict disease progression using CT vessel measurements and MRI. This method has been used to predict MRI ventilation from CT images,[10] as well as to predict disease progression in COPD using baseline and follow-up data according to disease phenotypes.[11] Application of machine learning in this case would include identifying participants at risk of disease progression based on vascular structure. The ground truth for this method would be based on patients who experienced an increase in ventilation defect percent or decline in lung function according to clinical PFT data. Input data would include maps of vascular structure, emphysema, and MR ventilation maps. Not only would this method be important for determining which participants are at risk of disease progression but could also elucidate relationships about ventilation/perfusion mismatch and what that means for COPD prognosis. Recently, researchers involved in the COPDGene study have proposed that perhaps COPD phenotypes may not exist, but rather a series of axes related to inflammation, disease trajectory, and genetic factors.[12] Further, they highlight the importance of chest CT in our

developing understanding of this disease. It is therefore important to continue to investigate the diagnostic and predictive role of imaging biomarkers to further elucidate factors related to disease morbidity and mortality.

3.5 Significance and Impact

This work contributes significantly to the literature as a novel study comparing CT vascular structure and MRI ventilation in COPD, and what this tells us about disease progression and functional changes. While changes to MRI ventilation did not correlate significantly with changes to vascular structure, it is likely that one change precedes the other, and depends on disease presentation. To our knowledge, this is the first study to compare clinically important biomarkers using multimodality imaging of both lung CT structure and MRI lung function in COPD. This work has a significant impact due to the importance of understanding ventilation-perfusion relationships in COPD, as well as supporting peripheral vascular structure as an important measurement in COPD progression. In the bigger picture, this work also supports the application of multimodality imaging which provides important structural and functional measurements.

3.6 References

1 Synn, A. J. *et al.* Radiographic pulmonary vessel volume, lung function and airways disease in the Framingham Heart Study. *Eur Respir J* **54**, doi:10.1183/13993003.00408-2019 (2019).

2 Takayanagi, S. *et al.* Longitudinal changes in structural abnormalities using MDCT in COPD: do the CT measurements of airway wall thickness and small pulmonary vessels change in parallel with emphysematous progression? *Int J Chron Obstruct Pulmon Dis* **12**, 551-560, doi:10.2147/copd.s121405 (2017).

3 Estepar, R. S. *et al.* Computed tomographic measures of pulmonary vascular morphology in smokers and their clinical implications. *Am J Respir Crit Care Med* **188**, 231-239, doi:10.1164/rccm.201301-0162OC (2013).

4 Patel, I. S. *et al.* Bronchiectasis, exacerbation indices, and inflammation in chronic obstructive pulmonary disease. *Am J Respir Crit Care Med* **170**, 400-407, doi:10.1164/rccm.200305-648OC (2004).

5 Pasteur, M. C., Bilton, D. & Hill, A. T. British Thoracic Society guideline for non-CF bronchiectasis. *Thorax* **65 Suppl 1**, i1-58, doi:10.1136/thx.2010.136119 (2010).

6 Chalmers, J. D., Aliberti, S. & Blasi, F. Management of bronchiectasis in adults. *Eur Respir J* **45**, 1446-1462, doi:10.1183/09031936.00119114 (2015).

7 Gevenois, P. A. *et al.* Comparison of computed density and microscopic morphometry in pulmonary emphysema. *Am J Respir Crit Care Med* **154**, 187-192, doi:10.1164/ajrccm.154.1.8680679 (1996).

8 Raghavan, D. & Jain, R. Increasing awareness of sex differences in airway diseases. *Respirology* **21**, 449-459, doi:10.1111/resp.12702 (2016).

9 Vidaillac, C., Yong, V. F. L., Jaggi, T. K., Soh, M. M. & Chotirmall, S. H. Gender differences in bronchiectasis: a real issue? *Breathe (Sheff)* **14**, 108-121, doi:10.1183/20734735.000218 (2018).

10 Westcott, A. *et al.* Chronic Obstructive Pulmonary Disease: Thoracic CT Texture Analysis and Machine Learning to Predict Pulmonary Ventilation. *Radiology* **293**, 676-684, doi:10.1148/radiol.2019190450 (2019).

11 Young, A. L. *et al.* Disease Progression Modelling in Chronic Obstructive Pulmonary Disease (COPD). *Am J Respir Crit Care Med*, doi:10.1164/rccm.201908-1600OC (2019).

12 Castaldi, P. J. *et al.* Machine Learning Characterization of COPD Subtypes: Insights from the COPDGene Study. *Chest*, doi:10.1016/j.chest.2019.11.039 (2019).

4 APPENDICES

Appendix A: Health Science Research Ethics Board Approval Notices

Western Research

Date: 17 January 2020

To: Dr. Grace Parraga

Project ID: 6014

Study Title: Longitudinal Study of Helium-3 Magnetic Resonance Imaging of COPD

Application Type: Continuing Ethics Review (CER) Form

Review Type: Delegated

REB Meeting Date: 28/Jan/2020

Date Approval Issued: 17/Jan/2020

REB Approval Expiry Date: 10/Feb/2021

Dear Dr. Grace Parraga,

The Western University Research Ethics Board has reviewed the application. This study, including all currently approved documents, has been re-approved until the expiry date noted above.

REB members involved in the research project do not participate in the review, discussion or decision.

Western University REB operates in compliance with, and is constituted in accordance with, the requirements of the TriCouncil Policy Statement: Ethical Conduct for Research Involving Humans (TCPS 2); the International Conference on Harmonisation Good Clinical Practice Consolidated Guideline (ICH GCP); Part C, Division 5 of the Food and Drug Regulations; Part 4 of the Natural Health Products Regulations; Part 3 of the Medical Devices Regulations and the provisions of the Ontario Personal Health Information Protection Act (PHIPA 2004) and its applicable regulations. The REB is registered with the U.S. Department of Health & Human Services under the IRB registration number IRB 00000940.

Please do not hesitate to contact us if you have any questions.

Sincerely,

Daniel Wyzynski, Research Ethics Coordinator, on behalf of Dr. Joseph Gilbert, HSREB Chair

Note: This correspondence includes an electronic signature (validation and approval via an online system that is compliant with all regulations).

Appendix B: Permissions for Reproduction of Scientific Articles

ELSEVIER LICENSE
TERMS AND CONDITIONS

Feb 14, 2020

This Agreement between Robarts Research Institute -- Andrea Barker ("You") and Elsevier ("Elsevier") consists of your license details and the terms and conditions provided by Elsevier and Copyright Clearance Center.

License Number	4767700103671
License date	Feb 14, 2020
Licensed Content Publisher	Elsevier
Licensed Content Publication	Elsevier Books
Licensed Content Title	Pediatric Critical Care
Licensed Content Author	Christopher A. D'Angelis,Jacqueline J. Coalson,Rita M. Ryan
Licensed Content Date	Jan 1, 2011
Licensed Content Pages	9
Start Page	490
End Page	498
Type of Use	reuse in a thesis/dissertation
Portion	figures/tables/illustrations

Number of figures/tables/illustrations	1
Format	both print and electronic
Are you the author of this Elsevier chapter?	No
Will you be translating?	No
Title	Multimodality imaging to investigate longitudinal functional consequences of vascular remodeling in COPD
Institution name	The University of Western Ontario
Expected presentation date	Mar 2020
Portions	Figure 36.1

CREATIVE COMMONS CORPORATION IS NOT A LAW FIRM AND DOES NOT PROVIDE LEGAL SERVICES. DISTRIBUTION OF THIS LICENSE DOES NOT CREATE AN ATTORNEY-CLIENT RELATIONSHIP. CREATIVE COMMONS PROVIDES THIS INFORMATION ON AN "AS-IS" BASIS. CREATIVE COMMONS MAKES NO WARRANTIES REGARDING THE INFORMATION PROVIDED, AND DISCLAIMS LIABILITY FOR DAMAGES RESULTING FROM ITS USE.

4.1.1 *License*

THE WORK (AS DEFINED BELOW) IS PROVIDED UNDER THE TERMS OF THIS CREATIVE COMMONS PUBLIC LICENSE ("CCPL" OR "LICENSE"). THE WORK IS PROTECTED BY COPYRIGHT AND/OR OTHER APPLICABLE LAW. ANY USE OF THE WORK OTHER THAN AS AUTHORIZED UNDER THIS LICENSE OR COPYRIGHT LAW IS PROHIBITED.

BY EXERCISING ANY RIGHTS TO THE WORK PROVIDED HERE, YOU ACCEPT AND AGREE TO BE BOUND BY THE TERMS OF THIS LICENSE. TO THE EXTENT THIS LICENSE MAY BE CONSIDERED TO BE A CONTRACT, THE LICENSOR GRANTS YOU THE RIGHTS CONTAINED HERE IN CONSIDERATION OF YOUR ACCEPTANCE OF SUCH TERMS AND CONDITIONS.

1. Definitions

a. **"Adaptation"** means a work based upon the Work, or upon the Work and other pre-existing works, such as a translation, adaptation, derivative work, arrangement of music or other alterations of a literary or artistic work, or phonogram or performance and includes cinematographic adaptations or any other form in which the Work may be recast, transformed, or adapted including in any form recognizably derived from the original, except that a work that constitutes a Collection will not be considered an Adaptation for the purpose of this License. For the avoidance of doubt, where the Work is a musical work, performance or phonogram, the synchronization of the Work in timed-relation with a moving image ("synching") will be considered an Adaptation for the purpose of this License.

b. **"Collection"** means a collection of literary or artistic works, such as encyclopedias and anthologies, or performances, phonograms or broadcasts, or other works or subject matter other than works listed in Section 1(g) below, which, by reason of the selection and arrangement of their contents, constitute intellectual creations, in which the Work is included in its entirety in unmodified form along with one or more other contributions, each constituting separate and independent works in themselves, which together are assembled into a collective whole. A work that constitutes a Collection will not be considered an Adaptation (as defined above) for the purposes of this License.

c. **"Distribute"** means to make available to the public the original and copies of the Work or Adaptation, as appropriate, through sale or other transfer of ownership.

d. **"License Elements"** means the following high-level license attributes as selected by Licensor and indicated in the title of this License: Attribution, Noncommercial, ShareAlike.

e. **"Licensor"** means the individual, individuals, entity or entities that offer(s) the Work under the terms of this License.

f. **"Original Author"** means, in the case of a literary or artistic work, the individual, individuals, entity or entities who created the Work or if no individual or entity can be identified, the publisher; and in addition (i) in the case of a performance the actors, singers, musicians, dancers, and other persons who act, sing, deliver, declaim, play in, interpret or otherwise perform literary or artistic works or expressions of folklore; (ii) in the case of a phonogram the producer being the person or legal entity who first fixes the sounds of a performance or other sounds; and, (iii) in the case of broadcasts, the organization that transmits the broadcast.

g. **"Work"** means the literary and/or artistic work offered under the terms of this License including without limitation any production in the literary, scientific and artistic domain, whatever may be the mode or form of its expression including digital form, such as a book, pamphlet and other writing; a lecture, address, sermon or other work of the same nature; a dramatic or dramatico-musical work; a choreographic work or entertainment in dumb show; a musical composition with or without words; a cinematographic work to which are assimilated works expressed by a process analogous to cinematography; a work of drawing, painting, architecture, sculpture, engraving or lithography; a photographic work to which are assimilated works expressed by a process analogous to photography; a work of applied art; an illustration, map, plan, sketch or three-dimensional work relative to geography, topography, architecture or science; a performance; a broadcast; a phonogram; a compilation of data to the extent it is protected as a copyrightable work; or a work performed by a variety or circus performer to the extent it is not otherwise considered a literary or artistic work.

h. **"You"** means an individual or entity exercising rights under this License who has not previously violated the terms of this License with respect to the Work, or who has received express permission from the Licensor to exercise rights under this License despite a previous violation.

i. **"Publicly Perform"** means to perform public recitations of the Work and to communicate to the public those public recitations, by any means or process, including by wire or wireless means or public digital performances; to make available to the public Works in such a way that members of the public may access these Works from a place and at a place individually chosen by them; to perform the Work to the public by any means or process and the communication to the public of the performances of the Work, including by public digital performance; to broadcast and rebroadcast the Work by any means including signs, sounds or images.

j. **"Reproduce"** means to make copies of the Work by any means including without limitation by sound or visual recordings and the right of fixation and reproducing fixations of the Work, including storage of a protected performance or phonogram in digital form or other electronic medium.

2. Fair Dealing Rights. Nothing in this License is intended to reduce, limit, or restrict any uses free from copyright or rights arising from limitations or exceptions that are provided for in connection with the copyright protection under copyright law or other applicable laws.

3. License Grant. Subject to the terms and conditions of this License, Licensor hereby grants You a worldwide, royalty-free, non-exclusive, perpetual (for the duration of the applicable copyright) license to exercise the rights in the Work as stated below:

a. to Reproduce the Work, to incorporate the Work into one or more Collections, and to Reproduce the Work as incorporated in the Collections;

b. to create and Reproduce Adaptations provided that any such Adaptation, including any translation in any medium, takes reasonable steps to clearly label, demarcate or otherwise identify that changes were made to the original Work. For example, a translation could be marked "The original work was translated from English to Spanish," or a modification could indicate "The original work has been modified.";

c. to Distribute and Publicly Perform the Work including as incorporated in Collections; and,

d. to Distribute and Publicly Perform Adaptations.

The above rights may be exercised in all media and formats whether now known or hereafter devised. The above rights include the right to make such modifications as are technically necessary to exercise the rights in other media and formats. Subject to Section 8(f), all rights not expressly granted by Licensor are hereby reserved, including but not limited to the rights described in Section 4(e).

4. Restrictions. The license granted in Section 3 above is expressly made subject to and limited by the following restrictions:

a. You may Distribute or Publicly Perform the Work only under the terms of this License. You must include a copy of, or the Uniform Resource Identifier (URI) for, this License with every copy of the Work You Distribute or Publicly Perform. You may not offer or impose any terms on the Work that restrict the terms of this License or the ability of the recipient of the Work to exercise the rights granted to that recipient under the terms of the License. You may not sublicense the Work. You must keep intact all notices that refer to this License and to the disclaimer of warranties with every copy of the Work You Distribute or Publicly Perform. When You Distribute or Publicly Perform the Work, You may not impose any effective technological measures on the Work that restrict the ability of a recipient of the Work from You to exercise the rights granted to that recipient under the terms of the License. This Section 4(a) applies to the Work as incorporated in a Collection, but this does not require the Collection apart from the Work itself to be made subject to the terms of this License. If You create a Collection, upon notice from any Licensor You must, to the extent practicable, remove from the Collection any credit as required by Section 4(d), as requested. If You create an Adaptation, upon notice from any Licensor You must, to the extent practicable, remove from the Adaptation any credit as required by Section 4(d), as requested.

b. You may Distribute or Publicly Perform an Adaptation only under: (i) the terms of this License; (ii) a later version of this License with the same License Elements as this License; (iii) a Creative Commons jurisdiction license (either this or a later license version) that contains the same License Elements as this License (e.g., Attribution-NonCommercial-ShareAlike 3.0 US) ("Applicable License"). You must include a copy of, or the URI, for Applicable License with every copy of each Adaptation You Distribute or Publicly Perform. You may not offer or impose any terms on the Adaptation that restrict the terms of the Applicable License or the ability of the recipient of the Adaptation to exercise the rights granted to that recipient under the terms of the Applicable License. You must keep intact all notices that refer to the Applicable License and to the disclaimer of warranties with every copy of the Work as included in the Adaptation You Distribute or Publicly Perform. When You Distribute or Publicly Perform the Adaptation, You may not impose any effective technological measures on the Adaptation that restrict the ability of a recipient of the Adaptation from You to exercise the rights granted to that recipient

under the terms of the Applicable License. This Section 4(b) applies to the Adaptation as incorporated in a Collection, but this does not require the Collection apart from the Adaptation itself to be made subject to the terms of the Applicable License.

c. You may not exercise any of the rights granted to You in Section 3 above in any manner that is primarily intended for or directed toward commercial advantage or private monetary compensation. The exchange of the Work for other copyrighted works by means of digital file-sharing or otherwise shall not be considered to be intended for or directed toward commercial advantage or private monetary compensation, provided there is no payment of any monetary compensation in con-nection with the exchange of copyrighted works.

d. If You Distribute, or Publicly Perform the Work or any Adaptations or Collections, You must, unless a request has been made pursuant to Section 4(a), keep intact all copyright notices for the Work and provide, reasonable to the medium or means You are utilizing: (i) the name of the Original Author (or pseudonym, if applicable) if supplied, and/or if the Original Author and/or Licensor designate another party or parties (e.g., a sponsor institute, publishing entity, journal) for attribution ("Attribution Parties") in Licensor's copyright notice, terms of service or by other reasonable means, the name of such party or parties; (ii) the title of the Work if supplied; (iii) to the extent reasonably practicable, the URI, if any, that Licensor specifies to be associated with the Work, unless such URI does not refer to the copyright notice or licensing information for the Work; and, (iv) consistent with Section 3(b), in the case of an Adaptation, a credit identifying the use of the Work in the Adaptation (e.g., "French translation of the Work by Original Author," or "Screenplay based on original Work by Original Author"). The credit required by this Section 4(d) may be implemented in any reasonable manner; provided, however, that in the case of a Adaptation or Collection, at a minimum such credit will appear, if a credit for all contributing authors of the Adaptation or Collection appears, then as part of these credits and in a manner at least as prominent as the credits for the other contributing authors. For the avoidance of doubt, You may only use the credit required by this Section for the purpose of attribution in the manner set out above and, by exercising Your rights under this License, You may not implicitly or explicitly assert or imply any connection with, sponsorship or endorsement by the Original Author, Licensor and/or Attribution Parties, as appropriate, of You or Your use of the Work, without the separate, express prior written permission of the Original Author, Licensor and/or Attribution Parties.

e. For the avoidance of doubt:
    i. **Non-waivable Compulsory License Schemes**. In those jurisdictions in which the right to collect royalties through any statutory or compulsory licensing scheme cannot be waived, the Licensor reserves the exclusive right to collect such royalties for any exercise by You of the rights granted under this License;

    ii. **Waivable Compulsory License Schemes**. In those jurisdictions in which the right to collect royalties through any statutory or compulsory licensing scheme can be waived, the Licensor reserves the exclusive right to collect such royalties for any exercise by You of the rights granted under this License if Your exercise of such rights is for a purpose or use which is otherwise than noncommercial as permitted under Section 4(c) and otherwise waives the right to collect royalties through any statutory or compulsory licensing scheme; and,

    iii. **Voluntary License Schemes**. The Licensor reserves the right to collect royalties, whether individually or, in the event that the Licensor is a member of a collecting society that administers voluntary licensing schemes, via that society, from any exercise by You of the rights granted under this License that is for a purpose or use which is otherwise than noncommercial as permitted under Section 4(c).

f. Except as otherwise agreed in writing by the Licensor or as may be otherwise permitted by applicable law, if You Reproduce, Distribute or Publicly Perform the Work either by itself or as part of any Adaptations or Collections, You must not distort, mutilate, modify or take other derogatory action in relation to the Work which would be prejudicial to the Original Author's honor or reputation. Licensor agrees that in those jurisdictions (e.g. Japan), in which any exercise of the right granted in Section 3(b) of this License (the right to make Adaptations) would be deemed to be a distortion, mutilation, modification or other derogatory action prejudicial to the Original Author's honor and reputation, the Licensor will waive or not assert, as appropriate, this Section, to the fullest extent permitted by the applicable national law, to enable You to reasonably exercise Your right under Section 3(b) of this License (right to make Adaptations) but not otherwise.

5. Representations, Warranties and Disclaimer

UNLESS OTHERWISE MUTUALLY AGREED TO BY THE PARTIES IN WRITING AND TO THE FULLEST EXTENT PERMITTED BY APPLICABLE LAW, LICENSOR OFFERS THE WORK AS-IS AND MAKES NO REPRESENTATIONS OR WARRANTIES OF ANY KIND CONCERNING THE WORK, EXPRESS, IMPLIED, STATUTORY OR OTHERWISE, INCLUDING, WITHOUT LIMITATION, WARRANTIES OF TITLE, MERCHANTABILITY, FITNESS FOR A PARTICULAR PURPOSE, NONINFRINGEMENT, OR THE ABSENCE OF LATENT OR OTHER DEFECTS, ACCURACY, OR THE PRESENCE OF ABSENCE OF ERRORS, WHETHER OR NOT DISCOVERABLE. SOME JURISDICTIONS DO NOT ALLOW THE EXCLUSION OF IMPLIED WARRANTIES, SO THIS EXCLUSION MAY NOT APPLY TO YOU.

6. Limitation on Liability. EXCEPT TO THE EXTENT REQUIRED BY APPLICABLE LAW, IN NO EVENT WILL LICENSOR BE LIABLE TO YOU ON ANY LEGAL THEORY FOR ANY SPECIAL, INCIDENTAL, CONSEQUENTIAL, PUNITIVE OR EXEMPLARY DAMAGES ARISING OUT OF THIS LICENSE OR THE USE OF THE WORK, EVEN IF LICENSOR HAS BEEN ADVISED OF THE POSSIBILITY OF SUCH DAMAGES.

7. Termination

a. This License and the rights granted hereunder will terminate automatically upon any breach by You of the terms of this License. Individuals or entities who have received Adaptations or Collections from You under this License, however, will not have their licenses terminated provided such individuals or entities remain in full compliance with those licenses. Sections 1, 2, 5, 6, 7, and 8 will survive any termination of this License.

b. Subject to the above terms and conditions, the license granted here is perpetual (for the duration of the applicable copyright in the Work). Notwithstanding the above, Licensor reserves the right to release the Work under different license terms or to stop distributing the Work at any time; provided, however that any such election will not serve to withdraw this License (or any other license that has been, or is required to be, granted under the terms of this License), and this License will continue in full force and effect unless terminated as stated above.

8. Miscellaneous

a. Each time You Distribute or Publicly Perform the Work or a Collection, the Licensor offers to the recipient a license to the Work on the same terms and conditions as the license granted to You under this License.

b. Each time You Distribute or Publicly Perform an Adaptation, Licensor offers to the recipient a license to the original Work on the same terms and conditions as the license granted to You under this License.

c. If any provision of this License is invalid or unenforceable under applicable law, it shall not affect the validity or enforceability of the remainder of the terms of this License, and without further action by the parties to this agreement, such provision shall be reformed to the minimum extent necessary to make such provision valid and enforceable.

d. No term or provision of this License shall be deemed waived and no breach consented to unless such waiver or consent shall be in writing and signed by the party to be charged with such waiver or consent.

e. This License constitutes the entire agreement between the parties with respect to the Work licensed here. There are no understandings, agreements or representations with respect to the Work not specified here. Licensor shall not be bound by any additional provisions that may appear in any communication from You. This License may not be modified without the mutual written agreement of the Licensor and You.

f. The rights granted under, and the subject matter referenced, in this License were drafted utilizing the terminology of the Berne Convention for the Protection of Literary and Artistic Works (as amended on September 28, 1979), the Rome Convention of 1961, the WIPO Copyright Treaty of 1996, the WIPO Performances and Phonograms Treaty of 1996 and the Universal Copyright Convention (as revised on July 24, 1971). These rights and subject matter take effect in the relevant jurisdiction in which the License terms are sought to be enforced according to the corresponding provisions of the implementation of those treaty provisions in the applicable national law. If the standard suite of rights granted under applicable copyright law includes additional rights not granted under this License, such additional rights are deemed to be included in the License; this License is not intended to restrict the license of any rights under applicable law.

https://creativecommons.org/licenses/by-nc-sa/3.0/legalcode

Appendix C: Curriculum Vitae

NAME: Andrea L. Barker Odhiambo

POST-SECONDARY EDUCATION AND DEGREES:

2018-2020	MSc in Medical Biophysics (Candidate) Department of Medical Biophysics **Western University, Canada** Supervisor: Dr. Grace Parraga
2014-2018	BSc (Honours) in Neuroscience & Mental Health *with distinction* Minor in Biology Minor in Psychology Department of Neuroscience **Carleton University, Canada** Supervisor: Dr. Matthew Holahan

RELATED WORK EXPERIENCE:

2016-2017	**Western University** *Research Assistant* Department of Kinesiology Supervisor: Dr. Kevin Shoemaker
2015-2017	**Carleton University** *Research Assistant* Department of Neuroscience Supervisor: Dr. Matthew Holahan
2016	**Western University** *Research Assistant* Fowler Kennedy Sport Medicine Clinic Supervisor: Dr. Lisa Fischer

2015 **Child & Parent Resource Institute (CPRI)**
Research Assistant
Department of Applied Research & Education
Supervisor: Ian Kerr

HONOURS AND AWARDS:

2019-2020 **Western Graduate Research Scholarship**
Institutional
$5000

2019-2020 **Frederick Banting and Charles Best Canada Graduate Scholarship (CGSM) in Health Research (CIHR)**
National
$17,500

2019-2020 **Queen Elizabeth II Graduate Scholarship in Science and Technology (QEII-GSST)**
Provincial (declined)
$15,000

2018-2019 **Western Graduate Research Scholarship**
Institutional
$5000

2018-2019 **Ontario Graduate Scholarship (OGS)**
Provincial
$15,000

2018-2019 **Ilan Levy Post-Graduate Scholarship**
National
$5000

2015-2019 **Dean's Honour List**
Institutional

2017 **YMCA Young Woman of Excellence Honouree**
Regional

2017-2018	**Joe Carter Scholarship** National **$5000**
2016-2017	**Ruth Lifeso Scholarship** Institutional **$5000**
2014, 2016-2017	**Gerhard Herzberg Scholarship** Institutional **$12,000**
2014-2015	**Faculty of Science Scholarship** Institutional **$1000**
2014-2015	**Kathleen Laing Memorial Scholarship** National **$5000**
2014-2017	**Clark Bursary** Provincial **$14,000**
2014-2017	**Bright Futures Bursary** Regional **$12,000**

PUBLICATIONS: (4)

In preparation (1)

1. **Barker AL**, SC Bureau, CC Marshall, MR Holahan. Characterizing concussion in a pediatric population: sex and age effects on symptom severity. *In preparation* for *British Journal of Sport Medicine.*

Published (3)

1. **Barker AL,** RL Eddy, JL MacNeil, M Kirby, DG McCormack, G Parraga. CT Pulmonary Vessels and MRI Ventilation in Chronic Obstructive Lung Disease: Relationship with worsening FEV_1 in the TINCan Cohort Study. *Academic Radiology (in press).*

2. MacNeil JL, DPI Capaldi, RL Eddy, A Westcott, AM Matheson, **AL Barker**, C Ong-Ly, DG McCormack, G Parraga. Multi-Parametric Response Maps: Pulmonary Imaging Phenotypes of Chronic Obstructive Pulmonary Disease. *Radiology*, 2020;295(1):227-236. doi: 10.1148/radiol.2020191735

3. MacNeil JL, DPI Capaldi, RL Eddy, A Westcott, AM Matheson, **AL Barker**, C Ong-Ly, DG McCormack, G Parraga. Development and Evaluation of Pulmonary Imaging Multi-Parametric Response Maps for Deep Phenotyping of Chronic Obstructive Pulmonary Disease. Proc. SPIE 10953, Medical Imaging 2019: Biomedical Applications in Molecular, Structural, and Functional Imaging, 109530J. doi: 10.1117/12.2512849

BOOK CHAPTERS: (1)

Submitted (1)

1. **Barker AL**, RL Eddy, H Yaremko, M Kirby, G Parraga. 2018. Medical Radiology: Diagnostic Imaging: "Structure-function imaging of asthma: Airway and ventilation biomarkers." Springer (08/2018).

PRESENTATIONS: (6)

1. **Barker AL,** RL Eddy, AM Matheson, A Westcott, AA Diaz, R San Jose Estepar, GR Washko, G Parraga. Are MRI Ventilation Defects and CT Vascular Pruning Related in Bronchiectasis and COPD Patients? London Imaging Discovery Day. June 2019; London ON.

2. **Barker AL**, RL Eddy, AM Matheson, A Westcott, R San Jose Estepar, AA Diaz, GR Washko, G Parraga. Bronchiectasis, Vascular Pruning and Ventilation Defects in COPD and Bronchiectatic Patients: Are They Related? American Thoracic Society. May 2019; Dallas TX.

3. **Barker AL**, A Westcott, RL Eddy, DG McCormack, G Parraga, A Ouriadov. Feasibility of Single Breath-hold Isotropic Voxel ^{129}Xe MRI in Patients. International Society of Magnetic Resonance in Medicine; May 2019; Montreal QC.

4. **Barker AL**, RL Eddy, AM Matheson, A Westcott, R San Jose Estepar, AA Diaz, GR Washko, G Parraga. Vascular Pruning and MRI Ventilation Defects in COPD and Bronchiectatic Patients. London Health Research Day; April 2019; London ON.

5. **Barker AL**, RL Eddy, AM Matheson, A Westcott, R San Jose Estepar, GR Washko, G Parraga. Is MRI Ventilation related to CT Vascular Structure in non-Cystic Fibrosis Bronchiectasis? Imaging Network of Ontario; March 2019; London ON.

6. **Barker AL**, SC Bureau, CC Marshall, MR Holahan. A comprehensive profile of reported symptoms in acute concussion patients in sport medicine clinics and emergency departments across Canada. In proceedings from the Young Researcher's Conference; May 2018; Ottawa ON.

ABSTRACTS: (13)

Accepted (4)

1. McIntosh MJ, RL Eddy, D Knipping, **AL Barker**, T Lindenmaier, C Yamashita, G Parraga. Response to benralizumab in severe asthsma: ^{129}Xe MRI, oscillometry and clinical measurements. American Thoracic Society Meeting. May 2020; Philadelphia PA.

2. **Barker AL**, RL Eddy, AM Matheson, A Westcott, R San Jose Estepar, AA Diaz, GR Washko, G Parraga. Vascular Structure and MRI Ventilation in Bronchiectasis and COPD. Robarts Research Retreat. June 2019; London ON.

3. **Barker AL**, RL Eddy, AM Matheson, A Westcott, R San Jose Estepar, AA Diaz, GR Washko, G Parraga. Vascular Structure and MRI Ventilation in Bronchiectasis and COPD. London Imaging Discovery Day. June 2019; London ON.

4. Matheson AM, RL Eddy, **AL Barker**, DG McCormack, G Parraga. Perfusion Abnormalities in COPD: How do Emphysema and Airways Contribute? American Thoracic Society Meeting. May 2020; Philadelphia, PA.

Submitted (0)

Published (9)

1. **Barker AL**, RL Eddy, AM Matheson, AR Westcott, GR Washko, G Parraga. Bronchiectasis, Vascular Pruning and Ventilation Defects in COPD and Bronchiectatic Patients: Are They Related? American Thoracic Society Meeting. May 2019; Dallas TX.

2. **Barker AL**, A Westcott, RL Eddy, DG McCormack, G Parraga, A Ouriadov. Feasibility of single breath-hold isotropic voxel ^{129}Xe MRI in patients. International Society for Magnetic Resonance in Medicine. May 2019; Montreal QC.

3. MacNeil JL, DPI Capaldi, RL Eddy, AR Westcott, AM Matheson, **AL Barker**, C Ong Ly, DG McCormack, G Parraga. Development and evaluation of pulmonary imaging multi-parametric response maps for deep phenotyping of chronic obstructive pulmonary disease. SPIE Medical Imaging. February 2019; San Diego CA.

4. MacNeil JL, RL Eddy, **AL Barker**, H Coxson, G Parraga. Multi-Parametric Response Maps: Phenotypes of COPD & Cannabis Smokers in the TINCan Cohort Study. Fleishner Society Meeting. March 29, 2019; Paris FR.

5. Harriss A, E Woehrle, **AL Barker**, E Moir, LK Fischer, DD Fraser, JK Shoemaker. The impact of aerobic exercise training on autonomic function in adolescent sport-related concussion. In proceedings from Experimental Biology. April 2018; San Diego CA.

6. Jacobs KG, E Woehrle, SO Smith, SA Klassen, RJ Knetsch, **AL Barker**, JK Shoemaker. Sex differences in heart rate response to isometric handgrip exercise with concurrent contralateral forearm somatosensory stimulation. In proceedings from Experimental Biology. April 2018; San Diego CA.

7. Woerhle E, KC Abbott, ME Moir, CS Balestrini, **AL Barker**, LK Fischer, DD Fraser, JK Shoemaker. Impaired heart rate response during brief 30% isometric handgrip in adolescents diagnosed with concussion. In proceedings from the Canadian Academy of Sport and Exercise Medicine. June 7-10, 2017; Mont-Tremblant QC.

8. Woehrle E, KC Abbott, AB Harris, ME Moir, CS Balestrini, **AL Barker**, LK Fischer, DD Fraser, JK Shoemaker. Autonomic dysregulation in heart rate responses to brief static handgrip exercise in concussed adolescents. In proceedings from Exercise is Medicine Canada National Student Conference. June 2017; London ON.

9. Woehrle E, KC Abbott, ME Moir, CS Balestrini, **AL Barker**, LK Fischer, DD Fraser, JK Shoemaker. Impaired heart rate response during brief 30% isometric handgrip in adolescents diagnosed with concussion. In proceedings from UHN Fifth Annual Symposium: Research on the Concussion Spectrum of Disorders. January 2017; Toronto ON.

POST-GRADUATE EXPERIENCES:

2020 **Conference Panelist**
Women in Science: Undergraduate Connect Conference
Western University